2017

The Formation of Polycyclic Aromatic Hydrocarbons from the Pyrolysis of Model 1-Alkene Fuels

Eva Christine Caspary
Louisiana State University and Agricultural and Mechanical College

Recommended Citation

Caspary, Eva Christine, "The Formation of Polycyclic Aromatic Hydrocarbons from the Pyrolysis of Model 1-Alkene Fuels" (2017). *LSU Doctoral Dissertations*. 4443.
https://repository.lsu.edu/gradschool_dissertations/4443

THE FORMATION OF POLYCYCLIC AROMATIC HYDROCARBONS FROM THE PYROLYSIS OF MODEL 1-ALKENE FUELS

A Dissertation

Submitted to the Graduate Faculty of the
Louisiana State University and
Agricultural and Mechanical College
in partial fulfillment of the
requirements for the degree of
Doctor of Philosophy

in

The Cain Department of Chemical Engineering

by
Eva Christine Caspary
B.S. University of Applied Sciences Mannheim, Germany, 2010
May 2017

Acknowledgements

First and foremost, I would like to thank my Ph.D. advisor, Prof. Mary J. Wornat. This work and experience would not have been possible without her guidance and wisdom. Apart from teaching me the importance of good scientific work, she has taught me how to be a successful human being on this earth. I would like to thank Prof. Wornat, for her unwavering support, for always believing in me, and for giving me the chance to personally and professionally grow during this experience. I will be forever grateful for the time Prof. Wornat has given me and for the many lessons I have learned from her.

Furthermore, I would like to thank the members of my doctoral committee: Prof. Francisco Hung, Prof. Michael Benton, Prof. John Flake, and Prof. Revati Kumar. Their time and input were helpful to my research. I would like to gratefully acknowledge BASF SE for funding part of my research. I would also like to thank Prof. Werner Schmidt for providing reference standards and UV spectra and for the many pleasant and insightful personal exchanges.

I am very grateful to the amazing administrative staff here in the Department of Chemical Engineering, Darla, Danny, Rachel, and Frank, for helping on so many occasions and for putting a smile on my face. Furthermore, I would like to thank the workshop staff, Paul and Joe, for their invaluable input and help in countless situations. I also want to gratefully acknowledge the Graduate School for financial help through the Coates award for travel to national and international conferences. I gratefully acknowledge the Combustion Institute for partially funding the travel to present posters at the International Symposia in Warsaw, Poland and San Francisco.

The first colleague I would like to thank is Dr. Nimesh Poddar, who has not only helped me get started in the beginning of my doctoral studies, but who has been a constant stream of

support and knowledge during my time as a graduate student. I would not be in the position to write this dissertation if it were not for Nimesh's steady help and input. Above being a colleague, I consider Nimesh to be my brother, and am beyond grateful for all the time he has spent helping me become the person I am today. Furthermore, I want to thank the rest of my academic family, Dr. Venkateswaran Subramanian Kalpathy, Ms. Elizabeth Hurst, Ms. Catherine Poddar, Dr. Sean Bagley, and Mr. Karthik Vutukuru, for the invaluable scientific discussions and the many laughs and heartfelt conversations that made the lab feel like home. I also would like to mention, that I am grateful to Dr. Aubrey Heath for her friendship during our time here at LSU. I would like to thank Ms. Melissa Walsh for her love for LSU, which led me to apply for this graduate program in the first place, and for her constant support throughout this process.

I would like to thank my family for all the love and support they have given me from far away. To my mother, Mrs. Ursula Kern, who has shown me what it means to be a strong woman and to fight for what is right; I am eternally grateful for all of her sacrifices that enable me to have this life. To my papa, Mr. Siggi Schoehl-Kern, for steadily standing by my side and teaching me the importance of thoroughness. To my sister, Ms. Alena Caspary, whom I love dearly, for her unwavering support and understanding. To my parents-in-law, Mr. Michael Schwartz and Mrs. Elaine Schwartz, for their many prayers and their love. And finally, I would like to thank the love of my life, Mr. Matthew Schwartz, for supporting me in countless ways, for encouraging me to be the best version of myself, and for loving me even in the hardest times.

Table of Contents

List of Tables

List of Figures

Abstract

To understand the role of 1-alkenes and allylic radicals in the reaction pathways leading to the formation and growth of polycyclic aromatic hydrocarbons (PAH), pyrolysis experiments have been performed with three 1-alkene fuels—propylene ($CH_2{=}CH{-}CH_3$), 1-butene ($CH_2{=}CH{-}CH_2{-}CH_3$), and 1-pentene ($CH_2{=}CH{-}CH_2{-}CH_2{-}CH_3$)—at temperatures of 600 – 1000 °C and a fixed residence time of 0.31 s. The experiments are carried out in an isothermal laminar-flow quartz-tube reactor.

Analyses of the pyrolysis products by gas-chromatographic and high-pressure liquid-chromatographic techniques reveal that the three fuels differ in: 1) their conversion behavior, 2) the relative amounts of the major C_2 – C_4 species produced, and 3) the propensity for PAH formation. The propylene pyrolysis experiments reveal that propylene's conversion becomes significant at temperatures $\geq$ 850 °C, where acetylene, propadiene, and propyne are produced in high yields and allyl and propargyl radicals are abundantly available for aromatic-growth reactions. In contrast, pyrolysis experiments with 1-pentene show that 1-pentene's conversion is appreciable already above 600 °C, but that a large portion of the reacted carbon is "tied up" in 1-pentene's highest-yield product ethylene. High yields of acetylene, propylene, propadiene, propyne, 1-butene, and 1,3-butadiene, however, and the readily formed allyl, propargyl, and butadienyl radicals result in increased formation of PAH from 1-pentene pyrolysis compared to propylene pyrolysis.

The 1-butene pyrolysis experiments reveal that 1-butene's conversion becomes substantial above 700 °C and that between 750 and 900 °C, 1-butene produces C_2 – C_4 products in higher yields compared to propylene or 1-pentene pyrolysis. The abundantly produced allyl, propargyl, methylallyl, and butadienyl radicals from 1-butene pyrolysis prove to be very effective aromatic-formation and -growth agents. Consequently, PAH products from 1-butene pyrolysis are both higher in number—69 two- to seven-ring product PAH having been identified, 67 of which for the first time from this fuel—and higher in yield (by factors of 2 – 6) than from the pyrolysis of the other two 1-alkene fuels. The findings of this experimental study unveil the importance of the molecular fuel structure and the critical role of allylic radicals in the formation and growth of PAH from 1-alkenes during fuel pyrolysis.

Chapter I. Introduction

1.1. Background and Motivation

The combustion of solid fuels is a big part of everyday life and is contributing significantly to our energy demands. Coal, for example, delivers 43 % of the world's electricity generation and 28 % of the world's total energy generation, and it is the world's most widely used source of energy for power generation [1-4]. It is predicted that in 2040, coal will still make up almost a third of the total energy demand [2]. The combustion of biomass-fuels currently accounts for 15% of the world's energy demands [5], and with the growing population and economy of developing countries, which heavily rely on biomass-based fuels, this percentage is predicted to rise in the future [6].

During the combustion of solid fuels, unwanted by-products are formed, many of which are considered harmful to the environment and to the human body. One class of unwanted by-products are the polycyclic aromatic hydrocarbons (PAH) [7,8]. The combustion of a solid fuel takes place within a diffusion flame, where high temperatures and oxygen-deficient or fuel-rich conditions are present. Under these conditions, devolatilization of the solid fuel occurs and the fuel is broken down into smaller fragments. These fuel fragments can then participate in pyrolytic reactions to produce PAH. This class of compounds is known to be a major contributor to emissions of small particles. These small particles can be inhaled and stay in the bronchioles and alveoli of the lung and can cause serious health problems, such as lung and heart diseases [9,10]. Additionally, PAH are considered to be precursors to soot [11-13] and some PAH have been found to exhibit carcinogenic and/or mutagenic activity [15-17]. Several studies have reported the formation of PAH products from numerous solid fuels [18-24]. It is important to study the formation and growth of PAH, so that cleaner, more environmentally friendly solid combustion processes can be designed.

Within the diffusion flame of a solid fuel, devolatilization processes lead to the production of smaller *n*-alkanes and alkyl fragments, which undergo dehydrogenation reactions to form alkenes. High yields of alkenes, especially of 1-alkenes, have been observed in the thermal decomposition products from coal and biomass [25-32]. 1-Alkenes and their decomposition products can undergo pyrolytic reactions leading to the formation of one-ring aromatics and PAH.

The purpose of this study is to better understand the role of 1-alkenes in reaction pathways leading to the formation and growth of PAH from solid fuel combustion. Since the composition of solid fuels is rather complex, representative 1-alkene fuels are used to perform fundamental pyrolysis studies and the resulting aliphatic and aromatic products are extensively characterized. It is particularly important to perform isomer-specific characterization of the PAH products, since their biological activity is very dependent on the structure of the compound [33]. Additionally, the absence or the presence of certain isomers can provide vital insight into the reaction pathways responsible for the formation and growth of PAH.

When pyrolyzed, 1-alkene fuels with ≥ 3 carbons can readily produce allylic radicals [37-57,66-69], which can reach high concentrations due to their resonance stability. Therefore, pyrolysis experiments with model 1-alkene fuels ≥ 3 carbons can help improve the understanding of the role of allylic radicals as participants in aromatic-ring-growth reactions. To understand the formation and growth reactions of PAH it is important that the products of the 1-alkene pyrolysis experiments be meticulously and extensively characterized. Particularly, the isomer-specific characterization of PAH products can help provide important mechanistic insights in the reaction routes leading to the formation and growth of PAH. Furthermore, the investigation of 1-alkenes with different chain-lengths can help pinpoint fuel-specific differences in the formation reactions of PAH.

For the purpose of this study, we have chosen to conduct pyrolysis experiments with three different 1-alkenes: the C_3 alkene propylene, the C_4 alkene 1-butene, and the C_5 alkene 1-pentene. The molecular structures and relevant bond-dissociation energies [34,35] of the three fuels are depicted in Figure 1.1. All three selected model 1-alkene fuels have been reported to be among the thermal decomposition products of coal and biomass [25-32]. Figure 1.1 reveals, that propylene's easiest-to-break bond is its allylic C-H bond, which has a bond-dissociation energy of 88.2 kcal/mole [34]. Breakage of this bond will lead to the formation of the allyl radical during the primary decomposition reaction of propylene. The weakest bonds of 1-butene and 1-pentene are their respective allylic C-C bonds with bond-dissociation energies of 75.9 kcal/mole for 1-butene and 74.3 kcal/mole for 1-pentene [34]. Therefore, both 1-butene and 1-pentene will also primarily decompose to the allyl radical. Additionally, breaking the second-weakest bonds of 1-butene and 1-pentene, their allylic C-H bonds, will lead to the formation of methylallyl and ethylallyl radical, respectively. Therefore, pyrolysis experiments with the three selected model 1-alkene fuels could help to not only reveal important findings about the influence

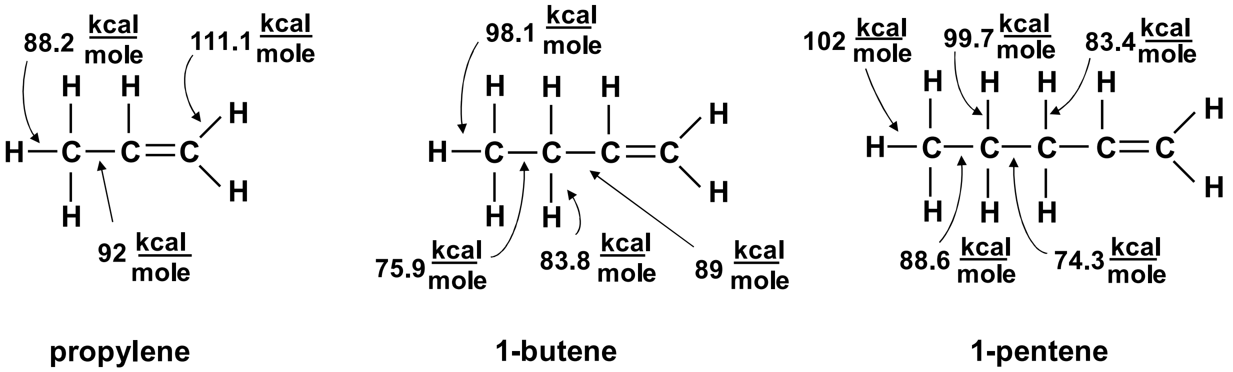

Figure 1.1. Molecular structures of propylene, 1-butene, and 1-pentene and relevant bond-dissociation energies [34,35].

of molecular fuel structure but also elucidate the role of the allyl, methylallyl, and ethylallyl radical in the formation and growth reactions of PAH. It is these questions that will be investigated in this experimental study.

1.2. Structure of Dissertation

The experimental methods and procedures of the pyrolysis experiments of the three fuels—propylene, 1-butene, and 1-pentene—are described in Chapter 2. The setup of the pyrolysis reactor, which consists of the gas delivery system, the reactor, and the product collection system, are presented and discussed in detail. Furthermore, the preparation of gas-phase and condensed-phase samples are explained. Finally, the analysis of the gas-phase products by gas chromatography with flame-ionization detection and thermal-conductivity detection, and the analysis of the condensed-phase products by gas-chromatography with flame-ionization detection and mass-spectrometric detection and by high-pressure liquid chromatography coupled with ultraviolet-visible spectrometric detection are described in Chapter 2.

The temperature-dependent yields of aliphatic and one-ring aromatic products from propylene pyrolysis, 1-butene pyrolysis, and 1-pentene pyrolysis are presented in Chapter 3. First, the conversion of the three investigated fuels is discussed, after which the yields of the aliphatic $C_1 – C_6$ hydrocarbon products are presented. The different decomposition reactions for propylene, 1-butene and 1-pentene pyrolysis are shown, along with formation reactions for the aliphatic products from each individual fuel. Then, the yields of one-ring aromatics are presented, and mechanistic implications for the formation of these products are discussed. At the end of Chapter 3, the temperature-dependent summed yields of aliphatic and one-ring aromatic products are shown and conclusions about the difference in these yield-trends for each investigated fuel are drawn.

The formation of PAH from propylene pyrolysis, 1-butene pyrolysis, and 1-pentene pyrolysis is discussed in Chapter 4. First, the summed yield of product PAH ≥ 2 rings from each pyrolysis set is shown and the findings from Chapter 3 are applied to explain the differences in the PAH yield for each individual fuel. Furthermore, the individually identified product PAH of the three pyrolysis sets at the highest investigated pyrolysis temperature, 1000 °C, are presented and fuel-specific differences are discussed. Finally, individual temperature-dependent yields of the quantified two- to seven-ring product PAH are presented, their formation reactions are discussed, and conclusions are drawn.

In the last chapter, Chapter 5, the present work is summarized and conclusions are drawn about the findings of this study, and recommendations for future work are given.

Chapter II. Experimental Methods and Procedures

2.1. Homogeneous Pyrolysis Reactor

The homogeneous pyrolysis reactor consists of a fuel delivery system, an isothermal quartz flow reactor, a Balston Teflon filter, and a product collection system. Figure 2.1. illustrates the scheme of the experimental setup of the pyrolysis experiments. Each of the components—the fuel delivery, the isothermal quartz flow reactor, and the product collection—are discussed in detail below.

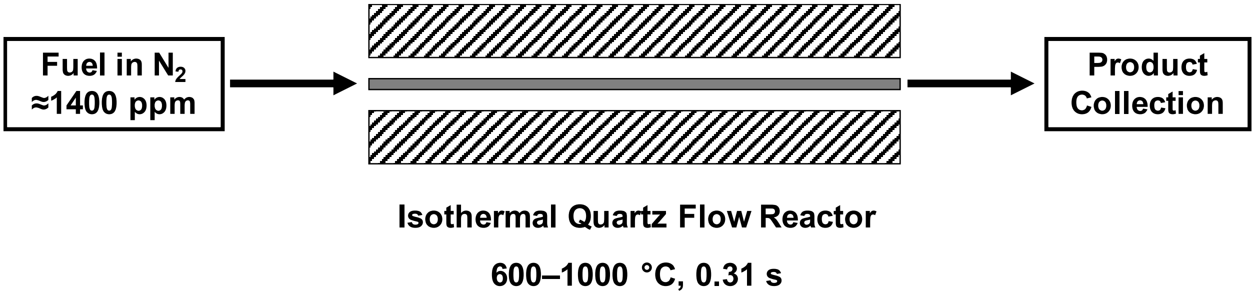

Figure 2.1. Reactor system for the pyrolysis experiments. Fuel concentrations are 1378 ppm for propylene, 1392 ppm for 1-butene, and 1410 ppm for 1-pentene.

2.1.1. Gas Delivery System

The three different gaseous alkene fuels, propylene, 1-butene, and 1-pentene, each come in a gas cylinder diluted in N_2. The concentrations of the fuels are 1378 ppm for propylene, which corresponds to a 0.413 mole-% carbon loading, 1392 ppm for 1-butene, corresponding to a carbon loading of 0.557 mole-%, and 1410 ppm for 1-pentene, equivalent to a 0.705 mole-% carbon loading of the reactor. For a given set of pyrolysis experiments, the respective fuel is being fed to the reactor by a mass flow controller. In front of the mass flow controller, a three-way valve is installed between the gas cylinder containing the feed gas and a gas cylinder containing ultra-high purity N_2. This setup allows the reactor to be flushed with pure nitrogen before and after each experimental run.

2.1.2. Reactor

The reactor consists of a quartz reactor tube, length 1.22 m, inner diameter, 2 mm, which is installed along the centerline of an electrically heated Lindberg/Blue M furnace. The furnace is controlled in three zones to ensure an isothermal temperature profile along the length of the reactor zone of 56 cm. At its respective ends the furnace is insulated with Moldatherm high-temperature ceramic-fiber plugs, and the quartz tube is kept at a temperature between 300 and 400 °C to ensure that there is no condensation of the fuel entering the reactor or the product mixture leaving the reactor. The furnace is calibrated in 50 °C increments at nine different temperatures ranging from 600 to 1000 °C. The calibration is carried out by measuring the temperature inside the reactor tube at every inch with a Type K thermocouple (Model: KMQXL-032U-40) and setting each of the three zones to the temperature that will result an isothermal temperature profile along the length of the reactor zone of 56 cm and a sharp drop in temperature before and after the reactor zone. The calibration for each reaction temperature can be found in Table A.1 in the Appendix. The fixed residence time of 0.31 s is achieved by setting the mass flow controller such that the flow through the reactor tube is 338 mL/min at reaction temperature. The reactor is designed such that it fulfills Lee's criteria [36] of idealized plug-flow at flows corresponding to residence times between 0.2 and 0.6 s. That means that upon exiting the reactor, a certain residence time can be attributed to the reaction products, and no corrections for mixing have to be applied. Before each experiment, the temperature inside of the reactor tube is measured along the centerline to verify the uniform calibration of the furnace. Furthermore, the flow rate setting of the mass flow controller is confirmed by attaching a bubble flow meter to the outlet of the reactor.

2.1.3. Product Collection

An experiment at each given reaction condition consists of three different runs: two runs to collect gas-phase products—one for the collection of $C_1 - C_6$ hydrocarbon products and one for the collection of product H_2—and a third run to collect the condensed-phase products, namely the one-ring aromatic products and product PAH ≥ 2 rings. The collection system for the condensed-phase products consists of a detachable quartz arm, in which the products are quenched to room temperature (quench time approximately 0.028 s) and are starting to condense, a Balston Teflon Filter, in which a portion of the lighter products and particles of solid carbon are collected, and a dichloromethane (DCM) solvent trap, where the majority of the condensed-phase products are collected. The collection of the gas-phase products also utilizes the quartz arm and the Balston Filter, but instead of a solvent bath, the system is connected to a Teflon gas sampling bag in which the gaseous product mixture is collected for analysis.

Prior to the collection of the gas-phase products at a given reaction condition, the product-gas mixture is allowed to bypass the gas sampling bag for 5 minutes, after which a two-way valve is turned so that the products are lead into the gas bag, where they are collected for 30 minutes. The products are then analyzed with gas chromatography and flame-ionization detection (GC/FID), for the $C_1 - C_6$ hydrocarbon products, or with gas chromatography and thermal conductivity detection (GC/TCD), for product H_2. The condensed-phase products are collected for 75 minutes in the DCM solvent bath, so as to obtain a high enough concentration of the products. After the sample of the liquid-phase product mixture is adequately prepared (as described below in Section 2.2), it is analyzed using gas chromatography and flame-ionization detection coupled with mass-spectrometric detection (GC/FID/MS), for the one- and two-ring aromatic products, and high-pressure liquid chromatography with ultraviolet-visible detection (HPLC/UV) for product PAH ≥ 2 rings.

2.2. Sample Preparation

2.2.1. Gas-Phase Products (C_1 – C_6 Hydrocarbons and H_2)

Immediately after the collection of gas-phase products, the gas sampling bag is connected to either the GC/FID, for analysis of C_1 – C_6 hydrocarbon products, or the GC/TCD, to measure product H_2. It is important that the time between collecting a gas-phase sample and analyzing it is kept both as short and as consistent as possible, to ensure that none of the heavier gas-phase products, such as benzene, partly condense in the gas bag. At each experimental condition, the product-gas mixture is also analyzed by a non-dispersive infrared detector (NDIR) to measure CO and CO_2. This is an effective additional step to ensure that the reactor system is leak-free, since there is no oxygen present in the fuel or the pyrolysis environment and therefore neither CO nor CO_2 can be products of the alkene pyrolysis experiments.

2.2.2. Condensed-Phase Products (Light Aromatics and PAH)

After the condensed-phase products are collected, the quartz arm and Balston filter are filled with DCM, sonicated for 5 minutes, and then thoroughly flushed with DCM to ensure that the entirety of the condensed-phase products is collected and dissolved in DCM. The product mixture is then filled into a Kuderna-Danish evaporator and concentrated to a volume of 10 ml. To analyze the one- and two-ring aromatic products 1 ml of the DCM/product mixture, representing 10% of the total volume and therefore 10% of the total amount of products, is transferred into a sample vial and analyzed on the GC/FID/MS. The remaining 90% are further concentrated until approximately 5 ml of the DCM/product mixture remain. This portion is used for analysis on the HPLC/UV. The liquid is solvent-exchanged under a nitrogen purge into dimethylsulfoxide (DMSO), a solvent that is compatible with the ones used as mobile phases in the HPLC analysis methods. The flow of the nitrogen is set such that is barely disturbs the surface of the DCM/product/DMSO mixture, so that the loss of one- and two-ring aromatic products due to evaporation is minimal. Because the more volatile one- and two-ring aromatic products are prone to evaporate during this process, these compounds are instead characterized from the 10% of the products shot on the GC/FID/MS.

2.3. Product Analysis

Of the products collected in the gas phase, the $C_1 - C_6$ hydrocarbon products are measured with GC/FID, while H_2 is measured using GC/TCD. Products in the condensed phase are measured with both GC/FID/MS and HPLC/UV. The more volatile one- and two-ring aromatics as well as some three-ring PAH—acenaphthylene, fluorene, phenanthrene, and anthracene—are analyzed by GC/FID/MS (the three-ring PAH are also analyzed using HPLC/UV.) PAH of three or more rings are not only less volatile but also have increasing numbers of isomers, which makes them optimal candidates for analysis by HPLC/UV. Since the UV spectrum is a fingerprint property of each individual PAH, HPLC/UV analysis enables us to isomer-specifically characterize the product PAH from our pyrolysis experiments. The analysis instruments and procedures for $C_1 - C_6$ hydrocarbon products, product H_2, light one- and two-ring aromatics, and product PAH are discussed in detail below.

For each fuel and each experimental condition, the carbon and hydrogen atoms of the unreacted fuel and the quantified products are summed up for the carbon-atom and hydrogen-atom balance, which is shown in Figure A.1 in the appendix. Figure A.1a shows, that at temperatures below 950 °C, the carbon-atom balances for propylene pyrolysis, 1-butene pyrolysis, and 1-butene pyrolysis is 97 % or higher. Only at the two highest temperatures, where solid carbon is observed in the reactor tube, is the carbon-atom balance below 97 %.

2.3.1. Analysis of Gas-Phase Products

2.3.1.1. $C_1 - C_6$ Hydrocarbon Products

The $C_1 - C_6$ hydrocarbon products are analyzed by an Agilent Model 6890/5973 gas chromatograph/flame-ionization detector (GC/FID). The product gases are separated using a GSGASPRO capillary column (Agilent J&W scientific) of length, 30 m, and inner diameter, 0.32 mm. The $C_1 - C_6$ products are separated using the following temperature program: hold at 35 °C for the first 2 min, then ramp at the rate of 5 °C/min for the next 13 min to 100 °C, followed by another ramp of 10 °C/min for the next 14 min to 240 °C, and finally a hold at 240 °C for 10 min. With the exception of vinylacetylene (C_4H_4) and cyclopentadiene (C_5H_6), the products are identified by matching their retention times and mass spectra to those of their respective reference standards. The flame-ionization detector is extensively calibrated for the $C_1 - C_6$ products with reference standards containing known concentrations of these products, and the resulting response factors are used to quantify the hydrocarbon products. The response factors are shown in Table A.2. Since there is no commercially available reference standard for cyclopentadiene, its identification is achieved by matching the product component's GC retention index with that of cyclopentadiene generated from the pyrolysis of dicyclopentadiene and by matching product component's mass spectrum with that of a reference standard in the NIST/EPA/NIH mass spectral library. Vinylacetylene is also identified by matching the product component's mass spectrum with that of a reference standard in the NIST/EPA/NIH mass spectral library.

2.3.1.2. Product H_2

H_2 is measured by an Agilent Model 6890 gas chromatograph/thermal-conductivity detector (GC/TCD). The product gases are separated on a HP plot Molsieve A capillary column (Agilent J&W scientific) of length, 25 m, and inner diameter, 0.53 mm. The temperature program used for the separation is as follows: hold at 35 °C for the first 20 min, then ramp at the rate of 5 °C/min for the next 30 min to 240 °C, and finally a hold at 240 °C for 50 min. The thermal-conductivity detector is calibrated by shooting known concentrations of H_2 onto the column. The response factor and elution time of H_2 on the GC/TCD are shown in Table A.2 in the Appendix.

2.3.1.3. CO and CO_2

Even though no CO or CO_2 is not formed during alkene pyrolysis, the gaseous products are analyzed for them to ensure that there are no leaks in the reactor system. The product sample is analyzed on two Horiba Model VIA-510 nondispersive infrared analyzers (NDIR), one for CO and one for CO_2. Before pumping the gas through the analyzers, a constant flow of ultra-high purity N_2 is led through the analyzers to equilibrate the NDIR.

2.3.2. Analysis of Condensed-Phase Products

2.3.2.1. Light Aromatics ≤ 2 Rings

As mentioned in Section 2.2.2., 10 % of the total amount of condensed-phase products (corresponding to a sample volume of 1 ml) are used for the analysis of lighter aromatic products up to three rings. The DCM/product mixture is analyzed on an Agilent Model 6890/5973 gas chromatograph/flame-ionization detector/mass spectrometer (GC/FID/MS). For FID analysis, 2 µl of sample are withdrawn and injected onto an HP-5MSi (Agilent J&W scientific) fused silica capillary column of 30 m length, 0.25 mm inner diameter, and 0.25 µm film thickness. Since the MSD is less sensitive than the FID, a larger sample volume of 10 µl is used for injection onto the mass detector. The FID and MSD analyses are performed during the same gas chromatographic run by consecutive injections of both samples onto their respective detectors. The product components are separated with the following temperature program: hold at 40 °C for the first 3 min, then ramp at the rate of 4 °C/min for the next 60 min to 280 °C, and finally a hold at 280 °C for 30 min. The one- to three-ring aromatics are identified by matching their GC elution times and mass spectra to those of reference standards. The two- and three-ring aromatics are additionally identified by matching their HPLC elution times and UV absorbance spectra with those of reference standards. The quantification of the products results from extensive calibration of the GC/FID by injecting known concentrations of reference standards onto the FID. These calibrations are presented in Table A.3.

2.3.2.2. PAH Products

The remaining 90 % of the DCM/product mixture is used to measure product PAH ≥ 3 rings by HPLC/UV analysis. Before any kind of analysis, the products are solvent-exchanged into 100 µl DMSO, a solvent that is compatible with all the mobile phases used in the HPLC method. The sample is then analyzed using a Hewlett-Packard Model 1050 chromatograph, coupled to a diode-array ultraviolet-visible absorbance detector (HPLC/UV). A sample volume of 25 µl is injected onto a Restek Pinnacle II PAH column (particle size, 4 µm; pore size, 110 Å; inner diameter, 4.6 mm; and length, 250 mm.) The PAH products are separated using a mobile flowrate of 1.4 ml/min with the following method of a time-programmed sequence of solvents: the method begins with 60:40 water:ACN; next, it ramps to pure ACN in 43 minutes; then ACN is isocratically held for 21 min; and finally it ramps to pure DCM in 43 min. After the products are separated, they pass through a UV diode-array detector, which simultaneously monitors five absorbance channels: 328–332 nm, 335–345 nm, 275–285 nm, 236–500 nm, and 190–520 nm. UV absorbance spectra, covering the range of 190–520 nm, are taken every 0.8 s at a resolution of 2 nm. Each individual PAH product's identity is established by matching its UV absorbance spectrum with a reference spectrum obtained from a reference standard of the compound or with a UV spectrum published in the literature. The major advantage of using UV absorbance detection for PAH analysis is that it allows for isomer-specific characterization of product PAH, since each PAH has a unique UV spectrum. Figure 2.2. shows the UV spectrum of a product component from 1-butene pyrolysis, in solid lines, that elutes at 42.2 minutes on our HPLC instrument and the UV spectrum of a reference standard of benzo[a]pyrene, in dashed lines, that also elutes at 42.2 minutes. It is apparent, that the UV spectrum of the product component matches very well with that of the reference standard. Furthermore, the retention time of the product component is

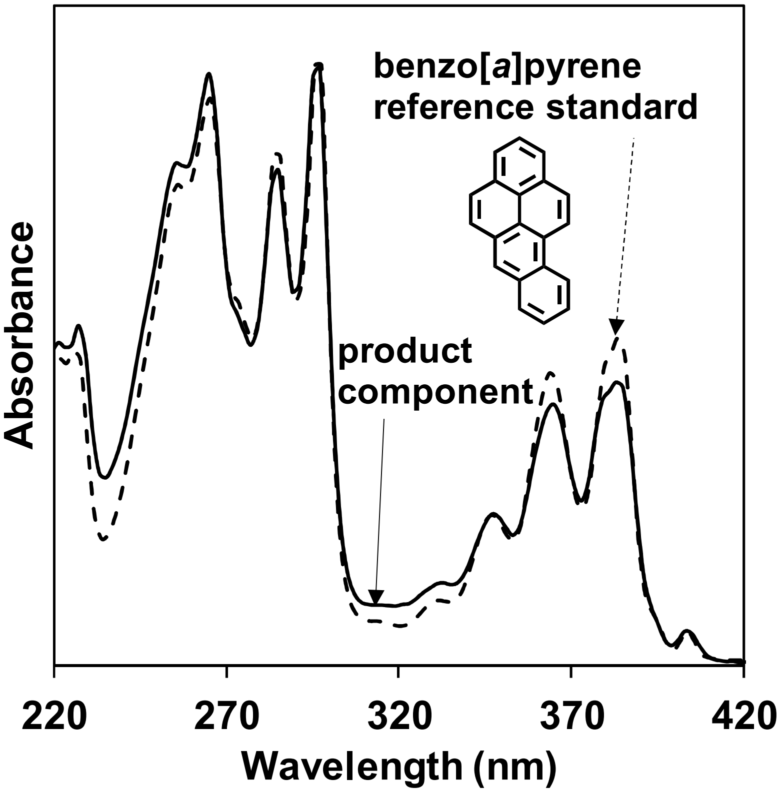

Figure 2.2. UV absorbance spectra of a pyrolysis-product component (solid line) and a reference standard of benzo[*a*]pyrene (dashed line).

identical to that of benzo[*a*]pyrene Therefore, the identity of the product component can be unequivocally determined as benzo[*a*]pyrene.

To quantify the product PAH, the instrument is calibrated with standard solutions of reference compounds at eight different concentrations ranging from 2.5 mg/l to 500 mg/l. Within this wide range of concentrations two different response factors, linear and non-linear, are determined for each given compound, and they are listed in Table A.4. It is not practical to calibrate our HPLC/UV instrument for all of the quantified PAH products, since some of the products do not have commercially available reference standards. In such cases, response factors of structurally similar compounds were used.

Chapter III. Aliphatic and One-Ring Aromatic Products from Propylene Pyrolysis, 1-Butene Pyrolysis, and 1-Pentene Pyrolysis

3.1. Fuel Conversion

Propylene pyrolysis, 1-butene pyrolysis, and 1-pentene pyrolysis experiments have been performed at nine temperatures between 600 and 1000 °C and at a fixed residence time of 0.31 s. To understand the decomposition behavior of the three different alkenes, we first look at the amount of unreacted fuel shown in Figure 3.1, where the amount is reported in % of the carbon fed to the reactor as carbon in the unreacted fuel exiting the reactor. The symbols represent the measured values obtained from the pyrolysis experiments: blue squares for unreacted propylene

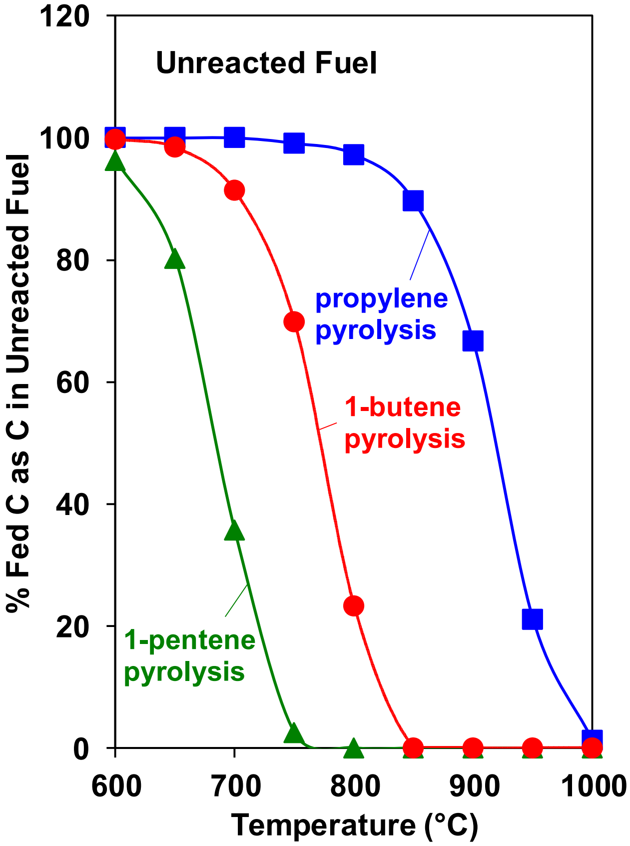

Figure 3.1. Yield, as function of temperature, of unreacted propylene from propylene pyrolysis (blue squares and curve), unreacted 1-butene from 1-butene pyrolysis (red circles and curve), and unreacted 1-pentene from 1-pentene pyrolysis (green triangles and curve) at 0.31 s.

from propylene pyrolysis, red circles for unreacted 1-butene from 1-butene pyrolysis, and green triangles for unreacted 1-pentene from 1-pentene pyrolysis.

Figure 3.1 reveals, that propylene is not very reactive at the lower pyrolysis temperatures. As the blue squares show in Figure 3.1, propylene is starting to react at 650 °C, however, it is only at temperatures above 850 °C, where propylene's conversion starts to become significant, and even at the highest investigated pyrolysis temperature, 1000 °C, a small fraction of the fuel remains unreacted. The reason for propylene needing relatively high temperatures for its decomposition is the bond-dissociation energy of propylene's easiest-to-break bond, shown in Figure 1.1. Propylene's weakest bond, the allylic C-H bond, requires 88.2 kcal/mole [34] to be broken into a hydrogen atom and the resonantly stabilized allyl radical. The allyl radical is also formed when the easiest-to-break bond of 1-butene, the allylic C-C bond, is broken. Figure 1.1 reveals that the bond-dissociation energy of this bond is 75.9 kcal/mole [34], which is significantly lower than that of propylene. This explains the much higher conversion of 1-butene at lower temperatures, as apparent from the red circles in Figure 3.1. At 700 °C, 1-butene's conversion is 9.7 % already and at 850 °C—where propylene's conversion only just reached 10.4 %—1-butene is almost completely (99.9 %) converted. 1-pentene is even more reactive than 1-butene is. The green triangles in Figure 3.1 show that already at 600 °C, only 96.3 % of the fed carbon is still accounted for by unreacted 1-pentene, corresponding to a fuel conversion of 3.7 % at the lowest investigated pyrolysis temperature. At 800 °C, 1-pentene's conversion is 99.9 % complete, while at the same temperature 1-butene's conversion is only 76.6%. The easiest-to-break-bond of 1-pentene is, just like for 1-butene, the allylic C-H bond, which has a bond-dissociation energy of 74.3 kcal/mole [34]. This value for 1-pentene is only 1.6 kcal/mole lower than that for 1-butene. Despite the similar bond-dissociation energies for these two alkene fuels, we have seen that 1-pentene is much more reactive than 1-butene. The reason for 1-pentene's higher reactivity is the composition of tits pyrolysis products. For example, Figure A.2 in the Appendix reveals that H_2 is produced during 1-pentene pyrolysis at temperatures 150 °C lower than during 1-butene pyrolysis and 200 °C lower than during propylene pyrolysis. This finding suggests, that there are more hydrogen atoms available at lower temperatures during 1-pentene pyrolysis compared to 1-butene or propylene pyrolysis and that these hydrogen atoms accelerate the 1-pentene decomposition reactions.

In the following section of this chapter we will investigate the decomposition reactions and formation of $C_1 – C_6$ aliphatic hydrocarbon products from each investigated fuel, and will pinpoint the pathways and products that contribute to the difference in conversion of the three fuels.

3.2. $C_1 – C_6$ Aliphatic Hydrocarbon Products

The temperature-dependent yields of the $C_1 – C_6$ aliphatic hydrocarbon products of propylene pyrolysis, 1-butene pyrolysis, and 1-pentene pyrolysis at 0.31 s are shown in Figures 3.2 – 3.5; where Figures 3.2 and 3.3 reveal the yields of the major $C_1 – C_5$ products, Figure 3.4 shows the yields of the minor $C_2 – C_6$ products, and Figure 3.5 depicts the yields of the trace $C_3 – C_5$ products of the three pyrolysis sets. To better compare the yields of products from different fuels, the yield of a given product is reported as % of the carbon fed to the reactor as carbon in the given product, and the different pyrolysis sets are color-coded as follows: blue circles and curves for product yields from propylene pyrolysis, red circles and curves for product yields from 1-butene pyrolysis, and green triangles and curves for product yields from 1-pentene pyrolysis. The major and minor $C_1 – C_6$ aliphatic hydrocarbon products of each fuel along with important decomposition and formation reactions are discussed in detail below.

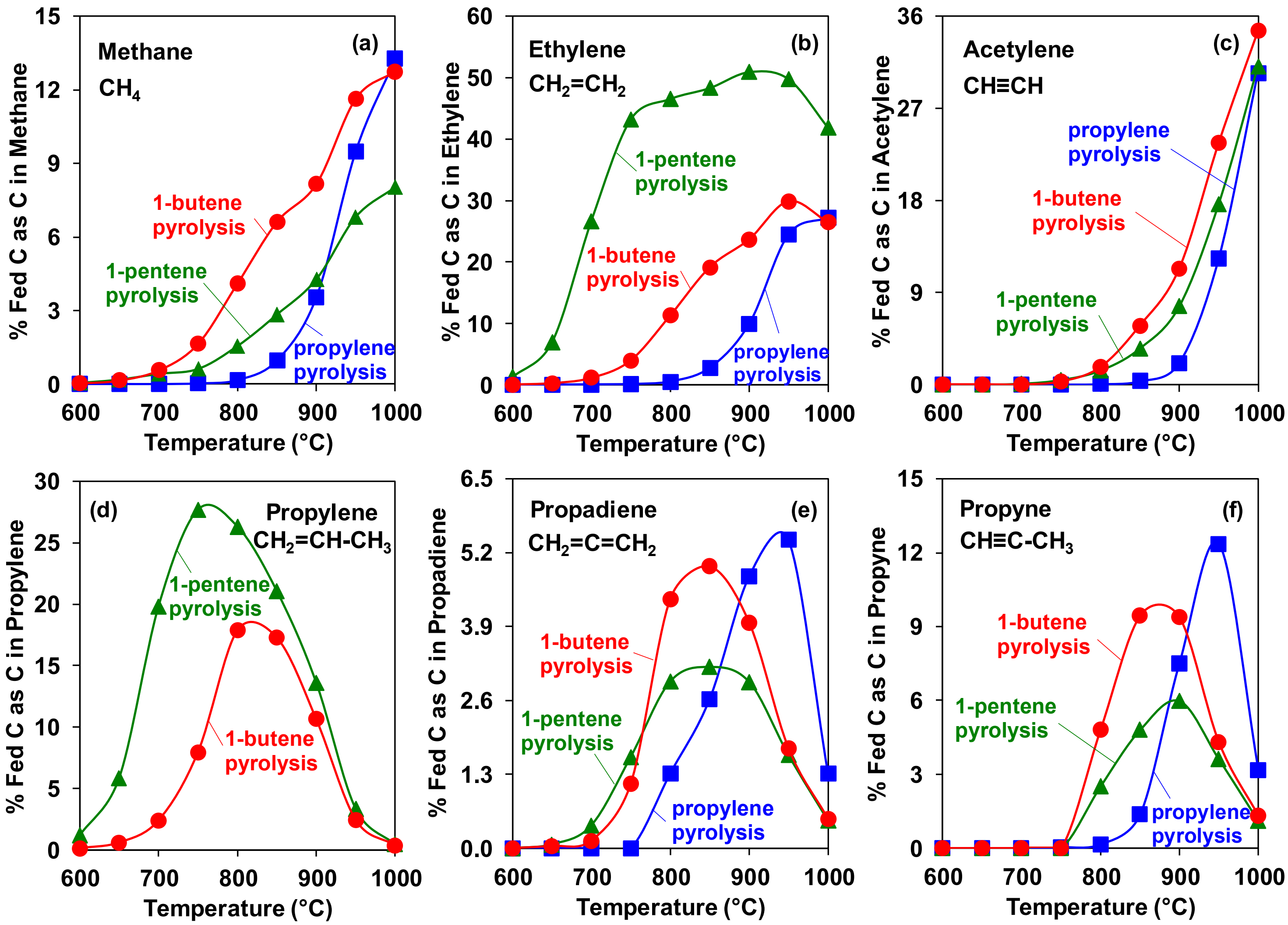

Figure 3.2. Yields, as functions of temperature, of the major $C_1 - C_3$ hydrocarbon products from propylene pyrolysis (blue squares and curves), 1-butene pyrolysis (red circles and curves), and 1-pentene pyrolysis (green triangles and curves), at 0.31 s: (a) methane, (b) ethylene, (c) acetylene, (d) propylene, (e) propadiene, and (f) propyne.

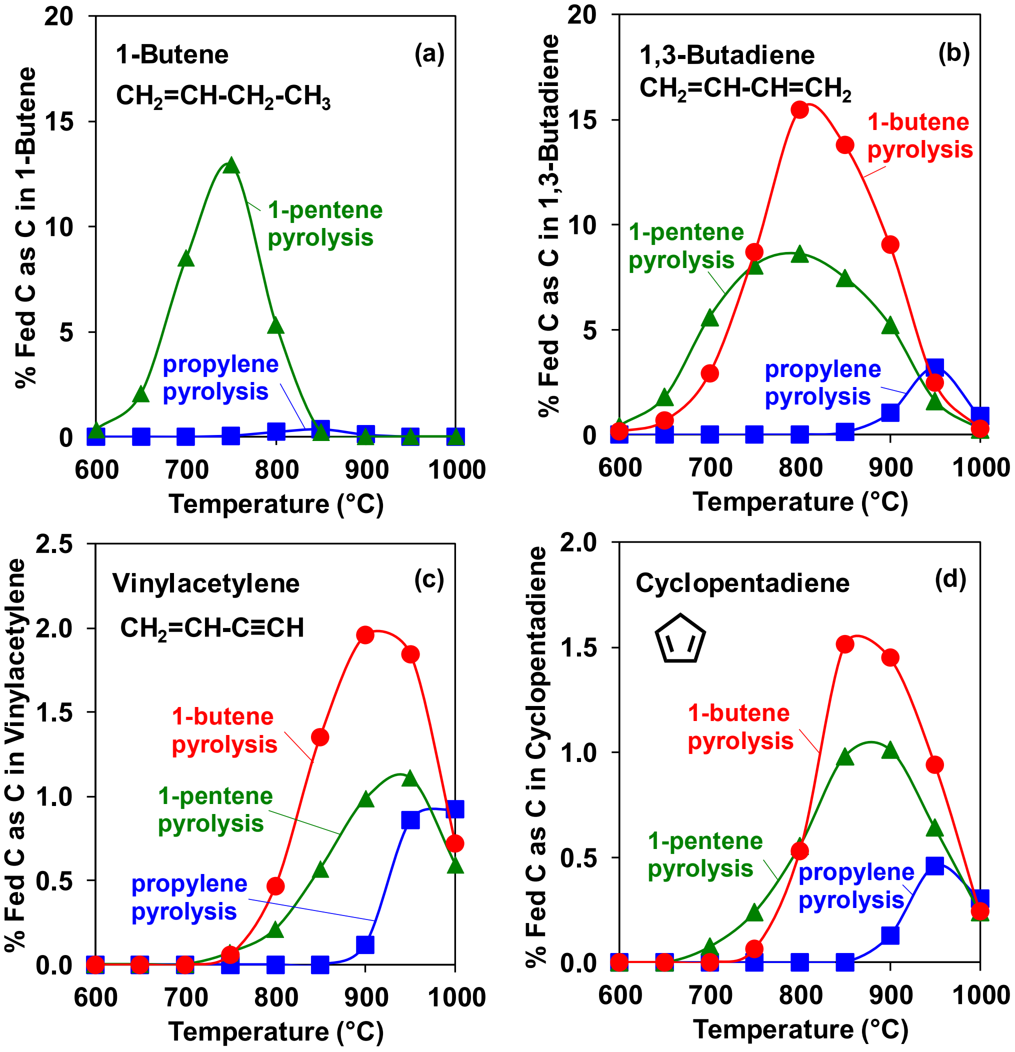

Figure 3.3. Yields, as functions of temperature, of the major C_4 and C_5 hydrocarbon products from propylene pyrolysis (blue squares and curves), 1-butene pyrolysis (red circles and curves), and 1-pentene pyrolysis (green triangles and curves) at 0.31 s: (a) 1-butene, (b) 1,3-butadiene, (c) vinylacetylene, and (d) cyclopentadiene.

3.2.1. Aliphatic Hydrocarbon Products of Propylene Pyrolysis

To investigate the aliphatic hydrocarbon products of propylene pyrolysis, we focus on the blue squares and curves of Figures 3.2 – 3.5. Propylene's major products are methane, ethylene, acetylene, propadiene, propyne, and 1,3-butadiene. As mentioned above in Chapter 3.1, the easiest-to-break bond of propylene is the allylic C-H bond, leading to the formation of a

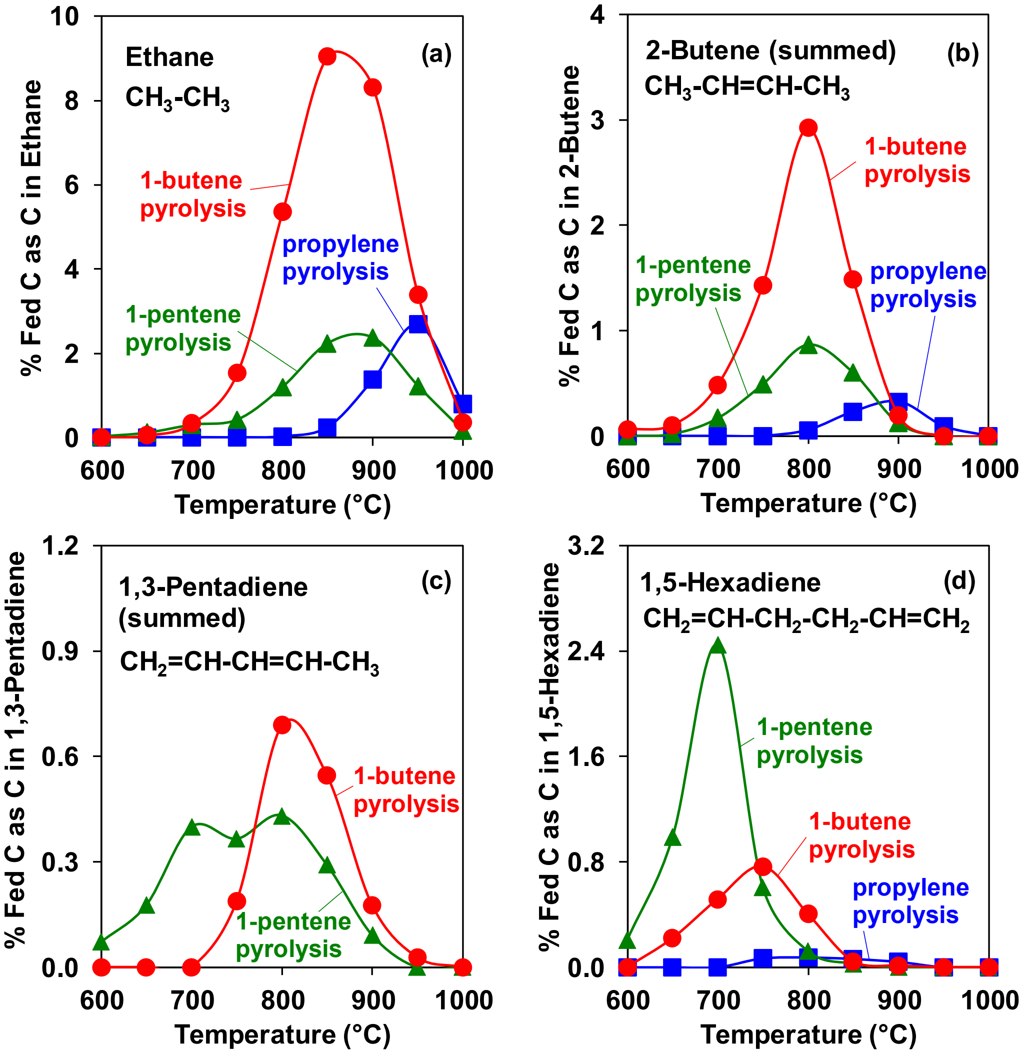

Figure 3.4. Yields, as functions of temperature, of minor C_2 – C_6 aliphatic hydrocarbon products from propylene pyrolysis (blue squares and curves), 1-butene pyrolysis (red circles and curves), and 1-pentene pyrolysis (green triangles and curves) at 0.31 s: (a) ethane, (b) summed yields of *cis*- and *trans*-2-butene, (c) summed yields of *cis*- and *trans*-1,3-pentadiene, and (d) 1,5-hexadiene.

hydrogen atom and the resonantly stabilized allyl radical, as shown in Reaction 1 [37-43]. The allyl radical can undergo hydrogen-atom loss to form propadiene, which is produced at temperatures above 750 °C, as Figure 3.2e illustrates. Propadiene then readily isomerizes to

$$\underset{\text{propylene}}{CH_2{=}CH{-}CH_3} \longrightarrow \underset{\text{allyl}}{CH_2{=}CH{-}\dot{C}H_2} + H \qquad (1)$$

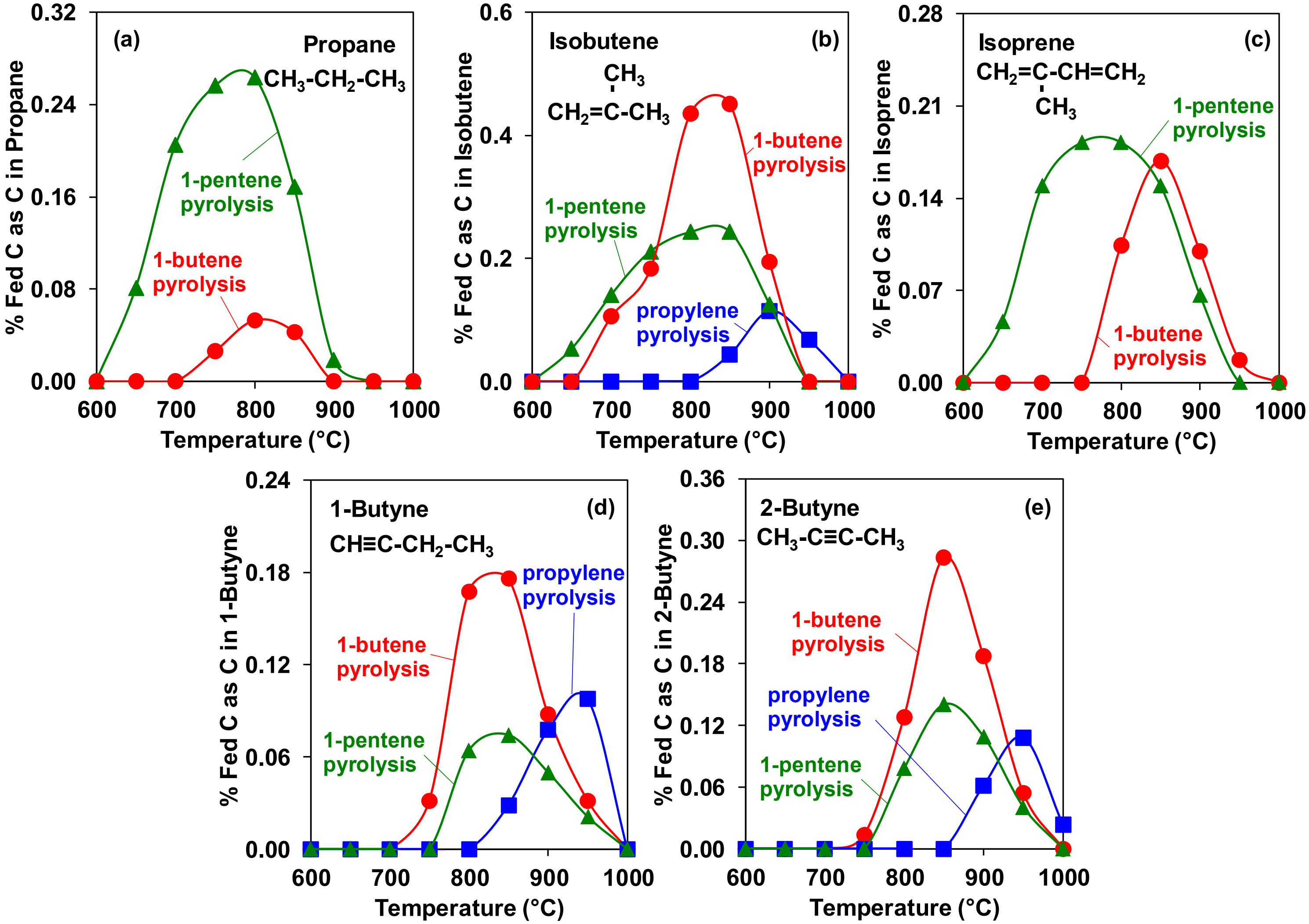

Figure 3.5. Yields, as functions of temperature, of trace $C_3 – C_5$ aliphatic hydrocarbon products from propylene pyrolysis (blue squares and curves), 1-butene pyrolysis (red circles and curves), and 1-pentene pyrolysis (green triangles and curves) at 0.31 s: (a) propane, (b) isobutene, (c) isoprene, (d) 1-butyne, and (e) 2-butyne.

propyne, whose yield is shown in Figure 3.2f. At ≥ 900 °C, more propyne than propadiene is produced. The yields of the two C_3H_4 isomers are increasing up to a temperature of 950 °C, after which they both decrease with a further increase in temperature. This observed behavior is due to the increased hydrogen-atom loss from propadiene and propyne to form another resonantly stabilized radical, the propargyl radical [44-54]. It has been previously shown that the propargyl radical plays an important role in aromatic ring-growth reactions [45-54,78]. Apart from forming the propargyl radical, propyne can also decompose to form methyl and acetylene [44,47,54]. The blue squares in Figure 3.2c reveal that indeed acetylene is a major product of propylene pyrolysis, whose yield keeps increasing with increasing pyrolysis temperature. Since acetylene's yield is much higher than that of propyne, there have to be additional pathways that contribute to the formation of acetylene. Another reaction that is important for the formation of acetylene is Reaction 2, the decomposition of propylene by breaking its vinylic C-C bond to form the vinyl and the methyl radical [37-43].

$$\underset{\text{propylene}}{CH_2{=}CH{-}CH_3} \longrightarrow \underset{\text{vinyl}}{CH_2{=}\dot{C}H} + \underset{\text{methyl}}{\dot{C}H_3} \qquad (2)$$

The addition of a hydrogen atom to methyl leads to the formation of methane, whose temperature-dependent yield is shown in Figure 3.2a. The vinyl radical can either lose a hydrogen atom and form acetylene [61,63-65], or it can gain a hydrogen atom and form ethylene, which is also a major product of propylene pyrolysis, as Figure 3.2b reveals. At the higher pyrolysis temperatures, ethylene can dehydrogenize and further contribute to the formation of acetylene. The recombination of two vinyl radicals leads to the formation of 1,3-butadiene. Figure 3.3b illustrates that the yield of 1,3-butadiene decreases between 950 and 1000 °C. Similar to propadiene and propyne, 1,3-butadiene can undergo hydrogen-atom loss at either its terminal or internal carbon atom, and form *n*-1,3-butadienyl and *i*-1,3-butadienyl radicals, respectively [54-60,62]. The *i*-1,3-butadienyl radical is resonantly stabilized, and it can play a major role in aromatic-ring-growth reactions, similar to other radicals with resonance stability that are available in the products. Both butadienyl radicals can undergo subsequent hydrogen-atom loss to form the C_4H_4 product vinylacetylene [62,63], which is formed at temperatures ≥ 900 °C, as shown in Figure 3.3c.

While not produced in very high yields, the C_5 product cyclopentadiene is important to mention since its relatively weak methylene C-H bond can easily be broken to produce the cyclopentadienyl radical. This radical is resonantly stabilized and therefore it can play an important role in aromatic-ring-growth reactions. Cyclopentadiene could be formed by the reaction of propargyl with ethylene, as shown in Reaction 3, and Figure 3.3d reveals that it is formed at temperatures above 850 °C and that its yield is increasing up to a temperature of 950 °C, after which it decreases with a further increase in temperature. Propargyl could also react with acetylene instead of with ethylene, which would lead to the direct formation of the cyclopentadienyl radical.

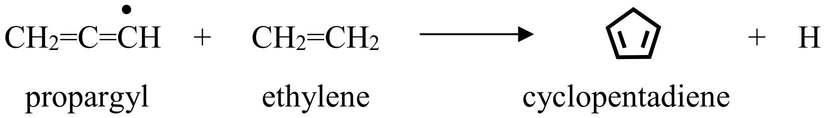

(3)

The recombination of methyl radicals leads to the formation of ethane, and the blue squares in Figure 3.4a reveal that propylene produces some ethane at temperatures above 800 °C. Ethane's yield reaches its peak at 950 °C, after which it decreases with a rise in temperature. Similar to ethane, 1,5-hexadiene is also formed from the recombination of two radicals, in this case two allyl radicals. Figure 3.4d shows that propylene produces minor amounts of 1,5-hexadiene at 750 – 900 °C, with its peak yield being at 800 °C. The 1,5-hexadiene that is formed readily decomposes to form two allyl radicals again. Other minor and trace products are 1- and 2-butene (shown in Figure 3.3a and 3.4b, respectively), isobutene (shown in Figure 3.5) and 1- and 2-butyne (shown in Figure 3.5d and 3.5e, respectively.)

As discussed in Section 3.1 above, 1-butene begins to react at lower temperatures than propylene, which is in part due to the lower bond-dissociation energy of 1-butene's easiest-to-break bond. In the following section we will discuss in detail the decomposition pathways of 1-butene pyrolysis and investigate additional reasons for 1-butene's higher conversion at lower temperatures compared to propylene.

3.2.2. Aliphatic Hydrocarbon Products of 1-Butene Pyrolysis

The red circles and curves of Figures 3.2. and 3.3 reveal that 1-butene's major products are methane, ethylene, acetylene, propylene, propadiene, propyne, and 1,3-butadiene. Similar to propylene, the first decomposition step of 1-butene leads to the formation of the allyl radical. Instead of allyl and H, however, 1-butene produces allyl and methyl, as shown in Reaction 4 [55-57]. This methyl radical can form methane by adding a hydrogen atom. Figure 3.2a reveals, that 1-butene produces methane at temperatures as low as 650 °C already, while propylene only does so at 800 °C. At temperatures between 600 and 950 °C, 1-butene produces more methane than propylene does. Only at the highest investigated temperature of 1000 °C is the methane yield from propylene pyrolysis slightly higher than that from 1-butene pyrolysis. The addition of a hydrogen atom to the allyl radical leads to the formation of propylene and Figure 3.2d shows that propylene's yield from 1-butene pyrolysis increases up to a temperature of 800 °C, after which it decreases with increasing temperature. By losing a hydrogen atom, allyl can form propadiene, and Figure 3.2e shows that propadiene is formed at temperatures as low as 650 °C and peaks in yield at 850 °C, after which propadiene's yield decreases with a further rise in temperature. Propadiene easily isomerizes to propyne, whose yield is shown in Figure 3.2f and which is produced in higher amounts than propadiene at temperatures between 850 °C and 1000 °C. As mentioned in Section 3.2.1, both of these C_3H_4 products are important sources of the resonantly stabilized propargyl radical [44-54], which is a vital participant in formation and growth reactions of aromatic products. It is important to note that these two C_3 compounds are formed at much lower temperatures from 1-butene pyrolysis compared to propylene pyrolysis, which suggests, that there is a larger amount of propargyl radicals available at lower temperatures from 1-butene pyrolysis than from propylene pyrolysis. It is only at temperatures of 900 °C and above, that propylene produces propadiene and propyne in higher yields than 1-butene does.

$$\underset{\text{1-butene}}{CH_2{=}CH\text{-}CH_2\text{-}CH_3} \longrightarrow \underset{\text{allyl}}{CH_2{=}CH\text{-}\overset{\bullet}{C}H_2} + \underset{\text{methyl}}{\overset{\bullet}{C}H_3} \qquad (4)$$

The second-weakest bond of 1-butene is its allylic C-H bond with a bond-dissociation energy of 83.8 kcal/mole [34]. This value is 4.4 kcal/mole lower than propylene’s weakest bond. Breaking 1-butene’s allylic C-H bond leads to Reaction 5, the formation of methylallyl and H [55-57]. The methylallyl radical is not formed in high amounts from propylene pyrolysis. Not only does the methylallyl radical increase the variety of abundant radicals in the 1-butene pyrolysis environment compared to propylene’s reaction environment, it is also a major source of the C_4 hydrocarbon product 1,3-butadiene. The methylallyl radical can form 1,3-butadiene by losing a hydrogen atom [55-58]. Figure 3.3b reveals that 1-butene produces a lot more 1,3-butadiene at

$$\underset{\text{1-butene}}{CH_2{=}CH\text{-}CH_2\text{-}CH_3} \longrightarrow \underset{\text{methylallyl}}{CH_2{=}CH\text{-}\overset{\bullet}{C}H\text{-}CH_3} + H \qquad (5)$$

temperatures below 950 °C than propylene does. Already at 600 °C some 1,3-butadiene is produced from 1-butene pyrolysis and at 800 °C, 15.5 % of the carbon fed to the reactor is accounted for by 1,3-butadiene. It is only at the two highest investigated temperatures, 950 and 1000 °C that propylene produces a slightly higher amount of 1,3-butadiene than 1-butene does. 1,3-butadiene readily loses a hydrogen atom to form either the *n*- or the *i*-butadienyl radical [54-60,62], both of which are participants in aromatic-ring-formation and -growth reactions. Furthermore, 1,3-butadiene can decompose according to Reaction 6 to form ethylene and vinyl [54-60,63,64].

$$\mathrm{H} + \underset{\text{1,3-butadiene}}{\mathrm{CH_2{=}CH{-}CH{=}CH_2}} \longrightarrow \underset{\text{ethylene}}{\mathrm{CH_2{=}CH_2}} + \underset{\text{vinyl}}{\overset{\bullet}{\mathrm{C}}\mathrm{H{=}CH_2}} \qquad (6)$$

Figure 3.2b shows that the yield of ethylene from 1-butene pyrolysis becomes significant at above 700 °C, and increases with increasing temperature up to 950 °C, where ethylene accounts for 29.9 % of the carbon fed to the reactor during 1-butene pyrolysis. The only temperature at which propylene pyrolysis produces more ethylene than 1-butene pyrolysis is 1000 °C, where ethylene's yield from 1-butene pyrolysis is 26.5 % of the fed carbon and ethylene's yield from propylene pyrolysis is 27.2 % of the fuel carbon. At higher temperatures, ethylene can dehydrogenize to form acetylene, whose yield is shown in Figure 3.2c. Acetylene production from 1-butene pyrolysis begins at 750 °C, becomes significant at 850 °C, and rapidly increases with rising temperature at 900 °C and above. Therefore, at 1000 °C, 34.6 % of the carbon fed to the reactor from 1-butene pyrolysis is accounted for by acetylene. The yield of acetylene is even higher than that of ethylene from 1-butene pyrolysis and therefore, dehydrogenation of ethylene cannot be the sole source of acetylene in the 1-butene reaction environment. Further ways acetylene is produced from 1-butene pyrolysis are, as previously mentioned in Section 3.2.1, hydrogen-atom loss from vinyl radicals [61,63-65] and decomposition of propyne to form acetylene and methyl [44,47,54]. At all investigated pyrolysis temperatures, 1-butene produces more acetylene than propylene does, which is an important finding since acetylene is known to play a key role in the formation and growth of aromatic products.

The C_4H_4 hydrocarbon vinylacetylene is a product of the dehydrogenation of butadienyl radicals [62,63], and its yield is shown in Figure 3.3c. Since 1-butene pyrolysis produces significantly more 1,3-butadiene than propylene does at temperatures < 950 °C, it makes sense that more vinylacetylene is produced from 1-butene pyrolysis than from propylene pyrolysis. Only at 1000 °C does propylene produce more vinylacetylene than 1-butene does. Another product important to mention is cyclopentadiene, whose yield is shown in Figure 3.3d. Hydrogen-atom loss of cyclopentadiene leads to the formation of the resonantly stabilized cyclopentadienyl radical, which can participate in aromatic-ring-formation reactions. As mentioned in Section 3.2.1, cyclopentadiene is formed through Reaction 3, propargyl addition to ethylene. Alternatively, if instead of ethylene the propargyl radical reacts with acetylene, the cyclopentadienyl radical is formed directly. Therefore, even if the yield of cyclopentadienyl is not very high, the cyclopentadienyl radical could still play an important role in the formation of aromatic products.

The minor products and trace products of 1-butene pyrolysis are shown in the red circles and curves in Figure 3.4 and 3.5. As Figure 3.4a shows, 1-butene produces ethane at temperatures > 600 °C, and ethane's yield is increasing with a rise in pyrolysis temperature up to 850 °C, ethane accounts for 9 % of the carbon fed to the reactor. Above 850 °C, ethane's yield is decreasing with increasing temperatures. Since ethane is formed from the recombination of two methyl radical and since 1-butene forms methyl radicals much more readily—primarily in Reaction 4—and at lower temperatures than propylene does, ethane's higher yield at lower temperatures from 1-butene pyrolysis is a logical result of the high availability of methyl radicals during 1-butene pyrolysis. At temperatures below 1000 °C, 1-butene produces up to 34 times more ethane than propylene does, indicating the higher abundance of methyl radicals in the 1-butene pyrolysis environment compared to the propylene pyrolysis environment. Another product that is produced in higher amounts and at lower temperatures from 1-butene compared to propylene is 2-butene, whose yield is shown in Figure 3.4b. 2-Butene can be formed by the recombination of a hydrogen atom with the resonance structure of the methylallyl radical. As mentioned in Section 3.2.1, 1,5-hexadiene is formed by recombination of two allyl radicals and since more allyl radicals are available at lower temperatures from 1-butene pyrolysis compared to propylene pyrolysis, more 1,5-hexadiene is formed from 1-butene than from propylene at temperatures below 850 °C, as shown in Figure 3.4d. A minor product that is not produced in measurable amounts from propylene pyrolysis is 1,3-pentadiene, which is a product of methyl reacting with the *i*-butadienyl radical. Figure 3.4c reveals, that 1,3-pentadiene's yield from 1-butene pyrolysis peaks at 800 °C, above which it decreases with increasing temperature.

In this section, we have learned that 1-butene pyrolysis produces high yields of C_2, C_3, and C_4 products, all of which are instrumental in the formation and growth reactions of one-ring aromatics and polycyclic aromatic hydrocarbons. Not only does 1-butene begin to react at much lower temperatures than propylene does, resulting in the availability of aromatic-growth agents at lower temperatures from 1-butene compared to propylene, 1-butene pyrolysis also leads to a more divers distribution of radicals and products—specifically C_4 species—compared to propylene pyrolysis. The latter finding suggests, that a larger number of reaction pathways can contribute to the formation and growth of aromatic products during 1-butene pyrolysis than during propylene pyrolysis. Therefore, we would expect that 1-butene pyrolysis leads to a higher yield of one-ring aromatic products and product PAH compared to propylene pyrolysis. In the following section we will examine the decomposition of the C_5 alkene 1-pentene and the formation of aliphatic hydrocarbon products from 1-pentene pyrolysis.

3.2.3. Aliphatic Hydrocarbon Products of 1-Pentene Pyrolysis

The green triangles and curves in Figures 3.2 and 3.3 reveal the yields of 1-pentene's major aliphatic hydrocarbon products. The major products of 1-pentene pyrolysis are ethylene, acetylene, propylene, propadiene, propyne, 1-butene, and 1,3-butadiene. Breaking 1-pentene's weakest bond, the allylic C-C bond, leads to the formation of allyl and ethyl radical, shown in Reaction 7 [66-69]. The allyl radical undergoes the same reactions as during propylene pyrolysis and 1-butene pyrolysis, mentioned in Section 3.2.1 and 3.2.2, respectively.

$$\underset{\text{1-pentene}}{CH_2{=}CH{-}CH_2{-}CH_2{-}CH_3} \longrightarrow \underset{\text{allyl}}{CH_2{=}CH{-}\overset{\bullet}{C}H_2} + \underset{\text{ethyl}}{\overset{\bullet}{C}H_2{-}CH_3} \qquad (7)$$

Addition of a hydrogen atom to the allyl radical leads to the formation of propylene, and since 1-pentene conversion is higher at lower temperatures compared to 1-butene conversion, more propylene is formed from 1-pentene pyrolysis than from 1-butene pyrolysis. Figure 3.2d reveals, that propylene is already formed during 1-pentene pyrolysis at 600 °C, and with increasing temperature, the yield of propylene rises. At 750 °C, propylene accounts for 27.7 % of the carbon fed to the reactor from 1-pentene pyrolysis, which is a factor of 3.5 times more than from 1-butene pyrolysis at the same temperature. Above 750 °C, the yield of propylene decreases with a further increase in temperature. However, at any investigated temperature 1-pentene produces more propylene than 1-butene does. The loss of a hydrogen atom from the allyl radical leads to the formation of propadiene, and the green triangles in Figure 3.4e reveal, that at temperatures of up to 750 °C, 1-pentene produces more propadiene than 1-butene or propylene does. At 800 and 850 °C, more propadiene is formed from 1-butene pyrolysis than from 1-pentene pyrolysis or propylene pyrolysis, and between 900 and 1000 °C, propylene produces more propadiene than 1-pentene or 1-butene does. As mentioned in the sections above, propyne is formed via isomerization of propadiene, and as Figure 3.2f reveals, 1-pentene forms propyne at temperatures above 750 °C. As we have learned in Section 3.2.1 and 3.2.1, hydrogen-atom loss of propadiene or propyne lead to the formation of propargyl [44-54].

The biggest difference in the primary decomposition reaction of 1-pentene compared to the other two investigated fuels is the formation of ethyl radical. This radical is very reactive and readily loses a hydrogen atom to form ethylene. It is apparent from Figure 3.2b that already at 600 °C, some ethylene is produced and that its yield is rapidly increasing up to 43 % of the fuel carbon at 750 °C, after which it is still increasing with increasing temperature, albeit not quite as drastically. At 900 °C, ethylene accounts for 51 % of the carbon fed to the reactor. Above 900 °C, ethylene's yields is decreasing with a further increase in temperature. However, even at the highest investigated pyrolysis temperature of 1000 °C, still 42 % of the carbon fed to the reactor is accounted for by ethylene. Ethylene is 1-pentene's highest-yield product at all investigated temperatures, and 1-pentene produces more ethylene than 1-butene or propylene does at any investigated temperature. The extremely high yields of ethylene from 1-pentene pyrolysis even at the higher temperatures render a large portion of the fuel carbon unavailable for aromatic-growth reactions. This finding would suggest, that the yields of aromatic products from 1-pentene pyrolysis might not be as high as they are from 1-butene pyrolysis. We will learn about the aromatic-formation and -growth behavior of our three fuels in the sections below.

Ethylene can dehydrogenate to form acetylene, and Figure 3.3c reveals that 1-pentene produces acetylene at temperatures of 700 °C and that acetylene's yield is rising with increasing temperature up to 1000 °C, where acetylene accounts for 31 % of the carbon fed to the reactor. Acetylene can also be formed from the decomposition of propyne [44,47,54] and the dehydrogenation of vinyl radical [61,63-65]. Between 800 and 1000 °C, 1-pentene produces up to 39 % less acetylene than 1-butene does.

Similar to the formation of methylallyl in Reaction 5 during 1-butene pyrolysis, the breaking of 1-pentene's allylic C-H bond leads to the formation of ethylallyl [67-69], as shown in Reaction 8. The ethylallyl radical, just like the methylallyl and allyl radical, has resonance stability, and it primarily decomposes according to Reaction 9, forming 1,3-butadiene and methyl radical [62].

$$\underset{\text{1-pentene}}{CH_2{=}CH\text{-}CH_2\text{-}CH_2\text{-}CH_3} \longrightarrow \underset{\text{ethylallyl}}{CH_2{=}CH\text{-}\overset{\bullet}{C}H\text{-}CH_2\text{-}CH_3} + H \tag{8}$$

$$\underset{\text{ethylallyl}}{CH_2{=}CH\text{-}\overset{\bullet}{C}H\text{-}CH_2\text{-}CH_3} \longrightarrow \underset{\text{1,3-butadiene}}{CH_2{=}CH\text{-}CH{=}CH_2} + \underset{\text{methyl}}{\overset{\bullet}{C}H_3} \tag{9}$$

The addition of a hydrogen atom to methyl leads to the formation of methane, and Figure 3.2a reveals that at all temperatures investigated, 1-pentene pyrolysis leads to the formation of less methane than 1-butene pyrolysis does, and that at temperatures higher than 900 °C, propylene produces more methane than 1-pentene does. The methyl radical can also recombine with allyl to form 1-butene, and Figure 3.3a reveals that 1-butene's yield from 1-pentene pyrolysis is increasing with increasing temperature up to 750 °C, where 13% of the fed carbon is accounted for by 1-butene. With a further increase in temperature, 1-butene is decomposing until 900 °C, where it is completely reacted. The decomposition of 1-butene is described in Section 3.2. The yield of 1,3-

butadiene from 1-pentene pyrolysis is shown in the green triangles in Figure 3.3b and we can see that at temperatures below 750 °C, 1-pentene produces more 1,3-butadiene than 1-butene or propylene does. Between 750 and 850 °C, 1-butene pyrolysis leads to the highest yield of 1,3-butadiene compared to 1-pentene pyrolysis and propylene pyrolysis. Only at the two highest temperatures does propylene produce more 1,3-butadiene than the two other investigated alkene fuels. As mentioned above, 1,3-butadiene can lose a hydrogen atom and form the *n*-butadienyl radical and the resonantly stabilized *i*-butadienyl radical [54-60,62]. Further dehydrogenation of 1,3-butadiene leads to the formation of the C_4H_4 hydrocarbon vinylacetylene [62,63], whose yield is shown in Figure 3.3c. 1,3-butadiene can also decompose to ethylene and vinyl according to Reaction 6 [54-60,63,64]. Figure 3.3d shows that cyclopentadiene is produced at lower temperatures from 1-pentene than from 1-butene or propylene, however at 800 °C and above, the yield of cyclopentadiene from 1-butene pyrolysis is higher than from 1-pentene pyrolysis.

The minor and trace products of 1-pentene pyrolysis are shown in the green triangles and curves in Figures 3.4 and 3.5. Figure 3.4a shows the yield of ethane and reveals that up to 900 °C, 1-pentene forms less ethane than 1-butene does, but more ethane than propylene does. Since ethane is formed from methyl/methyl recombination and methyl radicals are more readily available from 1-butene pyrolysis compared to 1-pentene pyrolysis, this trend in yield makes sense. Above 900 °C, ethane's yield from 1-pentene decreases with increasing temperature, which means that the ethane is dehydrogenating to ethylene. The summed yield of *cis*- and *trans*-1,3-pentadiene is shown in Figure 3.4c, and the green triangles reveal that 1-pentene forms small amounts of 1,3-pentadiene at 600 °C already. The two isomers of 1,3-pentadiene are formed from the loss of a hydrogen atom from the ethylallyl radical [68], which is formed in Reaction 8. As mentioned above, recombination of two allyl radicals leads to the formation of 1,5-hexadiene, and Figure 3.4d reveals, that at temperatures below 750 °C, 1-pentene produces up to 4.7 times more 1,5-hexadiene than 1-butene does. This finding can be attributed to the conversion of 1-pentene at much lower temperatures compared to 1-butene, which means that more allyl radicals are readily available from 1-pentene pyrolysis at lower temperatures than from 1-butene. 1,5-hexadiene primarily decomposes to form two allyl radicals again.

In this section we have learned that, while 1-pentene produces aliphatic products at temperatures lower than 1-butene or propylene does, the very high yield of ethylene make a large portion of 1-pentene's fuel carbon unavailable to participate in aromatic-ring-formation reactions. Apart from the carbon that is "trapped" in ethylene, 1-pentene produces high amounts of $C_2 - C_4$ compounds, many of which are effective aromatic-growth agents. We have further found that the 1-pentene reaction environment is rich in allyl, propargyl, methylallyl, butadienyl, and ethylallyl radicals, which play an important role in aromatic-growth-reactions. In the following section, we will investigate the formation of one-ring aromatic products from the three investigated 1-alkene fuels.

3.3. One-Ring Aromatic Products

The yields of one-ring aromatic products from propylene pyrolysis, 1-butene pyrolysis, and 1-pentene pyrolysis are revealed in Figure 3.6. The blue squares in Figure 3.6a show that propylene pyrolysis forms benzene at temperatures ≥ 900 °C, and that benzene's yield is increasing with increasing temperatures until at 1000 °C, 11.7 % of the carbon fed to the reactor from propylene pyrolysis is accounted for by benzene. Benzene formation starts at much lower temperatures from 1-butene pyrolysis compared to propylene pyrolysis. The red circles in Figure 3.6a reveal that 1-butene forms benzene at 750 °C, above which benzene's yield is increasing with rising temperature up to 950 °C. At these temperatures, 1-butene produces more benzene than

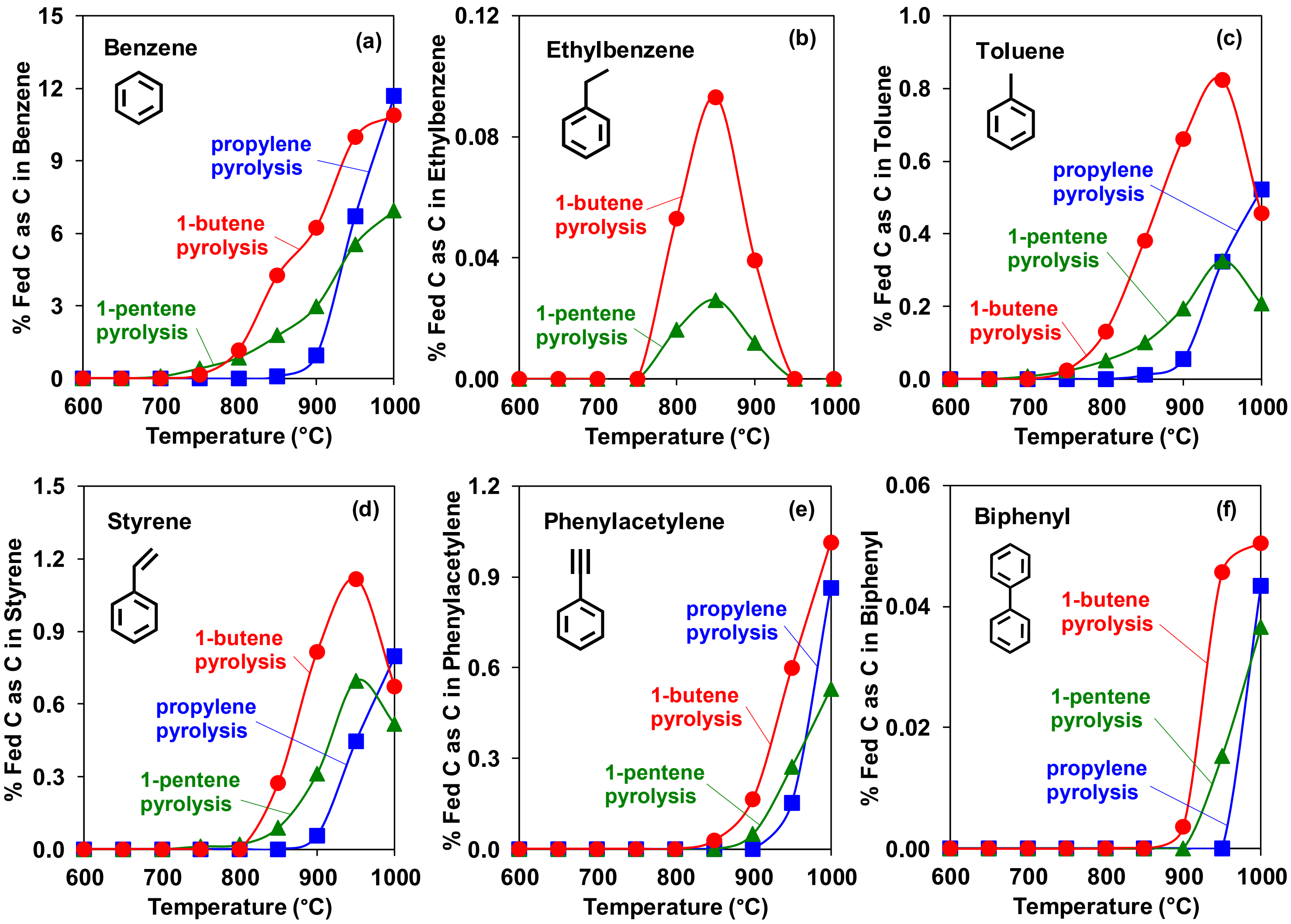

Figure 3.6. Yields, as functions of temperature, of one-ring aromatic products and biphenyl from propylene pyrolysis (blue squares and curves), 1-butene pyrolysis (red circles and curves), and 1-pentene pyrolysis (green triangles and curves) at 0.31 s: (a) benzene, (b) ethylbenzene, (c) toluene, (d) styrene, (e) phenylacetylene, and (f) biphenyl

propylene does. It is only at 1000 °C, when the rise in benzene's yield tapers off during 1-butene pyrolysis, that propylene produces more benzene than 1-butene does. 1-Pentene pyrolysis leads to benzene formation at even lower temperatures than 1-butene pyrolysis, as shown by the green triangles in Figure 3.6a. Already at 700 °C, a small amount of benzene is formed from 1-pentene pyrolysis, and with increasing temperature, benzene's yield is increasing. However, the yield of benzene is not increasing as steeply from 1-pentene pyrolysis compared to 1-butene pyrolysis or propylene pyrolysis. Hence that at 800 °C, more benzene is formed from 1-butene pyrolysis compared to 1-pentene pyrolysis, and at 950 °C, more benzene is formed from both 1-butene pyrolysis and propylene pyrolysis than it is from 1-pentene pyrolysis.

Four different reactions are responsible for the formation of benzene: propargyl/propargyl recombination [52], shown in Reaction 10, cross-reaction of propargyl radicals and allyl radicals [71-75], shown in Reaction 11, and reaction of acetylene with either the *n*-butadiene [60,75] or the *i*-butadiene radical [60,76], shown in Reaction 12 and Reaction 13, respectively. All three alkene pyrolysis systems produce plenty of allyl and propargyl radicals, although both 1-butene and 1-pentene form them at lower temperatures than propylene does. Therefore, Reactions 10 and 11 are prevalent in all three pyrolysis reaction environments. Since both 1-butene and 1-pentene produce significantly more 1,3-butadiene than propylene does, Reactions 12 and 13 are furthermore contributing to the formation of benzene during 1-butene pyrolysis and 1-pentene

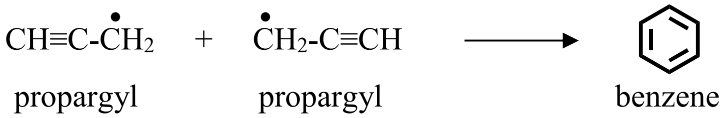
$$CH{\equiv}C\text{-}\overset{\bullet}{C}H_2 + \overset{\bullet}{C}H_2\text{-}C{\equiv}CH \longrightarrow \tag{10}$$

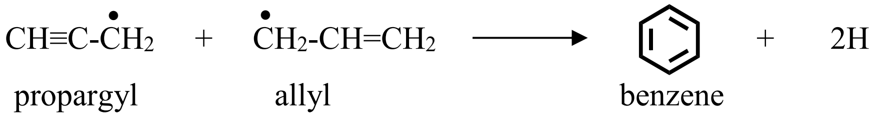
$$CH{\equiv}C\text{-}\overset{\bullet}{C}H_2 + \overset{\bullet}{C}H_2\text{-}CH{=}CH_2 \longrightarrow \quad + \quad 2H \tag{11}$$

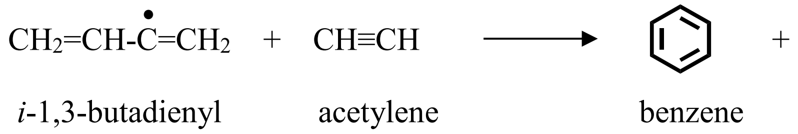

(12)

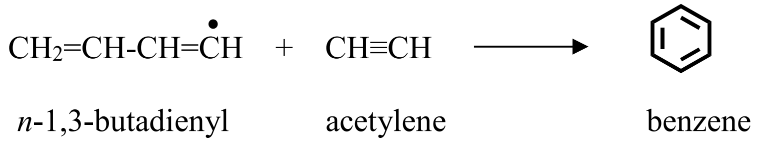

(13)

pyrolysis, while they do not play as a large of a role in the propylene pyrolysis environment. Due to the relatively high bond-dissociation energy of the aryl C-H bonds of benzene, the abstraction of a hydrogen atom to form a phenyl radical [70] requires higher reaction temperatures, which means that benzene is not very reactive at lower temperatures. Benzene's stability becomes evident when looking at Figure 3.6f, which shows that biphenyl's yields become significant only at temperatures > 900 °C, where phenyl becomes available and can react with benzene to form biphenyl.

At temperatures above 900 °C, reaction of phenyl with methyl (Reaction 14), vinyl, and acetylene lead to the formation of toluene, styrene, and phenylacetylene [78], whose temperature-dependent yields are shown in Figures 3.6c-e. We can see that benzene's yields are about an order of magnitude higher than the substituted one-ring aromatics, with the exception of the low-yield product ethylbenzene shown in Figure 3.6b. The substituted one-ring aromatics are more reactive than benzene, especially toluene, whose methyl C-H bond can much more easily be broken to lose a hydrogen atom and form the resonantly stabilized benzyl radical. Benzyl can react with methyl and form ethylbenzene. Figure 3.6c reveals, that toluene formation begins at 750 °C from 1-butene

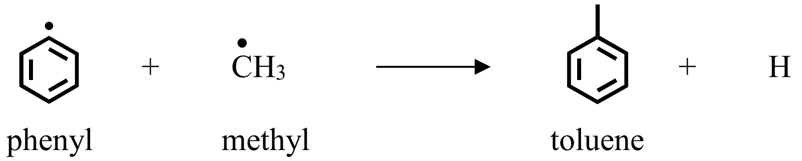

(14)

pyrolysis, as shown by the red circles, and at 700 °C from 1-pentene pyrolysis, as shown by the green triangles. At these temperatures, the phenyl radical is not yet readily available for reaction, which means that there has to be another source of toluene. Reaction 15 shows, that propargyl can react with 1,3-butadiene to form toluene. Furthermore, toluene can be formed from allyl/methylallyl combination [79]. As we have previously established, both

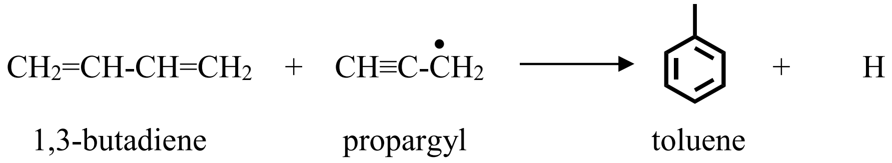

(15)

1,3-butadiene and C_3H_4 products are more abundant from 1-butene pyrolysis at temperatures above 750 °C. Therefore, it makes sense that more toluene is formed from 1-butene pyrolysis compared to 1-pentene pyrolysis, as is revealed in Figure 3.6c. The yield of toluene peaks at 950 °C for both 1-butene and 1-pentene pyrolysis and decreases with a further increase in temperature. This indicates that in both reaction systems, more toluene is "used up" by undergoing hydrogen-atom loss and forming the resonantly stabilized benzyl radical, which then can participate in the formation- and growth-reactions of PAH. In contrast, the blue squares in Figure 3.6c show that the yield of toluene from propylene pyrolysis is still increasing up to a temperature of 1000 °C.

If vinylacetylene reacts with *i*-butadienyl, styrene is formed, as shown in Reaction 16. Furthermore, the cyclopentadienyl radical can react with propargyl to from styrene, which is shown in Reaction 17 [60]. The blue squares of Figure 3.6d show, that propylene

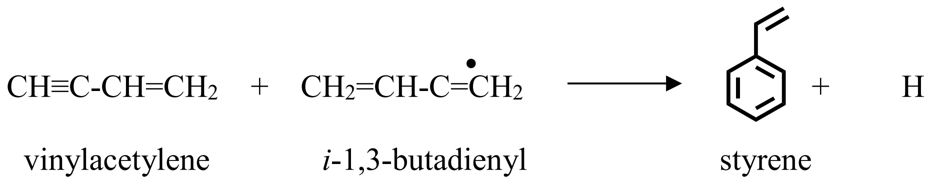

(16)

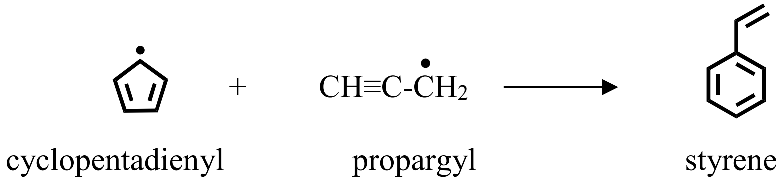

(17)

forms styrene at temperatures ≥ 900 °C, and that the yield of styrene is rising with increasing temperature, until at 1000 °C, styrene accounts for 0.8 % of the carbon fed to the reactor from propylene pyrolysis. 1-butene produces styrene at temperatures ≥ 850 °C, as shown by the red circles in Figure 3.6d, and styrene's yield is rising up to 1.1 % of the fed carbon at 950 °C, above which it decreases, indicating that more styrene is reacting than it is formed. At 1000 °C, propylene pyrolysis leads to a higher yield of styrene than 1-butene pyrolysis does. The green triangles in Figure 3.6d reveal that styrene formation from 1-pentene pyrolysis begins at 800 °C, which is 50 °C lower than for 1-butene pyrolysis; however, between 850 and 1000 °C, 1-butene produces up to 3 times more styrene than 1-pentene does. Analogous to the formation of acetylene from the dehydrogenation of ethylene, phenylacetylene can be formed from the dehydrogenation of styrene. Phenylacetylene's yields are shown in Figure 3.6e, which shows that more phenylacetylene is formed from 1-butene pyrolysis compared to propylene pyrolysis and 1-pentene pyrolysis at temperatures between 850 and 1000 °C.

3.4. Aliphatic and One-Ring Aromatic Products

In this chapter, we have discussed the key reactions for the decomposition of the three investigated pyrolysis fuels—propylene, 1-butene, and 1-pentene—and the formation of aliphatic and one-ring aromatic products. Figures 3.7a and 3.7b reveal the sum of the C_1 – C_6 aliphatic products and one-ring aromatic products, respectively. The different pyrolysis sets are presented in the same colors and symbols as in previous figures: blue squares and curves for propylene

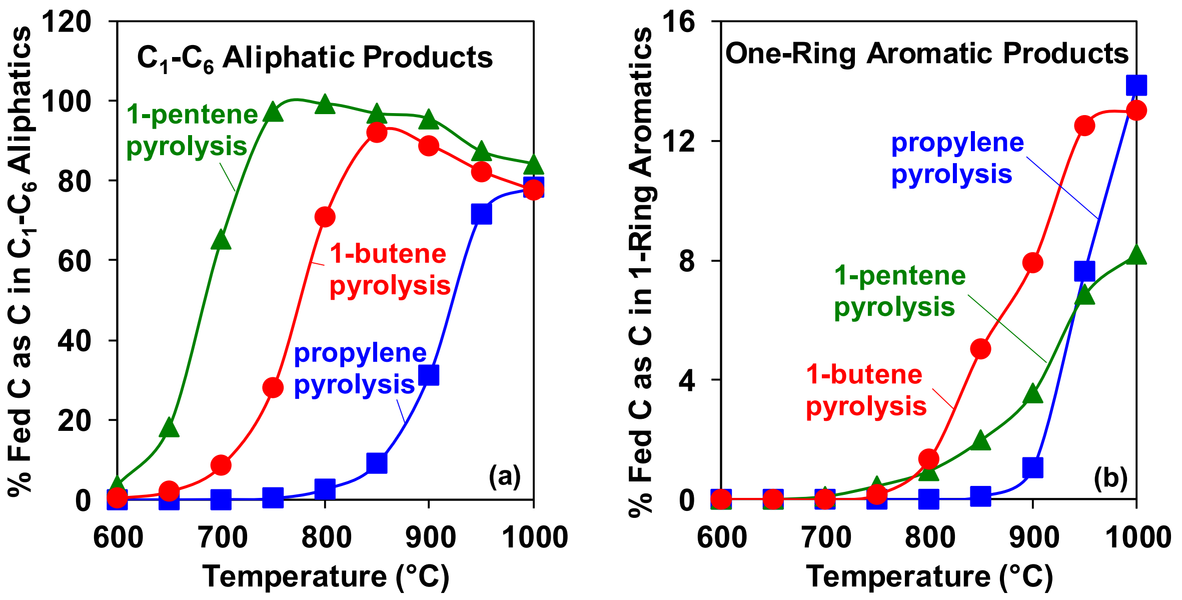

Figure 3.7. Yields, as functions of temperature, of classes of products from propylene pyrolysis (blue squares and curves), 1-butene pyrolysis (red circles and curves), and 1-pentene pyrolysis (green triangles and curves) at 0.31 s: (a) $C_1 - C_6$ aliphatic products and (b) one-ring aromatic products.

pyrolysis, red circles and curves for 1-butene pyrolysis, and green triangles and curves for 1-pentene pyrolysis.

We have established in Section 3.1 that propylene conversion begins at higher temperatures than 1-butene and 1-pentene conversion does. Therefore, the $C_1 - C_6$ aliphatic products are formed at higher temperatures from propylene pyrolysis compared to 1-butene or 1-pentene pyrolysis. Figure 3.7a shows, that the summed yield of aliphatic products from propylene produces becomes significant at temperatures above 800 °C and that it rapidly increases between 850 and 950 °C, above which it tapers off, so that at 1000 °C, $C_1 - C_6$ aliphatic hydrocarbon products account for 78.3 % of the carbon fed to the reactor during propylene pyrolysis. As we have learned in Section 3.2.1, propylene pyrolysis leads to the formation of large amounts of acetylene, a compound that is known to play a major role in formation- and growth-reactions of aromatic products. Furthermore, high yields of the two C_3H_4 isomers propadiene and propyne are produced during propylene pyrolysis, which provide ample amounts of the resonantly stabilized propargyl radical. The propylene pyrolysis environment is furthermore rich in allyl radicals and also contains butadienyl and cyclopentadienyl radicals, all of which are important participants in the formation of one-ring aromatic products, as we have established in Section 3.3. The conversion of the C_4 alkene 1-butene begins at temperatures much lower than that of propylene, and consequently, 1-butene pyrolysis leads to the formation of C_1 – C_6 aliphatic hydrocarbon products at lower temperatures than propylene pyrolysis does, as is depicted in Figure 3.7a. The yield of aliphatic products from 1-butene pyrolysis becomes significant at temperatures above 650 °C, and increases with increasing temperature up to 850 °C, at which 92 % of the carbon fed to the reactor is accounted for by C_1 – C_6 aliphatic hydrocarbons. With a further increase in temperature, the yield of aliphatic products decreases up to 1000 °C, where it accounts for 77.6 % of the carbon fed to the reactor during 1-butene pyrolysis. Since 1-butene produces acetylene and the C_3 products propylene, propadiene, and propyne in higher yields at lower temperatures than propylene does, they are available for reactions leading to aromatic products at lower temperatures compared to propylene pyrolysis. Additionally, as we have learned in Section 3.2.2, 1-butene pyrolysis leads to the formation of large amounts of 1,3-butadiene, which means that a lot more butadienyl radicals are available for ring-growth reactions. Furthermore, the formation of methylallyl radicals during the decomposition of 1-butene increases the variety of the radical pool in 1-butene pyrolysis compared to propylene pyrolysis. The green triangles in Figure 3.7a show that 1-pentene produces aliphatic products at 600 °C already, and that the summed yield of aliphatic products increases up to a temperature of 800 °C, where 99.3 % of the carbon fed to the reaction from 1-pentene pyrolysis is made up of C_1 – C_6 hydrocarbon products. Above 800 °C, the yield of aliphatic products is only slightly decreasing up to 1000 °C, where still 84.3 % of the fed carbon is accounted for by aliphatic products. The majority of this sum is made up of 1-pentene's highest-yield product ethylene, which "traps" a large portion of the carbon, making it unavailable to participate in reactions leading to the formation and growth of aromatic products. The carbon that is not tied up in ethylene is made up of acetylene and C_3 and C_4 species, which are key players in aromatic-growth reactions. Furthermore, ethyl and ethylallyl radicals are available in much higher amounts during 1-pentene pyrolysis compared to 1-butene or propylene pyrolysis.

While 1-pentene produces one-ring aromatic products at lower temperatures than 1-butene or propylene does, the yield of one-ring aromatics from 1-pentene pyrolysis does not increase as rapidly with increasing temperature compared to 1-butene or propylene pyrolysis, as the green triangles in Figure 3.7b reveal. Therefore, once the temperature reaches 800 °C, the yield of aliphatic products from 1-butene pyrolysis, as shown by the red circles in Figure 3.7b, is higher than from 1-pentene pyrolysis. At temperatures ≥ 800 °C, 1-butene produces up to 2.5 times more one-ring aromatic products than 1-pentene does. As is illustrated by the blue squares in Figure 3.7b, formation of the one-ring aromatic products from propylene becomes appreciable only above 900 °C and it is only 1000 °C, that propylene produces a slightly higher amount of one-ring aromatics than 1-butene does and a significantly higher amount than 1-pentene does. Especially noteworthy is the finding that between 800 and 950 °C, 1-butene produces more substituted one-ring aromatics compared to either 1-pentene or propylene pyrolysis, since the substituted one-ring aromatics are more susceptible to lose a hydrogen atom and participate in aromatic-ring-growth reactions.

Chapter IV. Polycyclic Aromatic Hydrocarbons from Propylene Pyrolysis, 1-Butene Pyrolysis, and 1-Pentene Pyrolysis

4.1. PAH Products from the Three Pyrolysis Sets

The three investigated alkene fuels—propylene, 1-butene, and 1-pentene—have been pyrolyzed at nine temperatures between 600 and 1000 °C at a fixed residence time of 0.31 s, and the condensed-phase products have been analyzed by GC/FID/MS, for the one- and two-ring aromatic products, and by HPLC/UV, for two-ring aromatic products and higher-ring-number PAH products. The sum of the individual temperature-dependent PAH-product yields from each fuel are presented in Figure 4.1, using the same color coding as in Chapter 3: blue squares for

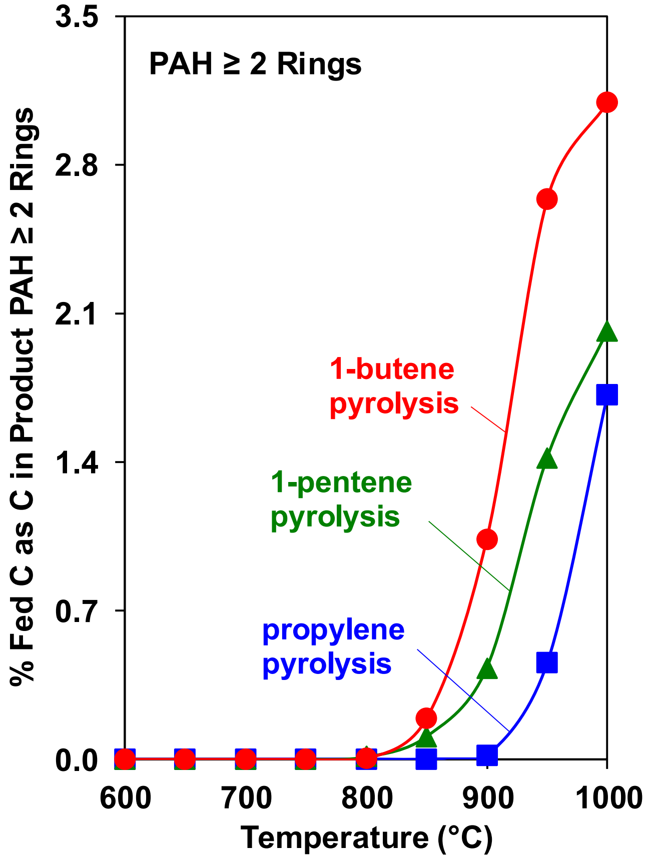

Figure 4.1. Yield, as function of temperature, of product PAH ≥ 2 rings from propylene pyrolysis (blue squares and curve), 1-butene pyrolysis (red circles and curve), and 1-pentene pyrolysis (green triangles and curve) at 0.31 s.

yields from propylene pyrolysis, red circles for yields from 1-butene pyrolysis, and green triangles for yields from 1-pentene pyrolysis.

Of all three investigated alkene fuels, propylene is the fuel with the lowest yield of PAH products at any of the investigated temperatures, when compared to 1-pentene and 1-butene. As shown by the blue squares in Figure 4.1, PAH yields from propylene pyrolysis become significant only at temperatures above 900 °C. After 900 °C, the summed yield of product PAH continues to rise with an increase in temperature, so that at 1000 °C, PAH products account for 1.7 % of the carbon fed to the reactor. The formation of PAH products from 1-pentene pyrolysis begins at lower temperatures than it does from propylene pyrolysis. The green triangles and curve in Figure 4.1 reveal that the PAH yield from 1-pentene pyrolysis becomes significant above 800 °C, and it rapidly increases with increasing temperature up to 950 °C. From 950 to 1000 °C, the summed yield of PAH products is still increasing, albeit with a smaller slope, so that at 1000 °C, 2.0 % of the carbon fed to the reactor are accounted for by PAH products from 1-pentene pyrolysis, which is almost 20 % more than from propylene pyrolysis. While the formation of product PAH from 1-butene pyrolysis begins at around the same temperature as that from 1-pentene pyrolysis, the summed yield of the PAH formed from 1-butene pyrolysis is larger than that from either 1-pentene or propylene pyrolysis at all investigated pyrolysis temperatures. The red circles Figure 4.1 show that the summed yield of PAH from 1-butene pyrolysis becomes larger than zero at 800 °C, after which it increases with a rise in temperature. At 1000 °C, 3.1 % of the carbon fed to the reactor from 1-butene pyrolysis is accounted for by PAH products, which is a factor of 1.5 times more than from 1-pentene pyrolysis and a factor 1.8 times more than from propylene pyrolysis. Not only does 1-butene produce a higher yield of PAH products than the other two fuels, it also leads to the formation of a larger number of individual product PAH. Figure 4.2 reveals the product

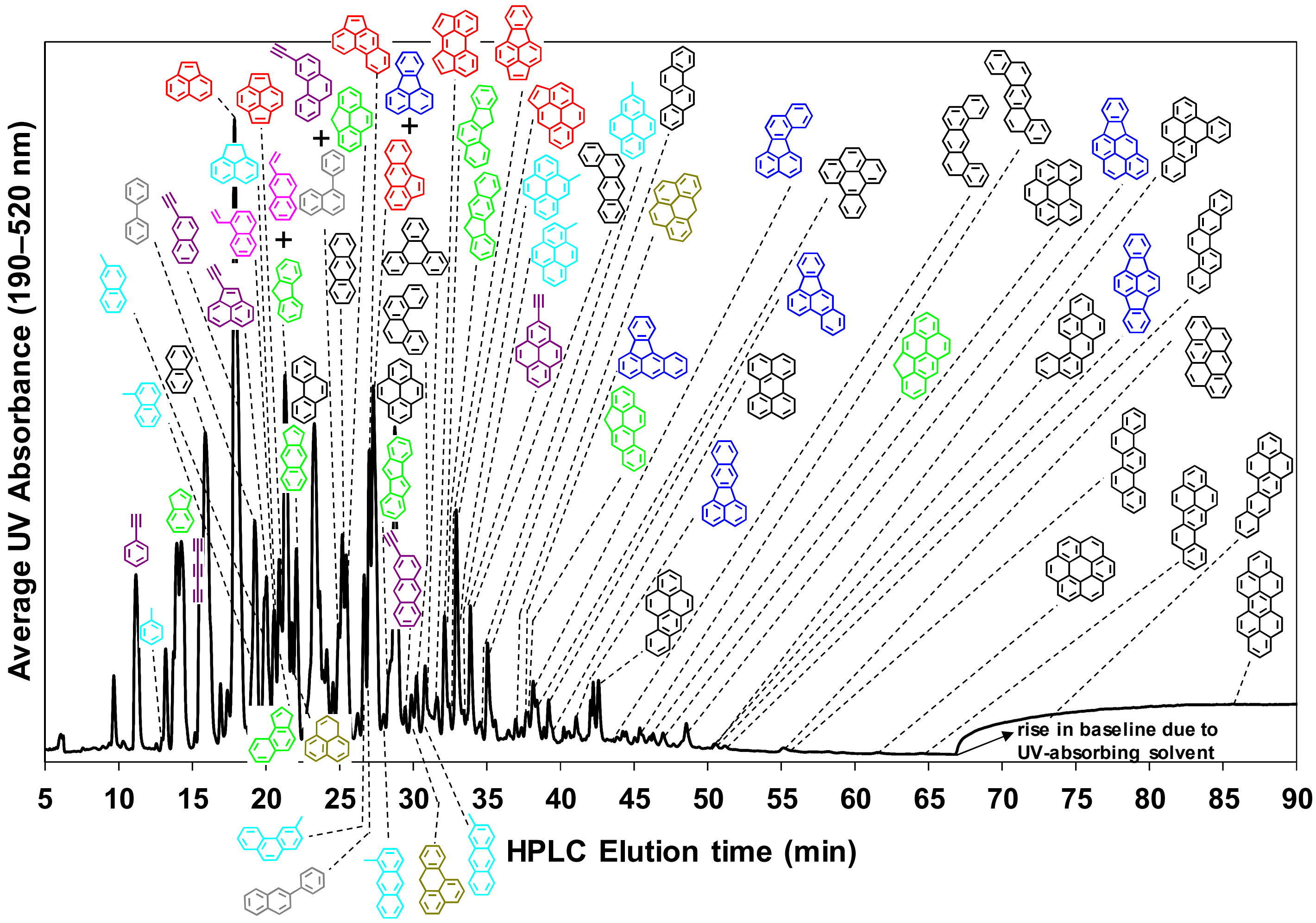

Figure 4.2. HPLC chromatogram of the products of 1-butene pyrolysis at 1000 °C and 0.31 s. The product compounds are color-coded by structural class: benzenoid PAH (black), ethynyl-substituted species (purple), vinyl-substituted PAH (pink), cyclopenta-fused PAH (red), fluoranthene benzologues (dark blue), indene benzologues (green), methyl substituted aromatics and acenaphthene (light blue), bi-aryls (grey), and phenalene-type compounds (olive). The names, molecular formulae, and structures of all the PAH products from 1-butene pyrolysis appear in Table A.5 in the Appendix.

chromatogram from 1-butene pyrolysis at 0.31 s and 1000 °C, the temperature at which the highest number of PAH are formed, and the 69 PAH that have been unequivocally identified by their UV spectra as products of 1-butene pyrolysis are shown. Of these 69 product PAH, 68 are reported here for the first time as products of 1-butene pyrolysis. The PAH range in size up to seven rings and are color-coded according to structural class: 23 benzenoid structures in black, 7 cyclopenta-fused PAH in red, 5 ethynyl-substituted species in purple, 7 fluoranthene benzologues in dark blue, 2 vinyl-substituted structures in pink, 10 indene benzologues in green, 8 methylated compounds and acenaphthene in light blue, 3 bi-aryls in grey, and 3 phenalene-type compounds in olive. The names and structures of all 69 PAH products are presented, sorted by molecular structure, in Table A.5 in the Appendix. Among the 69 identified product PAH shown in Figure 4.2 are the 64 PAH products that have been identified as products from 1-pentene pyrolysis (Figure A.3 and Table A.6) at 1000 °C and 0.31 s—all of which are reported here for the first time as products of 1-pentene pyrolysis——and the 59 PAH products that have been identified as products from propylene pyrolysis at the same condition (Figure A.4 and Table A.7). Since the pyrolysis of propylene has been studied more widely than that of 1-butene or 1-pentene, some information of PAH products from propylene pyrolysis is available [84]. However, still 35 of the 59 product PAH found in this work are reported here for the first time as products of propylene pyrolysis. No PAH products are formed during 1-pentene and propylene pyrolysis that are not also found in the product mixtures from 1-butene pyrolysis, and most of the additional products found from 1-butene pyrolysis are higher-ring-number PAH. This finding, along with the higher summed yield of PAH products from 1-butene pyrolysis suggests, that the reactions of PAH formation and growth are “further along” in the 1-butene pyrolysis environment compared to either the propylene or the 1-pentene pyrolysis environment.

In the following sections, we will investigate in detail the reactions leading to the different structural classes of product PAH formed during propylene, 1-butene, and 1-pentene pyrolysis. In order to understand the formation and growth reactions for PAH products, we first take a look at the smallest polycyclic products, the two-ring aromatic products.

4.2. Two-Ring Aromatic Products

Figure 4.3 reveals the yields of two-ring aromatic products from propylene pyrolysis (blue squares), 1-butene pyrolysis (red circles), and 1-pentene pyrolysis (green triangles), and the yields are reported as "% fed C as C in given product", in order to better compare between the three fuels. In the previous chapter we have learned that the various resonantly stabilized radicals that are present in the pyrolysis environments of the three investigated alkene fuels play a key role in the formation of one-ring aromatic products. We have also established that the one-ring product toluene is a ready source of the resonantly stabilized benzyl radical, which can react with the C_2 – C_4 species that are produced during the pyrolysis of either of the three fuels. Benzyl can react with acetylene [81,82], a product that is abundant in all three pyrolysis environments, and form indene, as shown in Reaction 18. Indene, whose temperature-dependent yields are revealed in Figure 4.3a, has the ability to form the resonance-stabilized indenyl radical, which is readily produced by breaking indene's methylene C-H bond. If benzyl radical reacts with propargyl instead of acetylene, naphthalene is formed [80,81], as shown in Reaction 19. Naphthalene's yields are shown in Figure 4.3b and similarly to benzene, fission of the aryl C-H bond of naphthalene to form

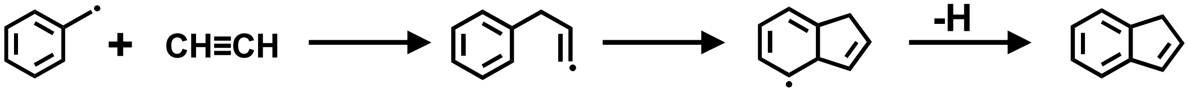

(18)

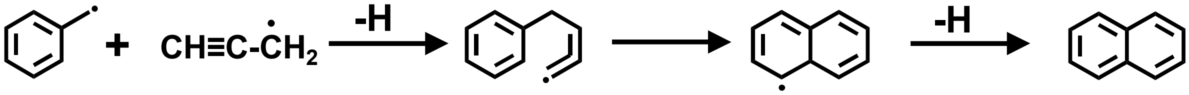

(19)

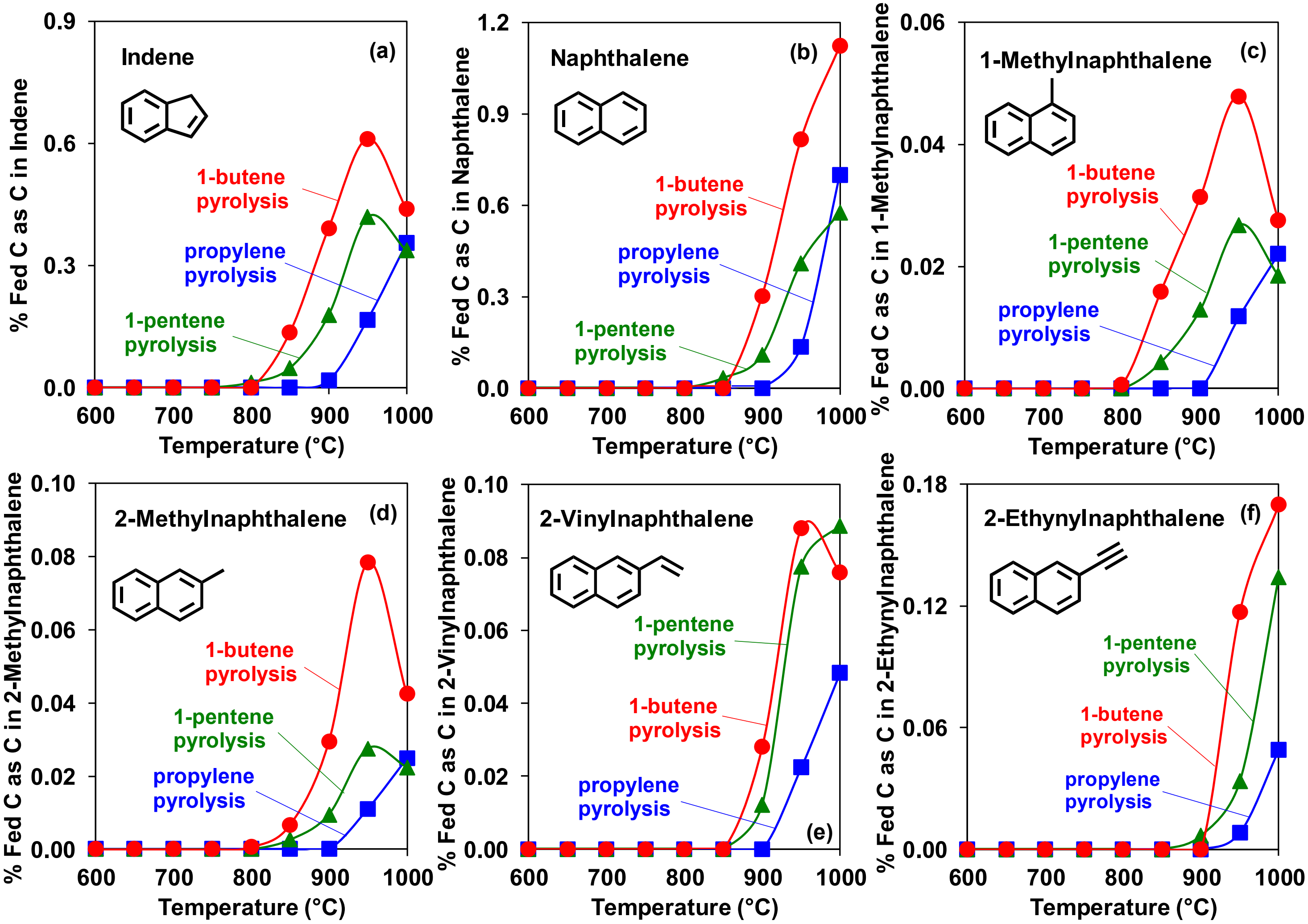

Figure 4.3. Yields, as functions of temperature, of two-ring aromatic products from propylene pyrolysis (blue squares and curves), 1-butene pyrolysis (red circles and curves), and 1-pentene pyrolysis (green triangles and curves) at 0.31 s: (a) indene, (b) naphthalene, (c) 1-methylnaphthalene, (d) 2-methylnaphthalene, (e) 2-vinylnaphthalene, and (f) 2-ethynylnaphthalene.

the naphthyl radical also requires high reaction temperatures. Evidence of the presence of the naphthyl radical at temperatures of 900 °C and above is found in Figure 4.3f, which shows that 2-ethynylnaphthalene is produced in significant amounts only at 950 and 1000 °C. Therefore, the major source of 2-ethynylnaphthalene seems to be Reaction 20, acetylene addition to the 2-naphthyl radical [80]. Analogous to toluene and styrene, methyl and vinyl radicals can combine with naphthyl radicals to form methyl- and vinylnaphthalenes. However, as Figures 4.3c and 4.3d reveal, both 1- and 2-methylnapthalene are already produced at temperatures below 900 °C from 1-pentene pyrolysis as well as from 1-butene pyrolysis. One other possible source of the formation of 1- and 2-methylnapthalene is the reaction of the benzyl radical with C_4 species, such as butadienyl radicals [81], which would account for the formation of methylnaphthalenes at temperatures below 900 °C, since both benzyl and C_4 species are readily available in the reaction environments of 1-butene as well as 1-pentene. As Figure 4.3e shows, both 1-butene and 1-pentene produce 2-vinylnaphthalene at 900 °C, while 2-vinylnaphthalene formation from propylene begins at 950 °C.

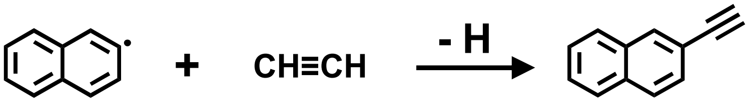

(20)

Additional to cross-reaction of the vinyl and 2-naphthyl radical, indenyl/allyl recombination could contribute further to the formation of 2-vinylnaphthalene, some of which can dehydrogenate to 2-ethynylnaphthalene. In order to understand the formation of 1-vinylnaphthalene, we turn our attention to Figure 4.4a, which shows that 1-vinylnaphthalene is formed in much lower amounts than its isomer with the vinyl substitution on the 2- position. This trend is, because 1-vinylnaphthalene readily cyclizes to form acenaphthene, whose yields are revealed in Figure 4.4b. Acenaphthene furthermore can undergo dehydrogenation to form acenaphthylene, whose yields are shown in Figure 4.4c. It is obvious that acenaphthylene's yields

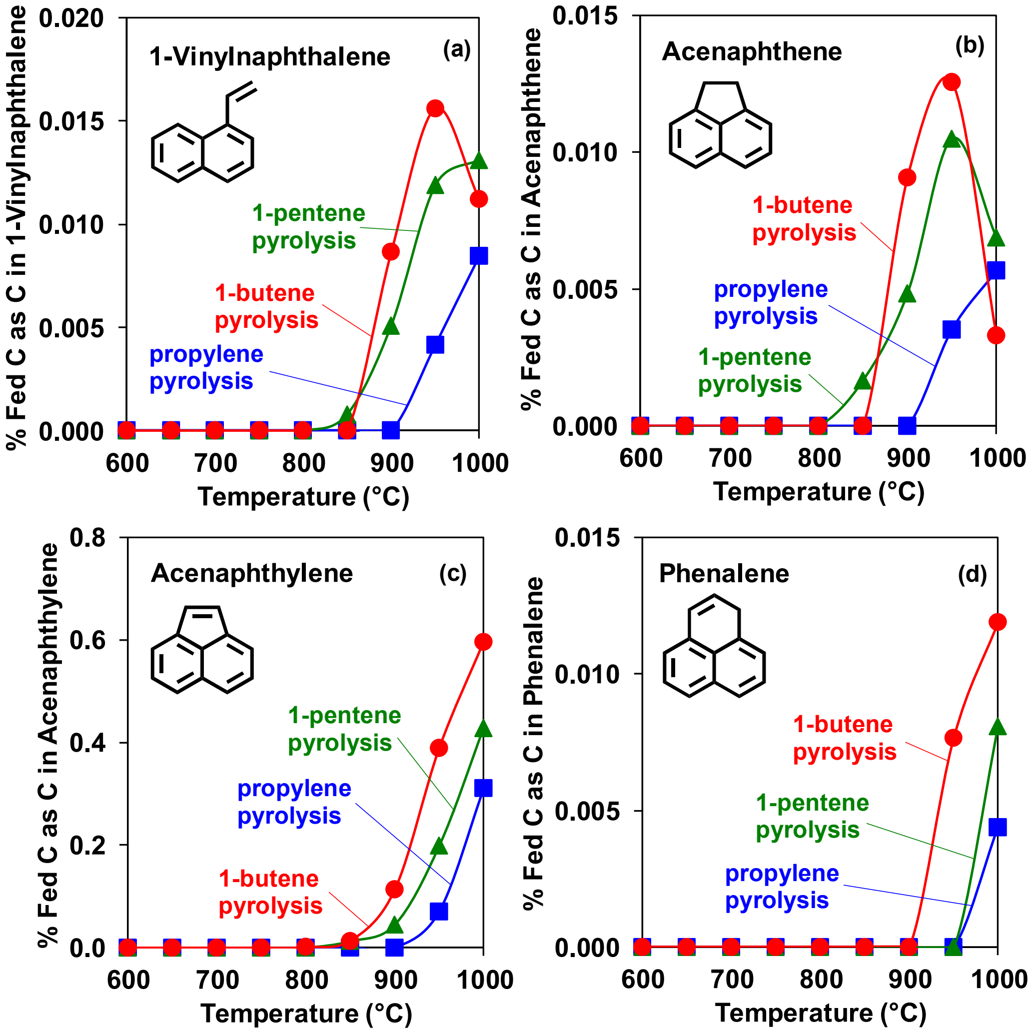

Figure 4.4. Product yields, as functions of temperature, from propylene pyrolysis (blue squares and curves), 1-butene pyrolysis (red circles and curves), and 1-pentene pyrolysis (green triangles and curves) at 0.31s: (a) 1-vinylnaphthalene, (b) acenaphthene, (c) acenaphthylene, and (d) phenalene.

are a lot higher from each of the three fuels than the yields of acenaphthene. Therefore, dehydrogenation of acenaphthene cannot be the sole source of acenaphthylene formation. When studying the two-ring aromatic products of the three pyrolysis sets, it becomes apparent that 1-ethynylnaphthalene is not observed as a product of any of the pyrolysis experiments. 1-

Ethynylnaphthalene is formed by acetylene addition to the 1-naphthyl radical, but once formed, it readily cyclizes to the energetically favored acenaphthylene, as shown in Reaction 21. Furthermore, the combination of indenyl and allyl radicals can also lead to the formation of acenaphthylene (Reaction 22) [82,83].

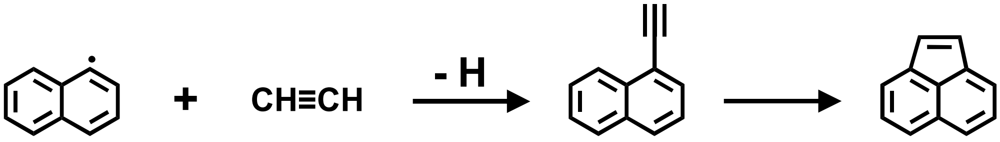

(21)

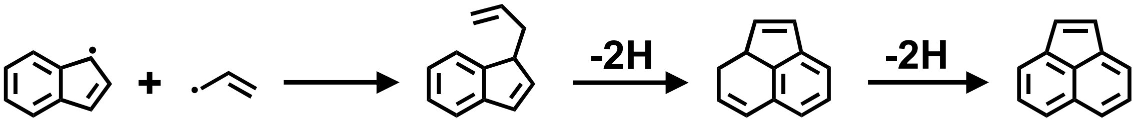

(22)

Another important group of PAH is phenalene and phenalene benzologues. The addition of C_3 radicals to the 1-naphthyl radical (Reaction 23), or acetylene addition to the 1-naphthylmethyl radical (Reaction 24) can lead to the formation of phenalene. As can be seen from Figure 4.4d, phenalene is not produced in large yields from either of the three pyrolysis fuels, however, phenalene readily produces the resonantly stabilized phenalenyl radical by breaking the relatively weak methylene C-H bond [85,86]. This radical, along with other radicals can react with C_3 and C_4 species, to form either another phenalene-type PAH or a benzenoid PAH.

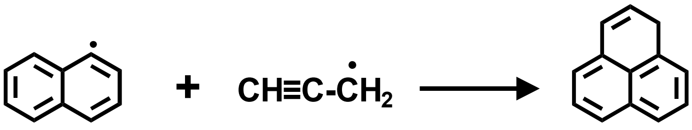

(23)

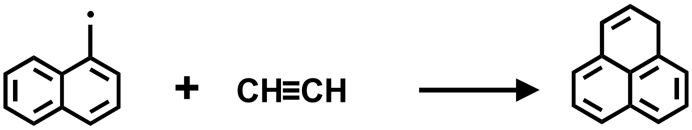

(24)

In this section we have learned how the different structural classes of two-ring aromatic products are formed during propylene pyrolysis, 1-butene pyrolysis, and 1-pentene pyrolysis. We have established, that $C_1 - C_4$ species react with phenyl and benzyl radicals to form PAH products of two rings. Since propylene requires much higher temperatures to convert than 1-butene or 1-pentene does, the yields of two-ring aromatic products from propylene pyrolysis become appreciable only above 900 °C, whereas they are already appreciable above 850 °C from 1-pentene pyrolysis and above 800 °C from 1-butene pyrolysis. Even though 1-pentene begins to react at much lower temperatures than 1-butene does, a large portion of the converted carbon from 1-pentene pyrolysis is "tied up" in ethylene. Therefore, more aliphatic and one-ring aromatic compounds and radicals are available for reaction in the 1-butene pyrolysis environment compared to the other two pyrolysis sets. In the following section, we will investigate the types of reactions leading to PAH products of higher ring number.

4.3. Higher-Ring Number PAH

The individual temperature-dependent yields of three- to seven-ring PAH products from propylene pyrolysis, 1-butene pyrolysis, and 1-pentene pyrolysis at 0.31 s are shown in Figures 4.5 – 4.13. The yield graphs are color-coded in accordance with the rest of the document: yields from propylene pyrolysis experiments are shown in blue squares, yields from 1-butene pyrolysis experiments are depicted in red circles, and yields from 1-pentene pyrolysis experiments are revealed in green triangles. Each figure-panel shows the yield of an individual PAH product with the exception of Figure 4.8d, which reveals the summed yield of benzo[*a*]fluorene and benzo[*b*]fluorene, since co-elution of the two isomers in the chromatograms obtained from the HPLC method used to analyze the pyrolysis products renders an accurate quantification of the individual products impossible. The structures of the individual product PAH that are shown in different colors according to their structural class in Figure 4.2—black for benzenoid PAH, purple for ethynyl-substituted PAH, pink for vinyl-substituted PAH, red for cyclopenta-fused PAH, dark

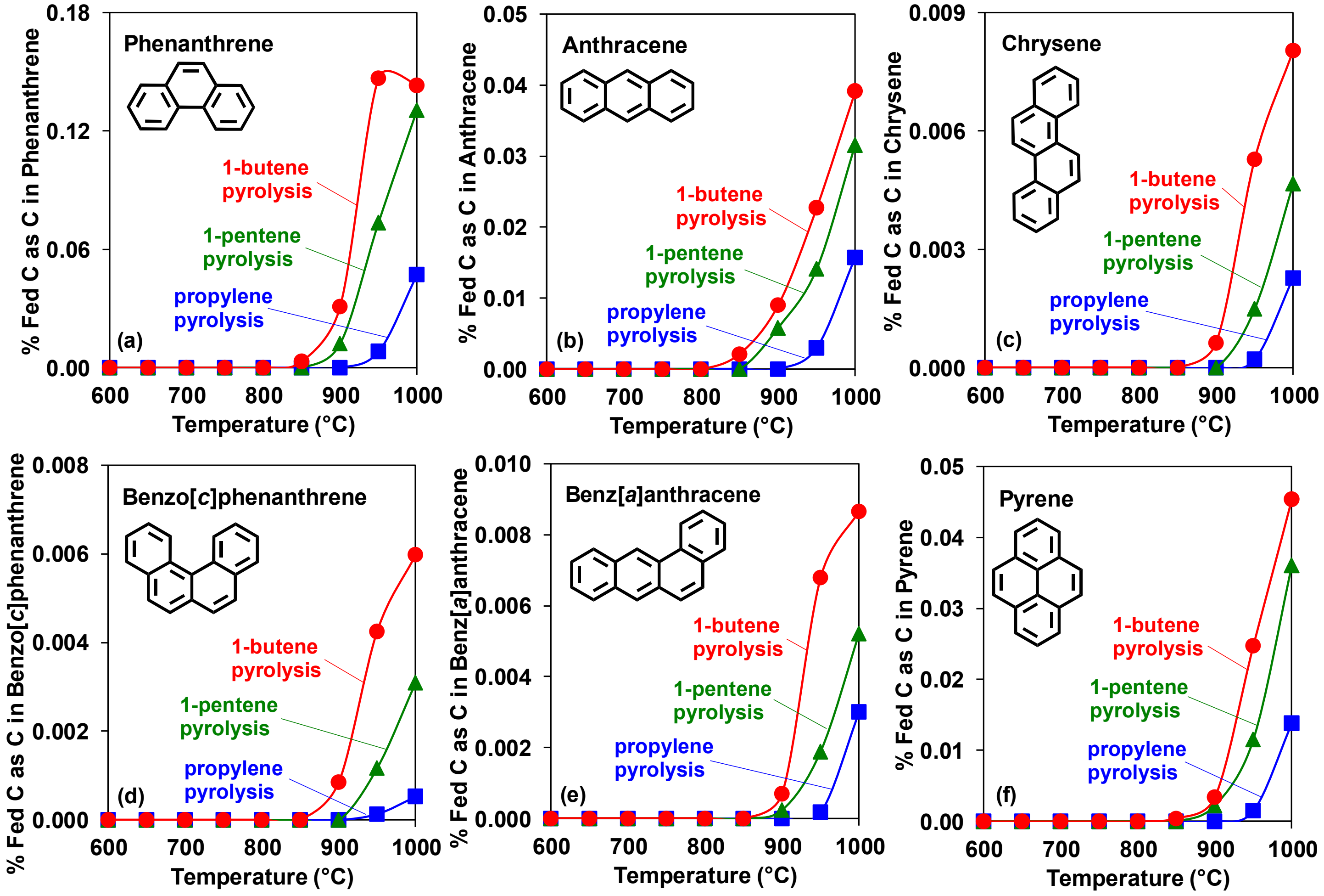

Figure 4.5. Yields, as functions of temperature, of benzenoid PAH products from propylene pyrolysis (blue squares and curves), 1-butene pyrolysis (red circles and curves), and 1-pentene pyrolysis (green triangles and curves) at 0.31 s: (a) phenanthrene, (b) anthracene, (c) chrysene, (d) benzo[*c*]phenanthrene, (e) benz[*a*]anthracene, and (f) pyrene.

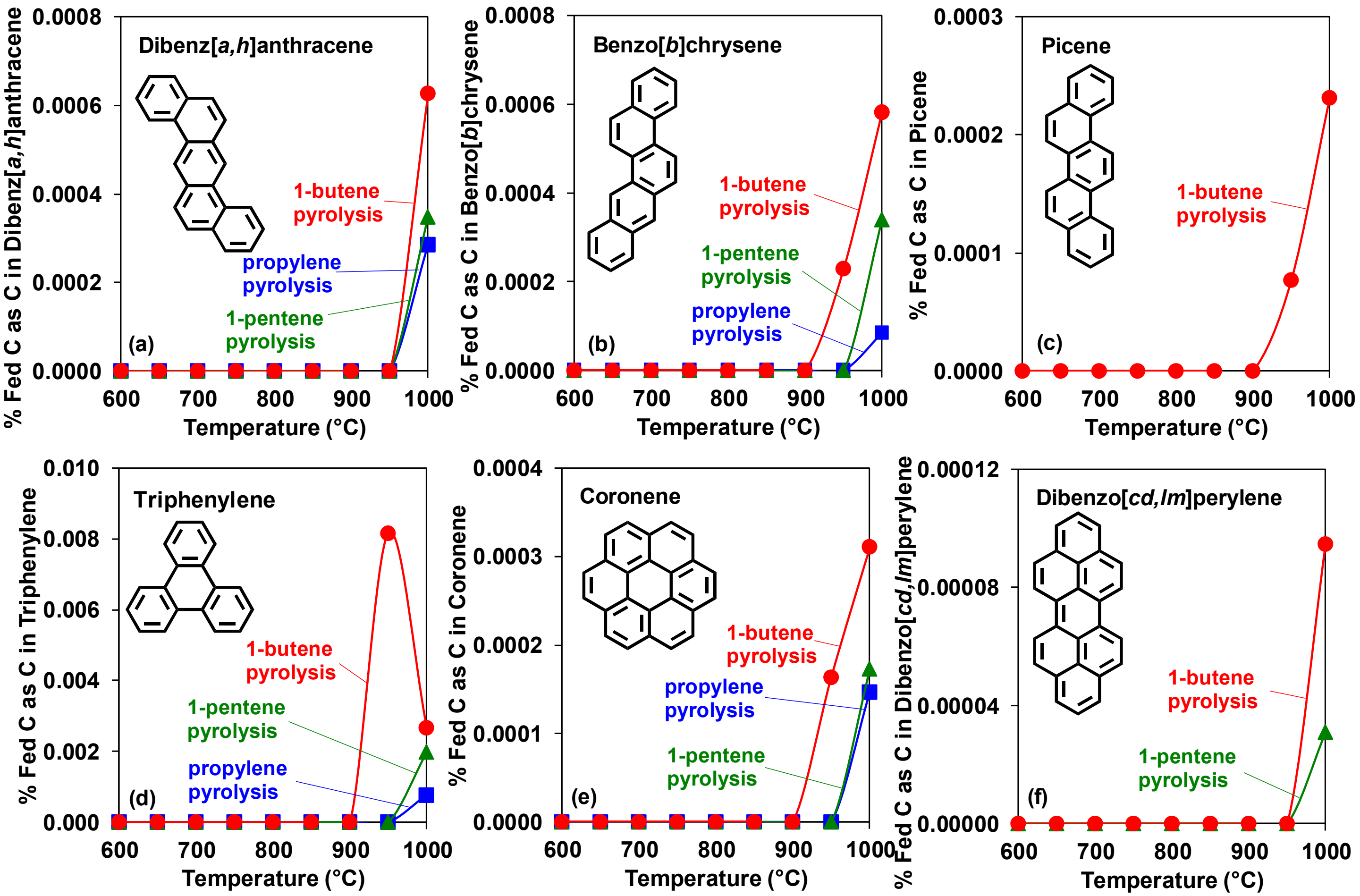

Figure 4.6. Yields, as functions of temperature, of benzenoid PAH products from propylene pyrolysis (blue squares and curves), 1-butene pyrolysis (red circles and curves), and 1-pentene pyrolysis (green triangles and curves) at 0.31 s: (a) dibenz[*a,h*]anthracene, (b) benzo[*b*]chrysene, (c) picene, (d) triphenylene, (e) coronene, and (f) dibenz[*cd,lm*]perylene.

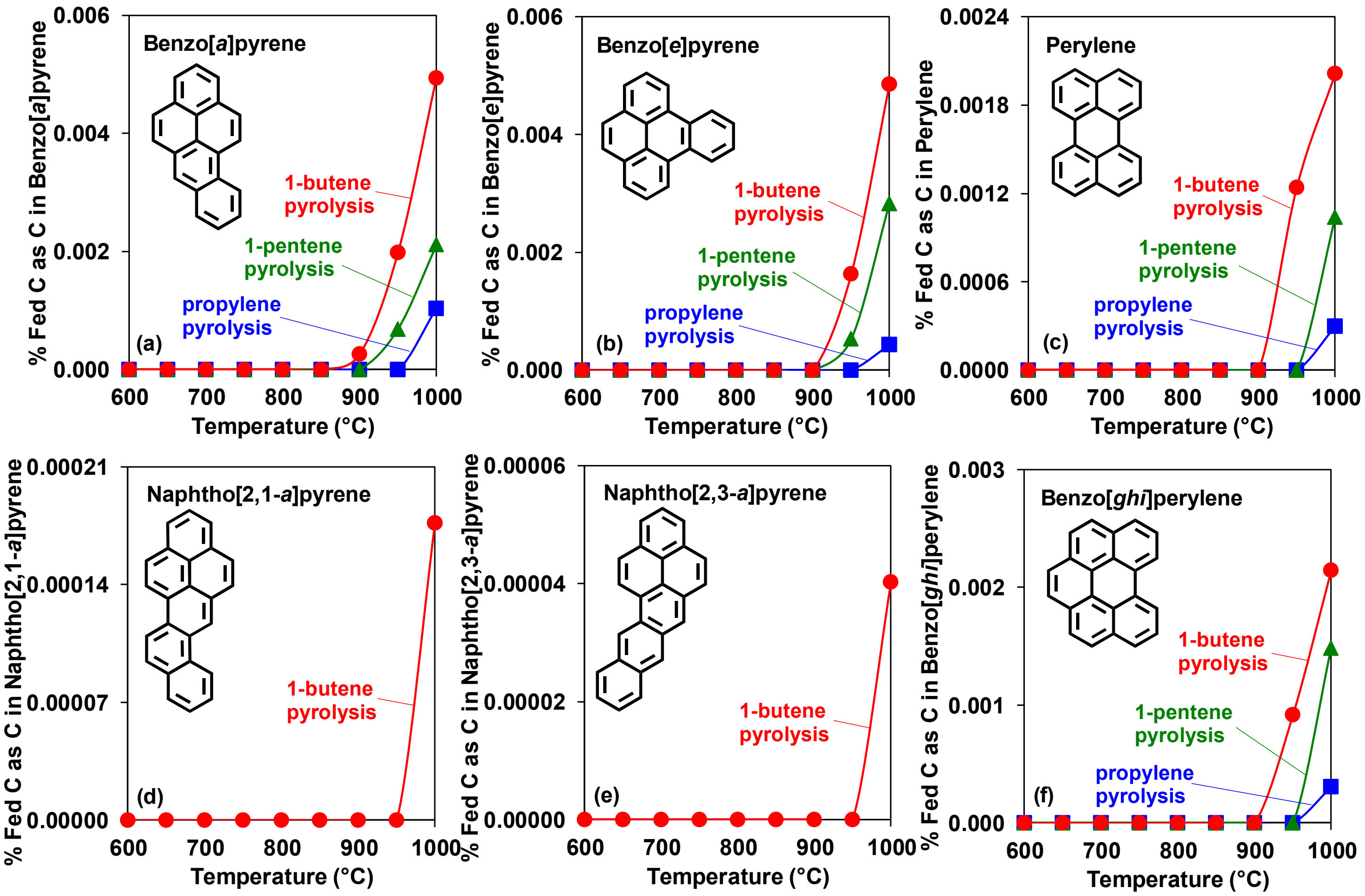

Figure 4.7. Yields, as functions of temperature, of benzenoid PAH products from propylene pyrolysis (blue squares and curves), 1-butene pyrolysis (red circles and curves), and 1-pentene pyrolysis (green triangles and curves) at 0.31 s: (a) benzo[*a*]pyrene, (b) benzo[*e*]pyrene, (c) perylene, (d) naphtho[2,1-*a*]pyrene, (e) naphtho[2,3-*a*]pyrene, and (f) benzo[*ghi*]perylene.

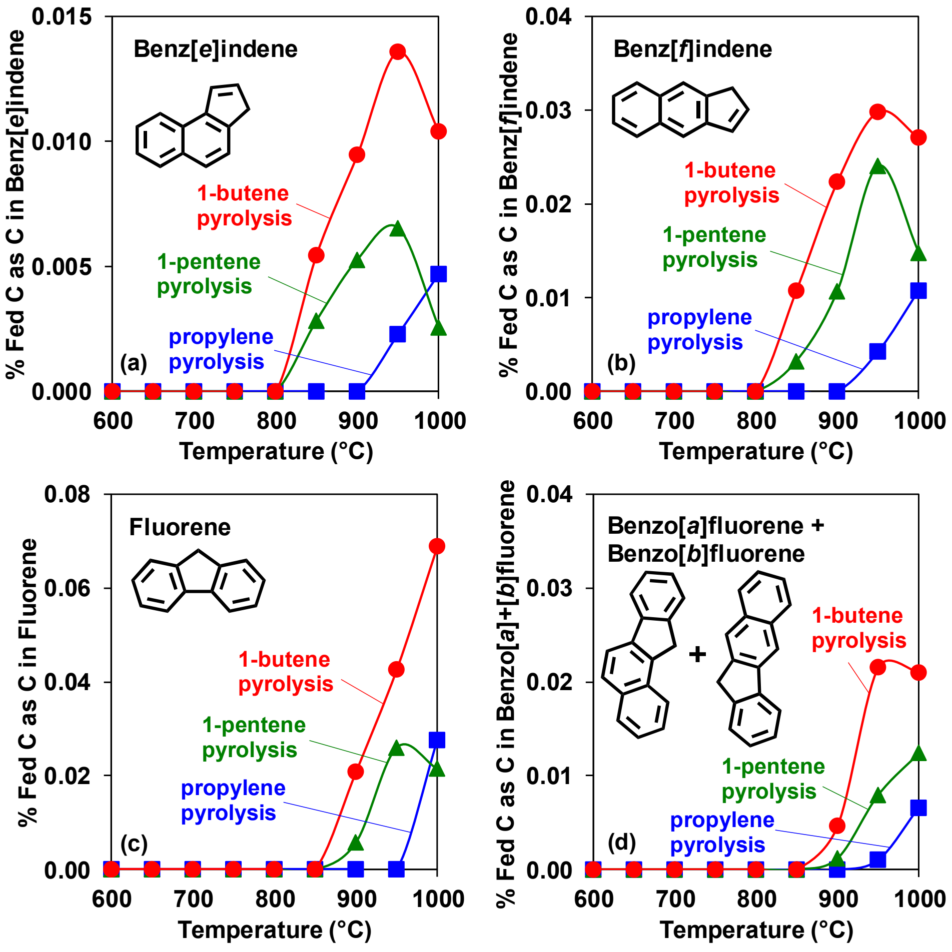

Figure 4.8. Yields, as functions of temperature, of product indene benzologues from propylene pyrolysis (blue squares and curves), 1-butene pyrolysis (red circles and curves), and 1-pentene pyrolysis (green triangles and curves) at 0.31 s: (a) benz[*e*]indene, (b) benz[*f*]indene, (c) fluorene, and (d) benzo[*a*]fluorene + benzo[*b*]fluorene.

blue for fluoranthene benzologues, green for indene benzologues, light blue for methyl-substituted aromatics and acenaphthene, grey for bi-aryls, and olive for phenalene-type compounds—are now shown in black in each panel of the Figures 4.5 – 4.13. The yields of product PAH ≥ 2 rings, summed by different structural classes, are presented in Figure 4.14. Figure 4.14a shows the summed yield of benzenoid product PAH ≥ 2 rings, which is made up of the individual product yields shown in Figures 4.3b, 4.5, and 4.6. It is apparent from Figure 4.14a that between 900 and

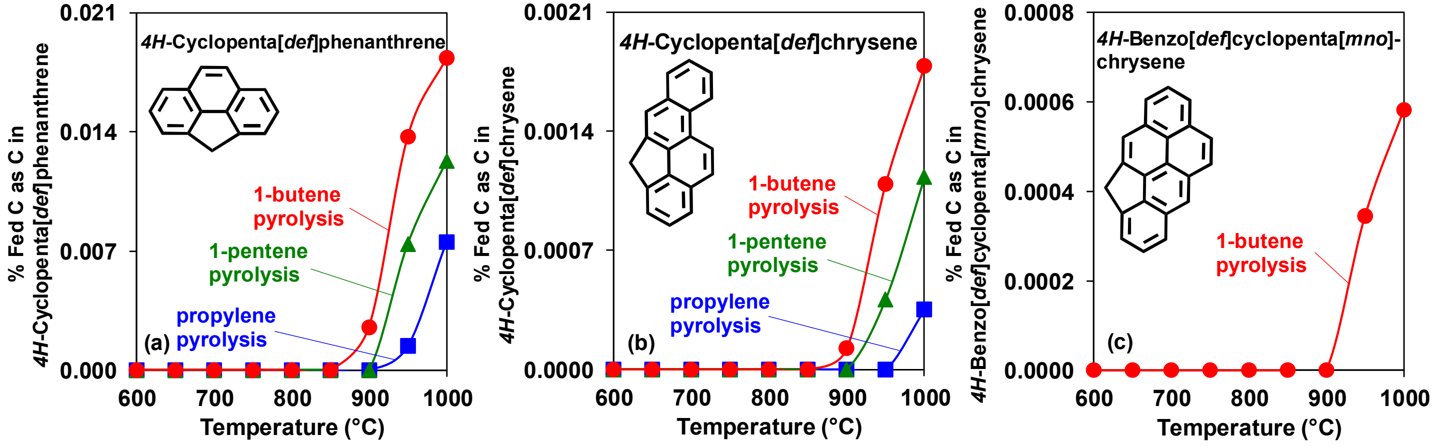

Figure 4.9. Yields, as functions of temperature, of product indene benzologues from propylene pyrolysis (blue squares and curves), 1-butene pyrolysis (red circles and curves), and 1-pentene pyrolysis (green triangles and curves) at 0.31 s: (a) 4*H*-cyclopenta[*def*]phenanthrene, (b) 4*H*-cyclopenta[*def*]chrysene, and (c) 4*H*-benzo[*def*]cyclopenta[*mno*]chrysene.

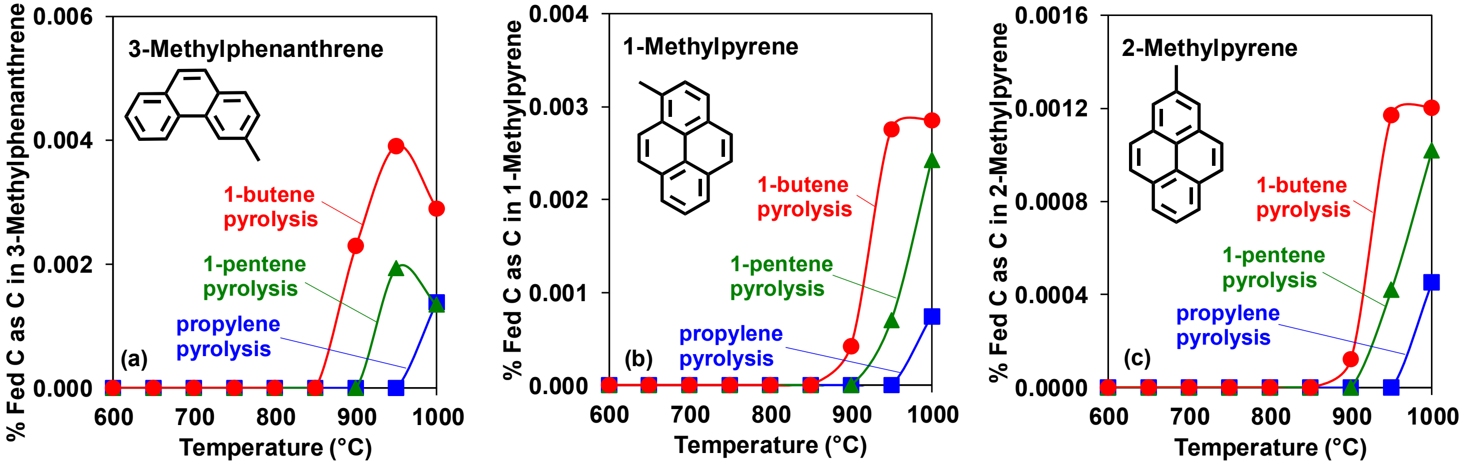

Figure 4.10. Yields, as functions of temperature, of methyl-substituted product PAH from propylene pyrolysis (blue squares and curves), 1-butene pyrolysis (red circles and curves), and 1-pentene pyrolysis (green triangles and curves) at 0.31 s: (a) 2-methylphenanthrene, (b) 1-methylpyrene, (c) 2-methylpyrene.

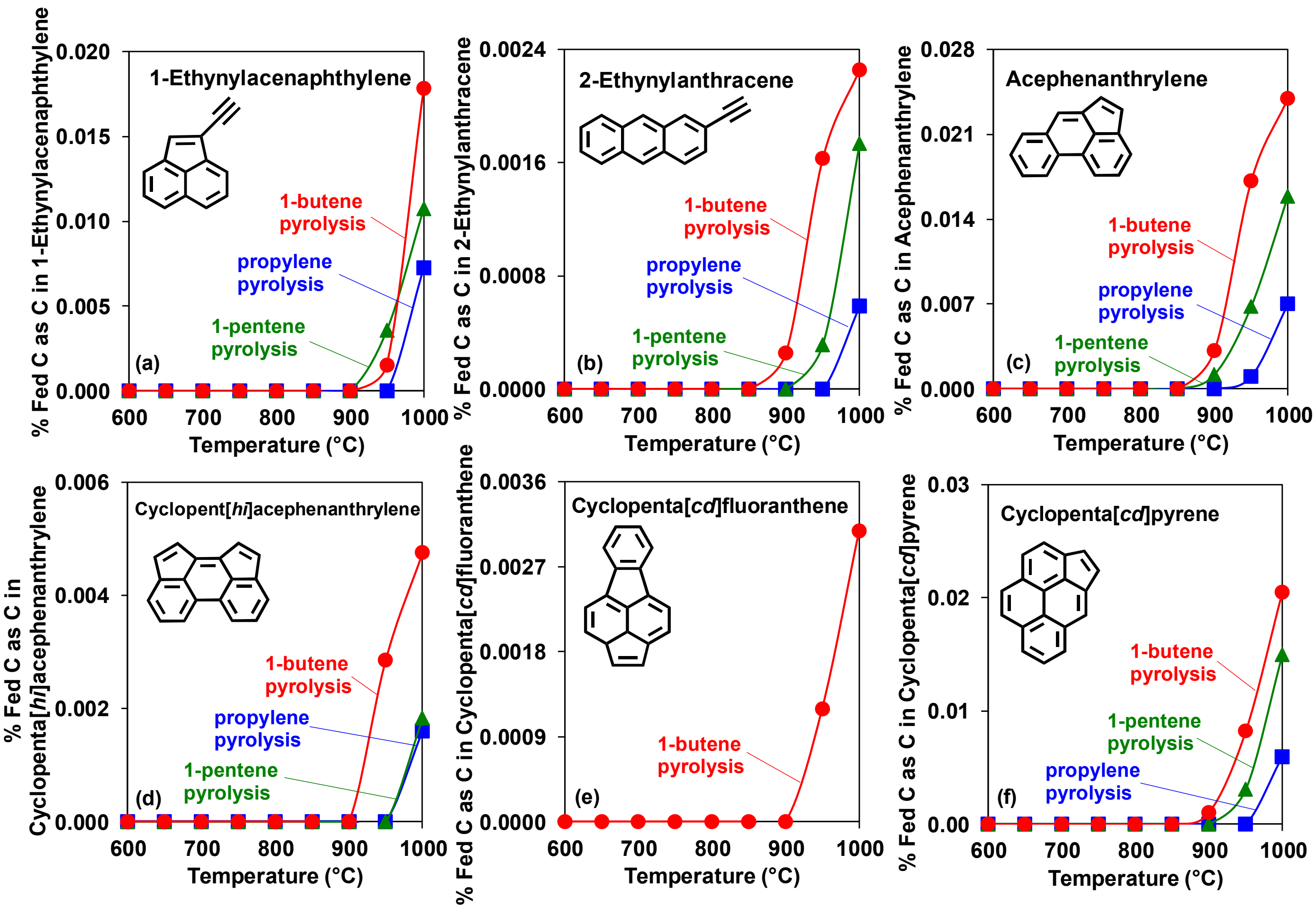

Figure 4.11. Yields, as functions of temperature, of ethynyl-substituted and cyclopenta-fused PAH products from propylene pyrolysis (blue squares and curves), 1-butene pyrolysis (red circles and curves), and 1-pentene pyrolysis (green triangles and curves) at 0.31 s: (a) 1-ethynylacenaphthylene, (b) 2-ethynylanthracene, (c) acephenanthrylene, (d) cyclopenta[*hi*]acephenanthrylene, (e) cyclopenta[*cd*]fluoranthene, and (f) cyclopenta[*cd*]pyrene.

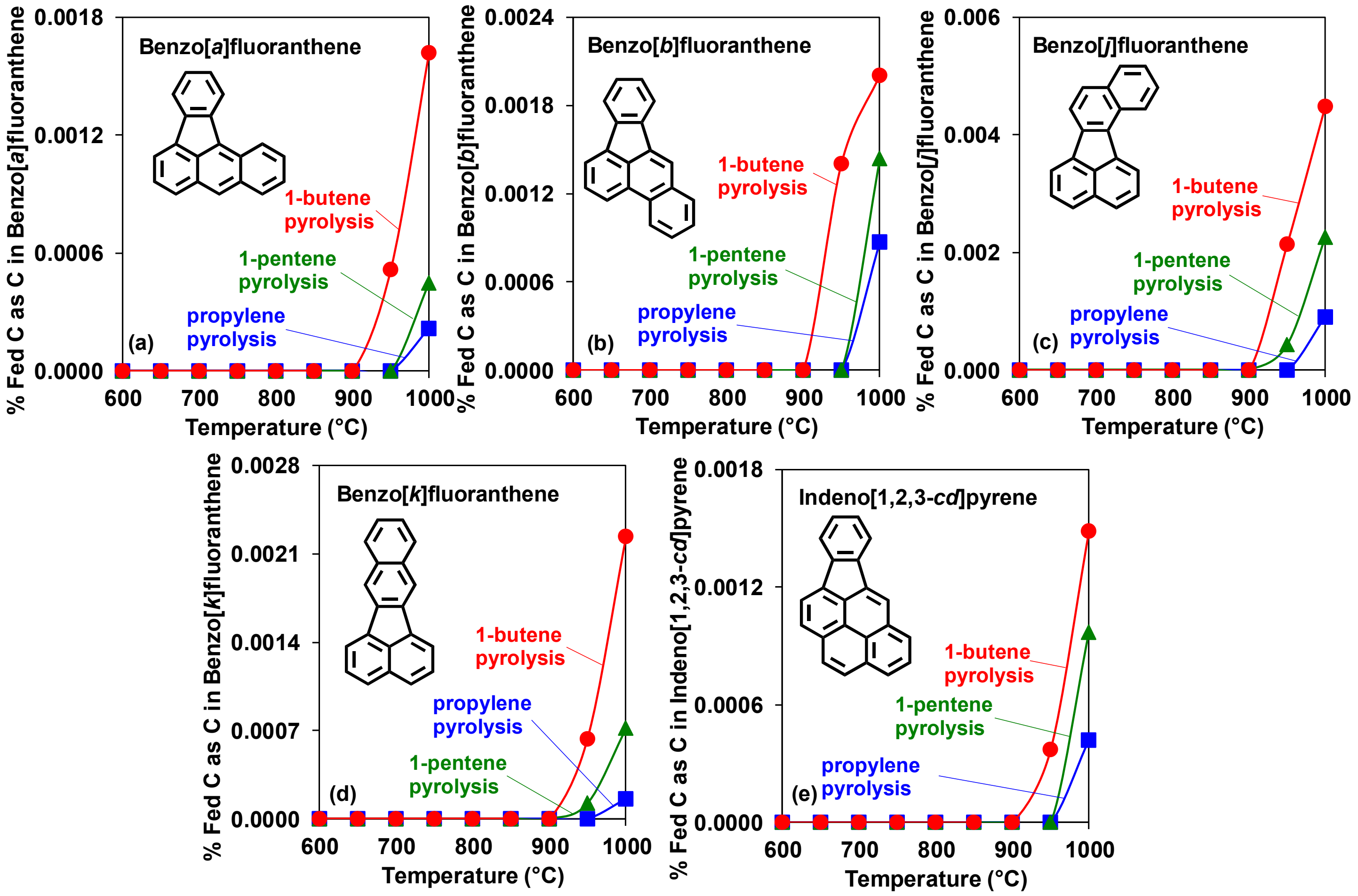

Figure 4.12. Yields, as function of temperature, of product fluoranthene benzologues from propylene pyrolysis (blue squares and curves), 1-butene pyrolysis (red circles and curves), and 1-pentene pyrolysis (green triangles and curves) at 0.31 s: (a) benzo[*a*]fluoranthene, (b) benzo[*b*]fluoranthene, (c) benzo[*j*]fluoranthene, (d) benzo[*k*]fluoranthene, (e) indeno[1,2,3-*cd*]pyrene.

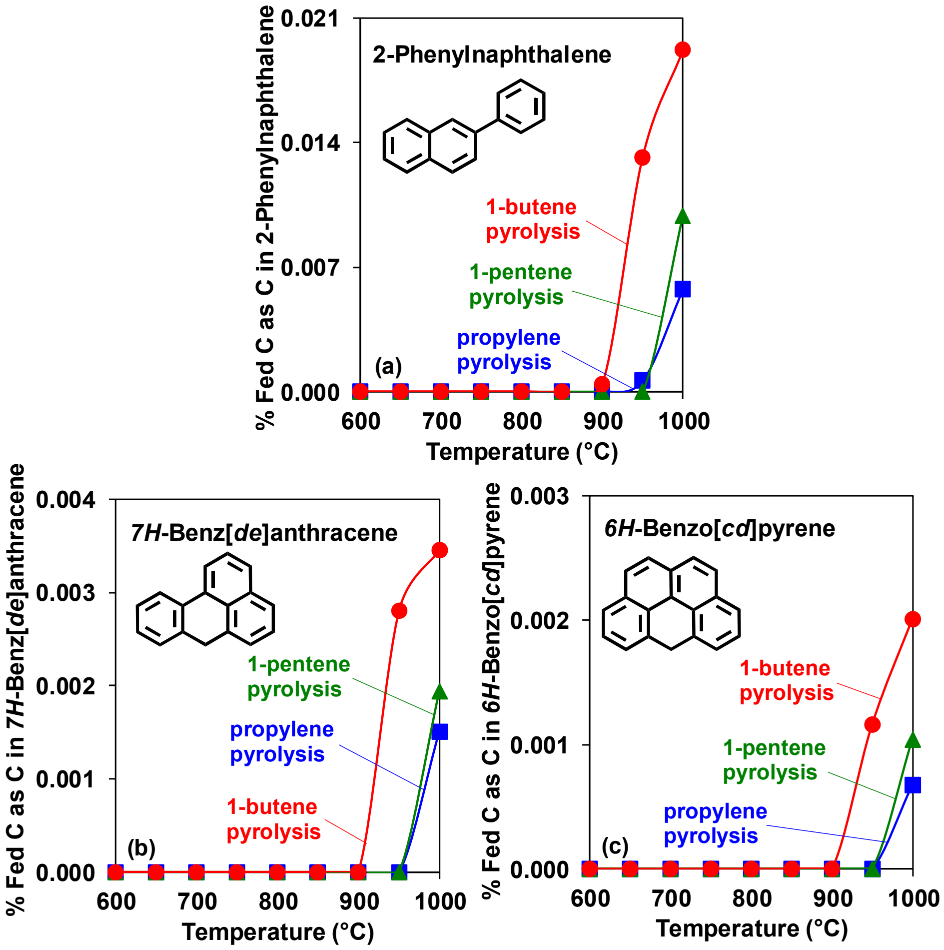

Figure 4.13. Yields, as functions of temperature, of bi-aryls and phenalene-type product compounds from propylene pyrolysis (blue squares and curve), 1-butene pyrolysis (red circles and curve), and 1-pentene pyrolysis (green triangles and curve) at 0.31 s: (a) 2-phenylnaphthalene, (b) 7*H*-benz[*de*]anthracene, (c) 6*H*-benzo[*cd*]pyrene.

1000 °C, 1-butene produces more benzenoid PAH than 1-pentene or propylene does. At 1000 °C, the yield of benzenoid PAH from 1-butene pyrolysis is 75 % and 78 % higher than from 1-pentene pyrolysis and propylene pyrolysis, respectively. Furthermore, we can see that PAH products with benzenoid structures are produced in the highest yields from all three 1-alkene fuels.

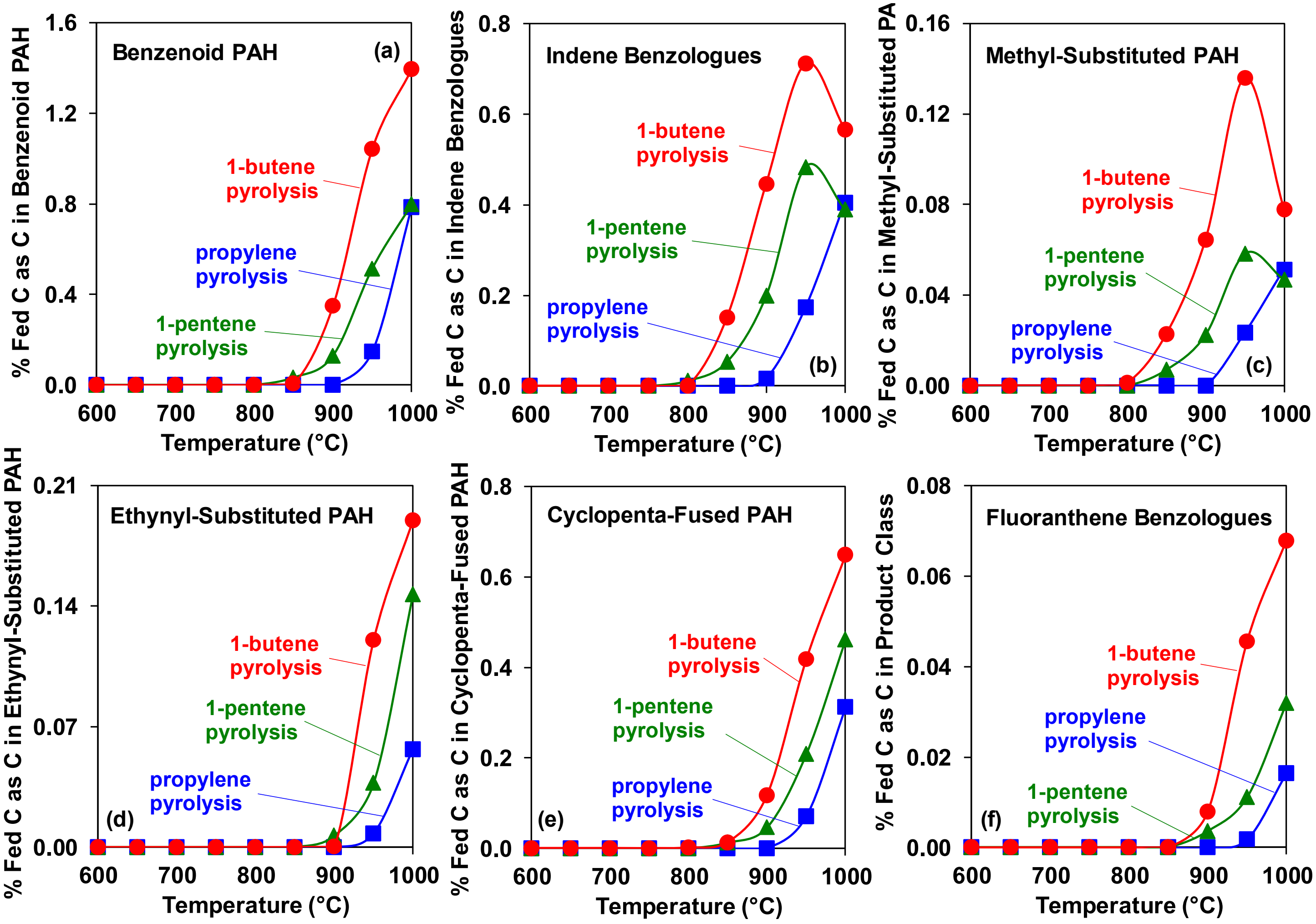

Figure 4.14. Yields, as functions of temperature, of product PAH ≥ 2 rings summed by structural class from propylene pyrolysis (blue squares and curves), 1-butene pyrolysis (red circles and curves), and 1-pentene pyrolysis (green triangles and curves) at 0.31 s: (a) benzenoid PAH, (b) indene benzologues, (c) methyl-substituted PAH, (d) ethynyl-substituted PAH, (e) cyclopenta-fused PAH, and (f) fluoranthene benzologues.

Similar to the formation of naphthalene by the combination of benzyl and propargyl, shown in Reaction 19, higher-ring number benzenoid PAH are formed by the reaction of arylmethyl radicals with propargyl radicals. The three-ring PAH phenanthrene, for example, can be formed by the reaction of the 2-naphthylmethyl radical with propargyl, as shown in Reaction 25.

Benzenoid PAH can furthermore be formed by the reaction of aryl radicals with C_4 species [80]. When using the example of phenanthrene, reaction of the 2-naphthyl radical with 1,3-butadiene or other C_4 species available in the reaction environment can lead to the formation of phenanthrene. As Figure 4.5a reveals, phenanthrene is formed in higher amounts from 1-butene pyrolysis compared to the other two pyrolysis sets, which can be explained with the ready availability of naphthyl, naphthylmethyl, and propargyl radicals as well as C_4 species during 1-butene pyrolysis. Further contributing to the formation of benzenoid product PAH is the reaction of phenalenyl-type radicals with C_3 radicals, for example, pyrene formation from combination of phenalenyl radical with propargyl, shown in Reaction 26. Again, the higher abundance of propargyl and phenalenyl radicals in the reaction environment of 1-butene compared to propylene and 1-pentene, leads to the formation of a higher yield of pyrene from 1-butene pyrolysis than from either 1-pentene or propylene pyrolysis, as shown in Figure 4.5f. Other phenalene-type compounds are 7*H*-benz[*de*]anthracene, and 6*H*-benzo[*cd*]pyrene, whose structures are show in grey in Figure 4.2 and whose yields are shown in Figures 4.13b and 4.13c, respectively. Analogous to phenalene, the methylene C-H bond of these compounds can easily be broken and lead to the

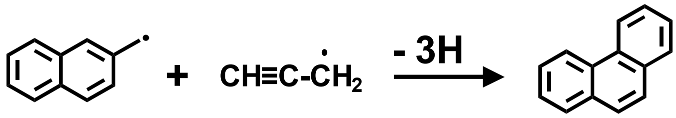

(25)

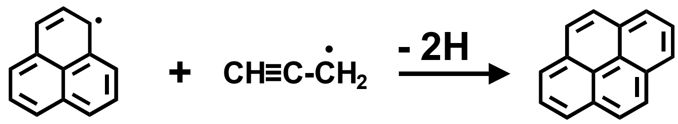

(26)

formation of the benz[*de*]anthracenyl and benzo[*cd*]pyrenyl radical, both of which are resonantly stabilized radicals. Benz[*de*]anthracenyl can react with propargyl to form either benzo[*e*]pyrene, whose yields are shown in Figure 4.7b, or perylene, whose yields are shown in Figure 4.7c. Reaction of benzo[*cd*]pyrenyl with propylene leads to the formation of benzo[*ghi*]perylene, whose yields are revealed in Figure 4.7f.

Similar to phenalene-type compounds, indene benzologues are susceptible to ring-growth reactions, since breaking their relatively weak methylene C-H bond leads to the formation of resonantly stabilized indenyl radicals. The individual product yields of the indene benzologues—whose structures appeared in light green in Figure 4.2—are shown in Figures 4.3a, 4.8, and 4.9, and the sum of these yields is presented in Figure 4.14b. Indene benzologues are formed by reaction of acetylene with arylmethyl radicals, analogous to the formation of indene, shown in Reaction 18. Furthermore, reaction of C_4 species with indene benzologues can lead to the formation of higher-ring-number indene benzologues. For example, fluorene reaction with a C_4 species, such as the butadienyl radical can lead to the formation of benzo[*a*]fluorene, whose yields—summed with benzo[*b*]fluorene's yields—are shown in Figure 4.8d.

Methyl-substituted PAH, structures that are depicted in light blue in Figure 4.2, are also susceptible to losing a hydrogen atom at their methyl site and forming a resonantly stabilized radical. The yield of methyl-substituted products from the three pyrolysis sets are shown in Figures 4.3c, 4.3d, and 4.10, and the sum of these product yields is shown in Figure 4.14c. Methyl-substituted PAH can be formed by methyl addition to aryl radicals, or by reaction of C_4 species with methyl-substituted product PAH to form higher-ring-number methyl-substituted PAH.

The yields of the products shown in the Figures 4.4c and 4.11c-f, whose structures are shown in red in Figure 4.2, are the cyclopenta-fused product PAH. The sum of the yields of cyclopenta-fused product PAH is shown in Figure 4.14e, and it can be seen that between 950 and 1000 °C, 1-butene pyrolysis leads to the formation of up to 2 times more cyclopenta-fused PAH than 1-pentene pyrolysis does, and up to 6 times more than propylene does. Analogous to Reaction 21, cyclopenta-fused PAH are formed by acetylene addition to aryl radicals, whose radical site is located at the valley carbon. For example, acetylene addition to the 1-pyrenyl radical leads to the formation of cyclopenta[*cd*]pyrene, whose yields are shown in Figure 4.11f. Furthermore, cyclopenta-fused PAH can be formed by the addition of resonance-stabilized C_3 radicals to indenyl-type radicals [80,82,83]. The formation of higher amounts of cyclopenta-fused PAH during 1-butene pyrolysis compared to the other two pyrolysis sets is an important finding, since C_4 addition to a cyclopenta-fused PAH can lead to the formation of fluoranthene benzologues [80].

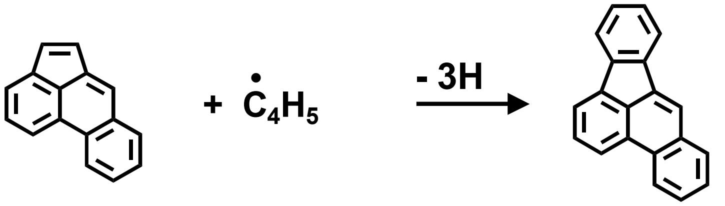

(27)

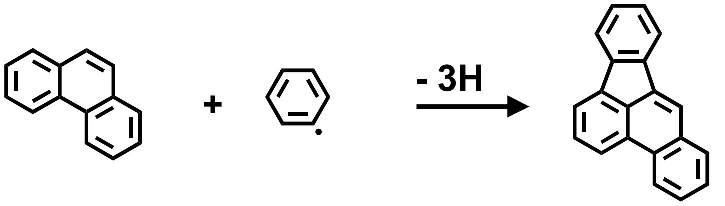

(28)

The individual yields of fluoranthene benzologues—whose structures are depicted in dark blue in Figure 4.2—are shown in Figure 4.12, and the summed yield of fluoranthene benzologues is revealed in Figure 4.14f. As shown in Reaction 27, the butadienyl radical can attack the isolated double bond of acephenanthrylene and form benzo[*b*]fluoranthene, whose yields are shown in Figure 4.12b. Benzo[*b*]fluoranthene can furthermore be formed by Reaction 28, phenyl addition to phenanthrene [80]. Since 1-butene produces higher amounts of all the ingredients leading to the formation of fluoranthene benzologues, 1-butene produces fluoranthene benzologues in yields up to 4 higher than 1-pentene does and up to 25 times higher than propylene does.

Chapter V. Conclusions and Recommendations for Future Work

5.1. Summary and Conclusions

The purpose of this experimental study has been to better understand the role of 1-alkenes and allylic radicals in the formation and growth reactions of PAH. To this end, pyrolysis experiments have been performed at nine temperatures between 600 and 1000 °C and a fixed residence time of 0.31 s, with three 1-alkene fuels: propylene (CH_2=CH–CH_3), 1-butene (CH_2=CH–CH_2–CH_3), and 1-pentene (CH_2=CH–CH_2–CH_2–CH_3). The experiments have been carried out in an isothermal laminar-flow quartz tube reactor, and the gas- and condensed-phase products have been analyzed in detail by GC/FID, for the C_1 – C_6 aliphatic hydrocarbon products; GC/TCD, for product H_2; GC/FID/MS, for one- and two-ring aromatic hydrocarbon products; and HPLC/UV, for PAH products.

The propylene pyrolysis experiments reveal that propylene conversion becomes significant at temperatures $\geq$ 850 °C and that it steeply increases with rising temperatures up to 1000 °C, where 98.8 % of propylene is converted. Propylene is found to produce acetylene, propadiene, and propyne in high yields and the radical pool of propylene pyrolysis is made up mostly of allyl and propargyl radicals. The abundantly produced C_2 and C_3 species participate in reactions leading to the formation of one-ring aromatic products, which are formed above 850 °C. At 1000 °C, 13.9 % of the carbon fed to the reactor from propylene pyrolysis is made up of one-ring aromatic products, the majority of which is accounted for by benzene, which is less reactive than its substituted counterparts. PAH products are found to be formed during propylene pyrolysis at temperatures $\geq$ 900 °C, and the PAH yield increases with a rise in temperature up to 1000 °C, where it reaches 1.7 % of the fed carbon. Extensive HPLC/UV analyses of the propylene pyrolysis product mixtures have led to the identification of 59 two- to seven-ring PAH products, 35 of which are reported here for the first time as products of propylene pyrolysis.

The 1-butene pyrolysis experiments show that 1-butene is more reactive than propylene is. 1-butene conversion becomes appreciable at temperatures > 700 °C and is almost fully complete (99.9%) by 850 °C, a temperature at which merely 10.3 % of propylene is converted during propylene pyrolysis. The major products of 1-butene pyrolysis are found to be methane, ethylene, acetylene, propylene, propadiene, propyne, and 1,3-butadiene. Since 1-butene's conversion begins at much lower temperatures compared to propylene, aliphatic products are formed at lower temperatures from 1-butene pyrolysis compared to propylene pyrolysis. At 850 °C, a temperature at which aliphatic products from propylene pyrolysis make up only 9.1% of the fed carbon, 92.1 % of the carbon fed to the reactor from 1-butene pyrolysis is accounted for by aliphatic hydrocarbon products. Therefore, important radicals that participate in aromatic formation reactions, such as allyl and propargyl, are available at lower temperatures for 1-butene pyrolysis than for propylene pyrolysis. Additionally, 1-butene readily produces methylallyl, a radical that is not present in the propylene pyrolysis environment. Furthermore, the yield of 1,3-butadiene from 1-butene pyrolysis is much higher than from propylene pyrolysis, resulting in the presence of ample amounts of butadienyl radicals, which contribute to the formation of one-ring aromatic products and PAH products. One-ring aromatic products are formed at ≥ 750 °C, and at 1000 °C, they make up 13 % of the carbon fed to the reactor from 1-butene pyrolysis. The facile formation, at relatively low temperatures, of one-ring aromatics from 1-butene pyrolysis—especially the more reactive substituted one-ring aromatics—leads to a higher yield of PAH products from 1-butene pyrolysis than from propylene pyrolysis. For 1-butene pyrolysis, PAH are produced at temperatures as low as 850 °C and rise in yield with increasing temperature, accounting, at 1000

°C, for 3.1 % of the 1-butene fuel carbon. (For propylene pyrolysis, product PAH account for only 1.7 % of the propylene fuel carbon at 1000 °C.) Furthermore, 1-butene produces a higher number of PAH products than propylene does. At 1000 °C and 0.31 s, 69 two- to seven-ring PAH products from 1-butene pyrolysis have been identified, in this study, by extensive HPLC/UV analyses; 67 of these 69 product PAH have never before been reported as products of 1-butene pyrolysis.

The 1-pentene pyrolysis experiments reveal that 1-pentene conversion begins at even lower temperatures than 1-butene conversion during 1-butene pyrolysis. At 600 °C, 1-pentene conversion has already reached 3.7 %, and it rapidly increases so that at 800 °C, 99.9 % of 1-pentene has reacted. This observed behavior is largely due to the facile formation of the reactive ethyl radical during the decomposition of 1-pentene. This ethyl radical readily loses a hydrogen atom to form ethylene so that at all investigated temperatures, ethylene is found to be the single highest-yield decomposition product of 1-pentene pyrolysis. Between 750 and 1000 °C, ethylene formed from 1-pentene pyrolysis accounts for 42 – 51% of the carbon fed to the reactor, while ethylene's yield from 1-butene or propylene pyrolysis never exceeds 30 % of the fuel carbon at any investigated temperature. Therefore, a large portion of the fuel carbon from 1-pentene pyrolysis is "tied up" in ethylene and unavailable for aromatic-formation and -growth reactions. Of the carbon that is not trapped in ethylene, a large portion is accounted for by 1-pentene's other high-yield products acetylene, propylene, propadiene, propyne, 1-butene, and 1,3-butadiene, and ample amounts of allyl, propargyl, methylallyl, butadienyl, and ethylallyl radicals are formed. At temperatures between 750 and 900 °C, the yields of these $C_2 – C_4$ species from 1-pentene pyrolysis are higher than they are from propylene pyrolysis, but lower than they are from 1-butene pyrolysis. Consequently, the yields of one-ring aromatic products at temperatures between 800 and 900 °C are up to 50 times higher from 1-pentene pyrolysis than they are from propylene pyrolysis, but up to 60 % lower compared to 1-butene pyrolysis. Thus, both the number and yield of PAH products from 1-pentene pyrolysis are higher than they are from propylene pyrolysis but lower compared to 1-butene pyrolysis. HPLC/UV analyses of the 1-pentene pyrolysis product mixtures reveal that at 1000 °C, 2 % of the carbon fed to the reactor is accounted for in the PAH products—a yield which, on a %-fed-carbon basis, is 1.8 times higher than that from propylene pyrolysis and 35 % lower than that from 1-butene pyrolysis. Furthermore, 64 individual two- to seven-ring PAH products have been identified from 1-pentene pyrolysis at 1000 °C, all of which are reported here as first-time identifications of PAH products from 1-pentene pyrolysis.

This experimental study of propylene pyrolysis, 1-butene pyrolysis, and 1-pentene pyrolysis has helped to elucidate the role allylic radicals play in the formation- and growth-reactions of one-ring aromatics and PAH. Not only have we learned that the allyl radical can participate in radical/radical combination reactions leading to the formation and growth of various aromatic products, but this study has also shown that the allyl radical is a rich source of the C_3H_4 isomers propadiene and propyne, which themselves readily form propargyl radical, a key player in aromatic-formation and -growth reactions. Moreover, we have established that the methylallyl radical not only participates in formation reactions leading to one-ring aromatic products, it also is a rich source of the C_4H_6 hydrocarbon 1,3-butadiene. Lastly, this study shows that ethylallyl radical also readily forms 1,3-butadiene, a product that easily dehydrogenates to form butadienyl radical, which plays an important role in reactions leading to the formation and growth of PAH.

With respect to fuel-specific differences, this study shows that it is not possible to make the assumption that 1-alkene fuels with higher carbon numbers or weaker bonds automatically lead to greater production of PAH. Rather, the experiments show that—even though 1-pentene has the highest number of carbons and its decomposition begins at the lowest temperature of the three 1-

alkene fuels investigated—1-pentene does not produce the highest yield or number of PAH products. The ready formation of the ethyl radical during the first decomposition reaction of 1-pentene leads to the formation of extremely high yields of ethylene, which proves to be unconducive to PAH formation in this reaction environment. This finding means that the fuel fragments formed during the initial decomposition reactions of a fuel have a crucial impact on the fuel's propensity to form one-ring aromatic products and PAH products.

All of the products that are identified in this study as major products and are shown to be key players in the reactions leading to the formation and growth of PAH from 1-alkene pyrolysis—acetylene, propylene, propadiene, propyne, 1-butene, and 1,3-butadiene—are also present in the devolatilization products of solid fuels. Therefore, this study's findings about the temperature-dependent yield behavior of these $C_2 - C_4$ products and the resonantly stabilized radical species they produce—allyl, propargyl, methylallyl, and butadienyl—are important for understanding the PAH formation- and growth-mechanisms from the combustion of solid fuels. Furthermore, since the thermal decomposition products from the three 1-alkene fuels investigated are also produced from many gaseous and liquid practical fuels, the findings uncovered in this study—both the effects of fuel structure on the yields and distribution of products as well as their temperature-dependent yield behavior—have extended applicability to the field of liquid and gaseous fuel combustion.

5.2. Recommendations for Future Work

This present study can be expanded by performing pyrolysis experiments of the three fuels at varying residence times, while keeping the pyrolysis temperature constant. Residence-time experiments are especially of interest for 1-pentene pyrolysis, due to the extremely high yields of ethylene formed from 1-pentene pyrolysis at 0.31 s. Particularly at higher temperatures, where ethylene can readily dehydrogenate and form acetylene (a key player in aromatic-formation and -growth reactions), 1-pentene pyrolysis experiments at higher residence times would be of interest. In comparison to 1-pentene pyrolysis experiments at 1000 °C and 0.31 s, preliminary experiments of 1-pentene pyrolysis at 1000 °C and 0.51 s have shown that the yield of ethylene is significantly lower, but the yield of PAH is higher. Experiments at a wider range of residence times would have to be performed in order to be able to adequately observe the effects of residence time on the product yields of 1-pentene pyrolysis.

To further extend the findings about the influence of molecular fuel-structure on the formation and growth reactions of PAH, it would be helpful to conduct pyrolysis experiments with an alkene fuel that is not a 1-alkene. A good candidate for such experiments would be the C_4 alkene 2-butene, since it has the same number of carbon and hydrogen atoms as 1-butene and only differs from its isomer by the position of the double bond within the fuel structure. The position of the double bond has a large influence on the bond-dissociation energies of the different molecular bonds within the fuel, and the decomposition behavior of the fuel is greatly affected by those bond-dissociation energies. Since, as we have shown in this study, the initial decomposition reactions of the fuel have a significant impact on the fuel's pyrolytic behavior, 2-butene pyrolysis experiments could help uncover the effects of the double bond placement on: 1) the conversion of the fuel, 2) the temperature-dependent yields of major aliphatic species produced, and 3) the fuel's propensity to form one-ring aromatic and PAH products.

The findings uncovered in this dissertation highlight the importance of resonantly stabilized radicals—especially allyl, propargyl, methylallyl, butadienyl, and ethylallyl, but also benzyl, indenyl, and phenalenyl—in the reactions leading to the formation and growth of aromatic compounds. Additionally, the 1-alkene pyrolysis experiments show that each of the investigated fuels produce a small amount of the C_5 hydrocarbon cyclopentadiene, which can readily undergo hydrogen-atom loss and form cyclopentadienyl radical. Cyclopentadienyl is another radical with resonance stability that can participate in reactions leading to the formation of one-ring aromatic products, as shown in Reaction 17 in Section 3.3, and PAH. Therefore, it would be useful to further investigate the role of cyclopentadienyl in the formation of aromatic compounds. To this end, 1-butene/dicyclopentadiene co-pyrolysis experiments could prove to be useful. Dicyclopentadiene is a compound that readily forms cyclopentadienyl radicals, and 1-butene would be a good choice for the co-pyrolysis experiments with dicyclopentadiene, since it reacts at relatively low temperatures and provides, as this study shows, many C_2 – C_4 species important for aromatic growth. The increase in concentration of cyclopentadienyl radicals provided from dicyclopentadiene could help elucidate the importance of reactions leading to one-ring aromatic products—such as the cross-reaction of cyclopentadienyl radicals with propargyl radicals to form styrene (Reaction 17)—and PAH.

References

[1] International Energy Outlook 2010, U. S. Department of Energy, Energy Information Administration (EIA), 2010 Report No. DOE/EIA-0484.

[2] Adam Sieminski, International Energy Outlook, Deloitte Oil and Gas Conference, Houston TX, 2013.

[3] M. Balat, *Energy Sources Part B* 5: 2010, 50-62.

[4] L. Ruth, *Journal of Energy Resources Technology* 123: 2001, 4-9.

[5] S. C. Bhattacharya, P. A. Salam, M. Sharma, *Energy* 25: 2000, 169-188.

[6] M. Balat, G. Ayar, *Energy Sources* 27: 2005, 931-940.

[7] E.B. Ledesma, M.A. Kalish, P.F. Nelson, M.J. Wornat, J.C. Mackie, *Fuel* 79: 2000, 1801-1814.

[8] R. Cypress, *Fuel Pro. Tech*. 15: 1987, 1-15.

[9] C.A.III. Pope, R.T. Burnett, M.J. Thun, E.E. Calle, D. Krewski, K. Ito, G.D; Thurston, *J. Am. Med. Assoc.* 287: 2002, 1132–1141.

[10] A. Nel, *Science* 308: 2005, 804–806.

[11] M. J. Wornat, A. F. Sarofim, J. P. Longwell, *Energy & Fuels* 1: 1987, 431-437.

[12] B. S. Haynes, H. G. Wagner, *Prog. Energy Combust. Sci.* 7: 1981, 229-273.

[13] J. D. Bittner, J. B. Howard, *Proc. Combust. Inst.* 18: 1981, 1105-1116.

[14] J. L. Durant, W. F. Busby, Jr., A. L. Lafleur, B. W. Penman, C. L. Crespi, *Mutation Research* 371: 1996, 123-157

[15] J. L. Durant, A. L. Lafleur, W. F. Busby, Jr., L. L. Donhoffner, B. W. Penman, C. L. Crespi, *Mut. Res.* 446: 1999, 1-14.

[16] J. B. Howard, J. P. Longwell, J. A. Marr, C. J. Pope, W. F. Busby, Jr., A. L. Lafleur, K. Taghizadeh, *Combust. Flame* 101: 1995, 262-270

[17] A. Dipple, R. C. Moschel, C. A. H. Bigger, *Chem. Carc.*: 1984, 41-164.

[18] M.J. Wornat, B.A. Vernaglia, A.L. Lafleur, E.F. Plummer, K. Taghizadeh, P.F. Nelson, C-Z. Li, A. Necula, L.T. Scott, *Proc. Combust. Inst*. 27: 1998, 1677-1686.

[19] M.J., Wornat, E.B. Ledesma, A.K. Sandrowitz, M.J. Roth, S.M. Dawsey, Y.L. Qiao, W. Chen, *Environ. Sci. Technol.* 35: 2001, 1943-1952.

[20] A.L. Lafleur, A.F. Sarofim, M.J. Wornat, *Energy Fuels* 7: 1993, 357-361.

[21] T.G. Benish, A.L. Lafleur, K. Taghizadeh, J.B. Howard, *Proc. Combust. Inst*. 26: 1996, 2319-2326.

[22] M.L. Somers, M.J. Wornat, *Polycyc. Arom. Comp.* 27: 2007, 27: 261-280.

[23] J.C. Fetzer, J.R. Kershaw, *Fuel* 74: 1995, 1533-1536.

[24] G. Grimmer, J. Jacob, G. Dettbarn, K.W. Naujack, *Fresenius' Z. Anal. Chem.* 322: 1985, 595-602.

[25] P.F. Nelson, I.W. Smith, R. J. Tyler, J. C. Mackies, *Energy Fuels* 2: 1988, 391-400.

[26] T. Streibel, R. Geißler, M. Saraji-Bozorgzad, M. Sklorz, E. Kaisersberger, T. Denner, R. Zimmermann, *J Therm Anal Calorim.* 96: 2009, 795–804

[27] W.H. Calkins, R.J. Tyler, *Fuel* 63: 1984, 487-494.

[28] M. Safarova, J. Kusy, L. Andel, *Fuel* 84: 2005, 2280–2285.

[29] R.J. Tyler, *Fuel* 59: 1980, 218-226.

[30] J.A. Caballero, R. Font, A. Marcilla, *J. Anal. Appl. Pyrolysis* 39: 1997, 161-183.

[31] M. Olsson, O. Ramnas and G. Petersson, *J. Anal. Appl. Pyrolysis* 71: 2004, 847-854.

[32] G. Barrefors, G. Petersson, *J. Chromatogr. A* 710: 1995, 71-77.

[33] W. Schmidt, G. Grimmer, J. Jacob, G. Dettbarn, K.W. Naujack, *Fresenius' Z. Anal. Chem.* 326: 1987, 401-413.

[34] Luo, Y.-R.; Handbook of Bond Dissociation Energies in Organic Chemistry, CRC Press, Boca Raton, FL, 2003

[35] S. Benson, *J. Chem. Educ.* 42: 1965, 502-518.

[36] Lee, J. C. Y. Simulations of Two-Dimensional Chemically Reactive Flows. Ph.D. Thesis, Princeton University, Princeton, 1996.

[37] E. Gorin, A.G. Oblad, R.F. Schmuck, *Ind. Eng. Chem.* 38: 1946, 1187–1193.

[38] M. Kamphus, M. Braun-Unkhoff, K. Kohse-Höinghaus, *Combust. Flame* 152: 2008, 28-59.

[39] G. A. Chappell, H. Shaw, *J. of Phys. Chem.* 72: 1968, 4672-4675.

[40] T. Kunugi, K. Soma, T. Sakai, *Ind. Eng. Chem. Res.* 9: 1970, 319-324.

[41] V. Subba Rao, G. B. Skinner, *J. of Phys. Chem*. 93: 1989, 1869-1876

[42] Y. Hidaka, T. Nakamura, H. Tanaka, A. Jinno, H. Kawano, T. Higashihara, *Ind. J. Chem. Kin.* 24: 1992, 761-780.

[43] S. G. Davis, C. K. Law, H. Wang, *Combust. Flame* 119: 1999, 375-399. (1999)

[44] H.Gg. Wagner, R. Zellner, *Ber. Bunsen-Ges. Phys. Chem.* 76: 1972, 518–25.

[45] C.H. Wu, R.D. Kern, *J. Phys. Chem.* 91: 1987, 6291–6296.

[46] Y. Hidaka, T. Nakamura, A. Miyauchi, T. Shiraishi, H. Kawano, *Int. J. Chem. Kinet.* 21: 1989, 643–666.

[47] P. Dagaut, M. Cathonnet, J-C. Boettner, *Combust. Sci. Technol.* 71: 1990, 111–128.

[48] P. Dagaut, M. Cathonnet, B. Aboussi, J-C. Boettner*, J. Chem. Phys. Phys.-Chem. Bio.* 1990, 87, 1159–1172.

[49] J. A. Miller, J. V. Volponi, J-F. Pauwels, *Combust. Flame* 105: 1996, 451–461.

[50] C. S. McEnally, L.D. Pfefferle, *Combust. Flame* 112: 1998, 545–558.

[51] S. G. Davis, C. K. Law, H.J. Wang, *Phys. Chem. A* 103: 1999, 5889–5899.

[52] T. Faravelli, A. Goldinaga, L. Zappella, E. Ranzi, P. Dagaut, M. Cathonnet, *Proc. Combust. Inst.* 28: 2000, 2601–2608.

[53] M. Kamphus, M. Braun-Unkhoff, K. Kohse-Höinghaus, *Combust. Flame* 152: 2008, 28–59.

[54] N. Hansen, J. A. Miller, P. R. Westmoreland, T. Kasper, K. Kohse-Höinghaus, J. Wang, T. Cool, *Combust. Flame* 156: 2009, 2153–2164.

[55] Y. Fenard, G. Dayma, F. Halter, F. Foucher, Z. Serinyel, P. Dagaut, *Energy Fuel* 29: 2015, 1107-1118.

[56] M. Schenk, L. Leon, K. Moshammer, P. Oßwald, T. Zeuch, L. Seidel, F. Mauss, K. Kohse-Höinghaus, *Combust. Flame* 160: 2013, 487-503.

[57] Y. Zhang, J. Cai, L. Zhao, J. Yang, H. Jin, Z. Cheng, Y. Li, L. Zhang, F. Qi, *Combust. Flame* 159: 2012, 905-917.

[58] J.L. Miller, *J. Phys. Chem. A* 108: 2004, 2268 – 2277.

[59] S.W. Benson, G.R.J. Haugen, *Phys. Chem.* 71: 1967, 1735–1746.

[60] J.A. Cole, J. D. Bittner, J. P. Longwell, J. B. Howard, *Combust. Flame* 56: 1984, 51-70.

[61] H. Wang, M. Frenklach, *Combust. Flame* 110: 1997, 173–221.

[62] J.H. Kiefer, H.C. Wei, R.D. Kern, C.H. Wu, *Int. J. Chem. Kinet*. 17: 1985, 225–253.

[63] Laskin, A.; Wang, H.; Law, C. K. *Int. J. Chem. Kinet.* 2000, 32, 589–614.

[64] Y. Hidaka, T. Higashihara, N. Ninomiya, H. Masaoka, T. Nakamura, H. Kawano, *Int. J. Chem. Kinet.* 28: 1996, 137–151.

[65] M. Frenklach, D.W. Clary, W.C. Gardiner Jr., S. E. Stein, *Proc. Combust. Inst*. 21: 1986, 1067–1076.

[66] S. Touchard, F. Buda, G. Dayma, P.A. Glaude, R. Fournet, F. Battin-Leclerc, *Int. J. Chem. Kin.* 37: 2005, 451-463.

[67] G. González Alatorre, H. Böhm, B. Atakan, K. Kohse-Höinghaus, *Z. f. Phys. Chem*. 215: 2001, 981-995.

[68] W. Tsang, *J. Phys. Chem. A* 110: 2006, 8501-8509.

[69] Y. Cheng, E. Hu, F. Deng, F. Yang, Y. Zhang, C. Tang, Z. Huang, *Fuel* 172: 2016, 263-272.

[70] N.B. Poddar, S. Thomas, M.J. Wornat, *Proc Combust. Inst*. 33: 2011, 541-548.

[71] Y. Georgievskii, J.A. Miller, S. Klippenstein, *Phys. Chem. Chem. Phys*, 9: 2007, 4259-4268.

[72] L.B. Harding, S.J. Klippenstein, *Proc. Combust. Inst.* 28: 2000, 1503-1509.

[73] J.A. Miller, S.J. Klippenstein, Y. Georgievskii, L.B. Harding, W.D. Allen, A.C. Simmonett, *J. Phys. Chem. A*, 114: 2010, 4881-4890.

[74] N. Hansen, J.A. Miller, T. Kasper, K. Kohse-Höinghaus, P.R. Westmoreland, J. Wang, T. Cool, *Proc. Combust. Inst.* 32: 2009, 623–630.

[75] M. B. Colket, *Proc. Comb. Inst.* 21: 1986, 851–864.

[76] H. Wang, M.J. Frenklach, *Phys. Chem.* 98: 1994, 11465–11489.

[77] S. Thomas, M.J. Wornat, *Proc Combust. Inst.* 32: 2009, 615-622.

[78] NB. Poddar, S. Thomas, M.J. Wornat, *Proc Combust. Inst.* 34: 2013, 1775-1783.

[79] K. Wang, S.M. Villano, A.M Dean, *Phys. Chem. Chem. Phys.* 17: 2015, 6255-6273.

[80] N.B. Poddar, An Experimental Investigation of the Role of Small Hydrocarbons and Combustion-Generated Nanoparticles on the Formation and Growth Reactions of Polycyclic Aromatic Hydrocarbons During the Pyrolysis of a Model-Fuel and Hydrocarbon Gases, Ph.D. Thesis, Department of Chemical Engineering, Louisiana State University, 2012.

[81] J. D. Bittner, J. B. Howard, *Proc. Comb. Inst.* 18: 1981, 1105–1116.

[82] Y. Li, J. Cai, L. Zhang, J. Yang, Z. Wang, F. Qi, *Proc. Combust. Inst.* 33: 2011, 617-624.

[83] S. B. Dworkin, Q. Zhang, M. J. Thomson, N. A. Slavinskaya, U. Riedel, *Combust. Flame* 158: 2011, 1682–1695.

[84] K. Norinaga, O. Deutschmann, N. Saegusa, J-I. Hayashi, *J. Anal. Appl. Pyrolysis* 86: 2009, 148-160.

[85] S.V. Kalpathy, N.B. Poddar, S.P. Bagley, M.J. Wornat, *Proc. Combust. Inst.* 35: 2015, 1833 -1841.

[86] S.V. Kalpathy, N.B. Poddar, E.A. Hurst, E.C. Caspary, M.J. Wornat, *Proc. Combust. Inst.* 36: 2017, 965-973.

Appendix: Supplemental Materials

Table A.1. Temperature calibrations of furnace at nine temperatures between 600 and 1000 °C.

Desired Temperature (°C)	Temperature (°C) at Distance from Front of Reactor (inch)											
	9	11	13	15	17	19	21	23	25	27	29	31
600	592	596	602	599	600	600	600	600	600	601	600	598
650	647	649	653	648	651	650	649	650	650	652	650	644
700	686	694	703	698	700	700	700	701	700	702	700	698
750	738	744	752	748	750	749	750	750	750	752	750	744
800	797	798	903	799	801	800	800	800	800	803	800	798
850	841	849	851	852	850	852	850	850	850	852	850	843
900	893	898	903	899	900	900	900	900	900	903	901	893
950	938	945	951	949	951	953	952	951	952	953	950	942
1000	991	997	1002	1000	1001	1001	1000	1000	999	1003	1001	991

Table A.2. Response factors and GC retention times for the C_1 – C_6 hydrocarbons (FID) and for H_2 (TCD).

Compound	Retention Time	Response Factor (ppm/area)
methane	0.95	5.063
ethane	1.40	2.672
ethylene	1.76	2.656
acetylene	2.88	2.043
propane	3.73	1.725
propylene	6.88	1.833
propadiene	7.05	1.830
1-butene	12.88	1.383
propyne	12.92	1.718
1,3-butadiene	13.87	1.376
trans-2-butene	14.12	1.383
isobutene	14.33	1.383
cis-2-butene	14.60	1.383
vinylacetylene	15.79	1.376
1-pentene	17.70	1.073
1-butyne	18.06	1.376
isoprene	19.08	1.172
cyclopentadiene	19.32	1.172
trans-1,3-pentadiene	19.80	1.172
cis-1,3-pentadiene	19.87	1.172
2-butyne	20.67	1.376
1,5-hexadiene	21.87	0.967
benzene	22.60	0.967
H_2	1.56	35.080

Table A.3. Response factors and GC retention times for one- and two-ring aromatics.

Compound	Retention Time	Response Factor ((mg/ml)/area)
toluene	7.2	3.87E-09
ethylbenzene	10.4	3.82E-09
phenylacetylene	11.0	3.74E-09
styrene	11.5	3.80E-09
indene	17.9	6.08E-09
naphthalene	22.7	5.43E-09
2-methylnaphthalene	26.5	5.29E-09
1-methylnaphthalene	27.1	5.29E-09
biphenyl	29.3	6.13E-09
2-vinylnaphthalene	29.9	5.29E-09
2-ethynylnaphthalene	30.9	5.29E-09
acenaphthylene	31.5	5.33E-09
fluorene	35.4	5.24E-09
phenanthrene	40.8	5.23E-09
anthracene	41.0	5.47E-09

Table A.4. Response factors and HPLC retention times for PAH.

Compound	Retention Time	Linear Range Concentration (mg/ml) = m * area	Non-linear Range Concentration (mg/ml) = m1 * area + m2 *area ^2	
		m	m1	m2
naphthalene	15.3	2.08E-05	3.38E-08	3.56E-05
acenaphthylene	17.1	2.09E-05	1.02E-08	3.19E-05
acenaphthene	19.9	1.68E-05	2.21E-08	3.08E-05
fluorene	20.8	1.37E-05	1.41E-08	3.39E-05
phenanthrene	22.6	9.10E-06	8.18E-09	2.00E-05
anthracene	24.4	3.75E-06	1.34E-08	1.78E-05
fluoranthene	26.4	1.60E-05	3.06E-09	2.12E-05
pyrene	28.0	1.49E-05	3.61E-09	2.04E-05
benz[*a*]anthracene	33.2	1.10E-05	2.76E-09	1.63E-05
chrysene	34.3	1.16E-05	3.59E-09	1.69E-05
benzo[*b*]fluoranthene	38.7	1.19E-05	1.34E-09	1.56E-05
benzo[*k*]fluoranthene	40.6	1.16E-05	1.22E-09	1.47E-05
benzo[*a*]pyrene	42.2	1.67E-05	1.02E-09	2.00E-05
dibenz[*a,h*]anthracene	45.1	1.30E-05	1.77E-09	1.62E-05
benzo[*ghi*]perylene	46.8	1.82E-05	1.17E-09	2.26E-05
indeno[1,2,3-*cd*]-pyrene	48.2	1.36E-05	5.14E-10	1.61E-05

Table A.5. PAH products of 1-butene pyrolysis in Figure 4.2.

Product Name (by Class)	**Formula**	**Structure**	**First-Time Identification as Product of 1-Butene Pyrolysis?**
Benzenoid PAH (black structures in Figure 4.2.)			
Naphthalene	$C_{10}H_8$	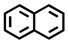	
Phenanthrene	$C_{14}H_{10}$	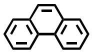	✓
Anthracene	$C_{14}H_{10}$	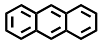	✓
Pyrene	$C_{16}H_{10}$	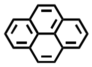	✓
Benzo[*c*]phenanthrene	$C_{18}H_{12}$	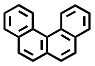	✓
Triphenylene	$C_{18}H_{12}$	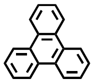	✓
Benz[*a*]anthracene	$C_{18}H_{12}$	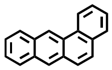	✓
Chrysene	$C_{18}H_{12}$	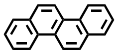	✓
Benzo[*e*]pyrene	$C_{20}H_{12}$	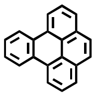	✓
Perylene	$C_{20}H_{12}$	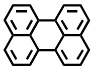	✓
Benzo[*a*]pyrene	$C_{20}H_{12}$	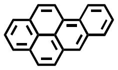	✓

Table A.5. *(continued)*

Product Name (by Class)	**Formula**	**Structure**	**First-Time Identification as Product of 1-Butene Pyrolysis?**
Benzo[*ghi*]perylene	$C_{22}H_{12}$	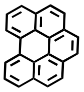	✓
Anthanthrene	$C_{22}H_{12}$	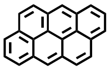	✓
Dibenz[*a,j*]anthracene	$C_{22}H_{14}$	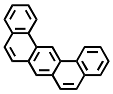	✓
Dibenz[*a,h*]anthracene	$C_{22}H_{14}$	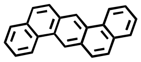	✓
Benzo[*b*]chrysene	$C_{22}H_{14}$	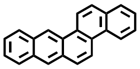	✓
Picene	$C_{22}H_{14}$	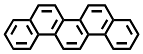	✓
Coronene	$C_{24}H_{12}$	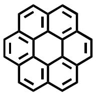	✓
Naphtho[1,2-*a*]pyrene	$C_{24}H_{14}$	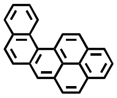	✓
Dibenzo[*a,e*]pyrene	$C_{24}H_{14}$	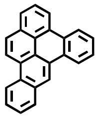	✓
Naphtho[2,1-*a*]pyrene	$C_{24}H_{14}$	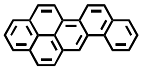	✓

Table A.5. *(continued)*

Product Name (by Class)	**Formula**	**Structure**	**First-Time Identification as Product of 1-Butene Pyrolysis?**
Naphtho[2,3-*a*]pyrene	$C_{24}H_{14}$	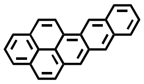	✓
Dibenzo[*cd,lm*]perylene	$C_{26}H_{14}$	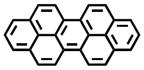	✓
Fluoranthene Benzologues (dark blue structures in Figure 4.2.)			
Fluoranthene	$C_{16}H_{10}$	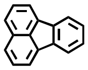	✓
Benzo[*a*]fluoranthene	$C_{20}H_{12}$	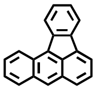	✓
Benzo[*j*]fluoranthene	$C_{20}H_{12}$	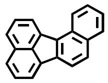	✓
Benzo[*b*]fluoranthene	$C_{20}H_{12}$	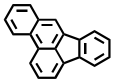	✓
Benzo[*k*]fluoranthene	$C_{20}H_{12}$	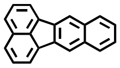	✓
Indeno[1,2,3-*cd*]pyrene	$C_{22}H_{12}$	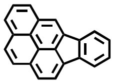	✓
Indeno[1,2,3-*cd*]fluoranthene[a]	$C_{22}H_{12}$	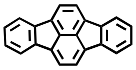	✓

Table A.5. *(continued)*

Product Name (by Class)	**Formula**	**Structure**	**First-Time Identification as Product of 1-Butene Pyrolysis?**
Indene Benzologues (green structures in Figure 4.2.)			
Indene	C_9H_8	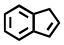	
Fluorene	$C_{13}H_{10}$	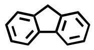	✓
Benz[*e*]indene	$C_{13}H_{10}$	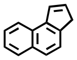	✓
Benz[*f*]indene	$C_{13}H_{10}$	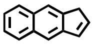	✓
4*H*-Cyclopenta[*def*]phenanthrene	$C_{15}H_{10}$	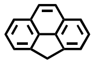	✓
Inden[2,1-*a*]indene	$C_{16}H_{10}$	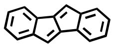	✓
Benzo[*a*]fluorene	$C_{17}H_{12}$	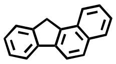	✓
Benzo[*b*]fluorene	$C_{17}H_{12}$	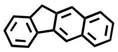	✓
4*H*-Cyclopenta[*def*]chrysene	$C_{19}H_{12}$	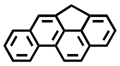	✓
4*H*-Benzo[*def*]-cyclopenta[*mno*]chrysene	$C_{21}H_{12}$	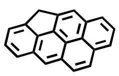	✓
Cyclopenta-Fused PAH (red structures in Figure 4.2.)			
Acenaphthylene	$C_{12}H_8$	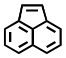	✓

Table A.5. *(continued)*

Product Name (by Class)	**Formula**	**Structure**	**First-Time Identification as Product of 1-Butene Pyrolysis?**
Pyracylene	$C_{14}H_8$	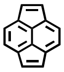	✓
Acephenanthrylene	$C_{16}H_{10}$	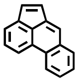	✓
Aceanthrylene	$C_{16}H_{10}$	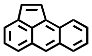	✓
Cyclopent[*hi*]acephenanthrylene	$C_{18}H_{10}$	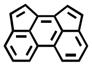	✓
Cyclopenta[*cd*]pyrene	$C_{18}H_{10}$	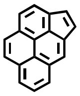	✓
Cyclopenta[*cd*]fluoranthene	$C_{18}H_{10}$	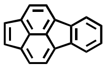	✓
Ethynyl-Substituted Species (purple structures in Figure 4.2.)			
2-Ethynylnaphthalene	$C_{12}H_8$	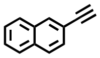	✓
1-Ethynylacenaphthylene	$C_{14}H_8$	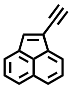	✓
3-Ethynylphenanthrene	$C_{16}H_{10}$	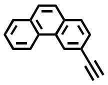	✓
2-Ethynylanthracene	$C_{16}H_{10}$	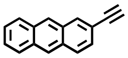	✓

Table A.5. *(continued)*

Product Name (by Class)	**Formula**	**Structure**	**First-Time Identification as Product of 1-Butene Pyrolysis?**
2-Ethynylpyrene	$C_{18}H_{10}$	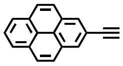	✓
Bi-aryls (gray structures in Figure 4.2.)			
Biphenyl	$C_{12}H_{10}$	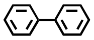	✓
1-Phenylnaphthalene	$C_{16}H_{12}$	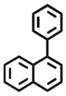	✓
2-Phenylnaphthalene	$C_{16}H_{12}$	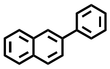	✓
Methyl-Substituted Aromatics and Acenaphthene (light blue structures in Figure 4.2.)			
1-Methylnaphthalene	$C_{11}H_{10}$	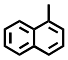	✓
2-Methylnaphthalene	$C_{11}H_{10}$	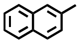	✓
3-Methylphenanthrene	$C_{15}H_{12}$	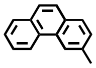	✓
1-Methylanthracene	$C_{15}H_{12}$	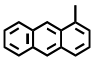	✓
2-Methylanthracene	$C_{15}H_{12}$	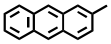	✓
1-Methylpyrene	$C_{17}H_{12}$	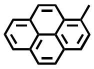	✓

Table A.5. *(continued)*

Product Name (by Class)	**Formula**	**Structure**	**First-Time Identification as Product of 1-Butene Pyrolysis?**
2-Methylpyrene	$C_{17}H_{12}$	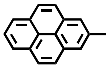	✓
4-Methylpyrene	$C_{17}H_{12}$	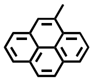	✓
Acenaphthene	$C_{12}H_{10}$	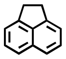	✓
Vinyl-Substituted Aromatics (pink structures in Figure 4.2.)			
1-Vinylnaphthalene	$C_{12}H_{10}$	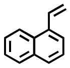	✓
2-Vinylnaphthalene	$C_{12}H_{10}$	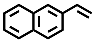	✓
Phenalene-Type Compounds (olive structures in Figure 4.2.)			
Phenalene	$C_{13}H_{10}$		✓
7*H*-Benz[*de*]anthracene	$C_{17}H_{12}$	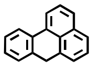	✓
6*H*-Benzo[*cd*]pyrene	$C_{19}H_{12}$	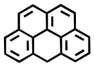	✓

[a] Indeno[1,2,3-*cd*]fluoranthene is an indeno-fused fluoranthene.

Table A.6. PAH products of propylene pyrolysis in Figure A.3.

Product Name (by Class)	**Formula**	**Structure**	**First-Time Identification as Product of Propylene Pyrolysis?**
Benzenoid PAH (black structures in Figure A.3.)			
Naphthalene	$C_{10}H_8$	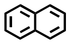	
Phenanthrene	$C_{14}H_{10}$	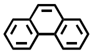	
Anthracene	$C_{14}H_{10}$	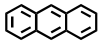	
Pyrene	$C_{16}H_{10}$	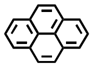	
Benzo[*c*]phenanthrene	$C_{18}H_{12}$	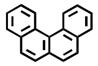	✓
Triphenylene	$C_{18}H_{12}$	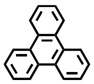	✓
Benz[*a*]anthracene	$C_{18}H_{12}$	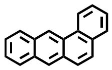	
Chrysene	$C_{18}H_{12}$	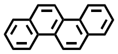	
Benzo[*e*]pyrene	$C_{20}H_{12}$	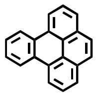	
Perylene	$C_{20}H_{12}$	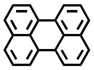	
Benzo[*a*]pyrene	$C_{20}H_{12}$	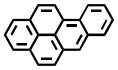	

Table A.6. *(continued)*

Product Name (by Class)	**Formula**	**Structure**	**First-Time Identification as Product of Propylene Pyrolysis?**
Benzo[*ghi*]perylene	$C_{22}H_{12}$	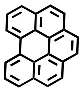	
Anthanthrene	$C_{22}H_{12}$	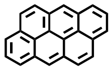	
Dibenz[*a,h*]anthracene	$C_{22}H_{14}$	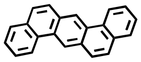	✓
Benzo[*b*]chrysene	$C_{22}H_{14}$	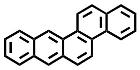	✓
Coronene	$C_{24}H_{12}$	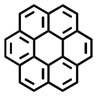	
Fluoranthene Benzologues (dark blue structures in Figure A.3.)			
Fluoranthene	$C_{16}H_{10}$	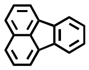	
Benzo[*a*]fluoranthene	$C_{20}H_{12}$	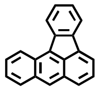	✓
Benzo[*j*]fluoranthene	$C_{20}H_{12}$	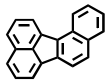	✓
Benzo[*b*]fluoranthene	$C_{20}H_{12}$	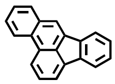	✓
Benzo[*k*]fluoranthene	$C_{20}H_{12}$	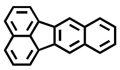	

Table A.6. *(continued)*

Product Name (by Class)	**Formula**	**Structure**	**First-Time Identification as Product of Propylene Pyrolysis?**
Indeno[1,2,3-*cd*]pyrene	$C_{22}H_{12}$	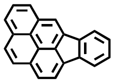	
Indene Benzologues (green structures in Figure A.3.)			
Indene	C_9H_8	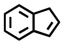	
Fluorene	$C_{13}H_{10}$	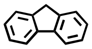	
Benz[*e*]indene	$C_{13}H_{10}$	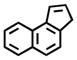	✓
Benz[*f*]indene	$C_{13}H_{10}$	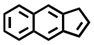	✓
4*H*-Cyclopenta[*def*]phenanthrene	$C_{15}H_{10}$	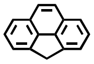	
Inden[2,1-*a*]indene	$C_{16}H_{10}$	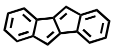	✓
Benzo[*a*]fluorene	$C_{17}H_{12}$	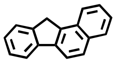	✓
Benzo[*b*]fluorene	$C_{17}H_{12}$	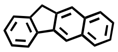	✓
4*H*-Cyclopenta[*def*]chrysene	$C_{19}H_{12}$	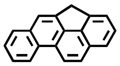	
Cyclopenta-Fused PAH (red structures in Figure A.3.)			
Acenaphthylene	$C_{12}H_8$	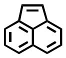	

Table A.6. *(continued)*

Product Name (by Class)	**Formula**	**Structure**	**First-Time Identification as Product of Propylene Pyrolysis?**
Pyracylene	$C_{14}H_8$	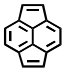	✓
Acephenanthrylene	$C_{16}H_{10}$	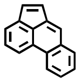	
Aceanthrylene	$C_{16}H_{10}$	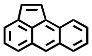	✓
Cyclopent[*hi*]acephenanthrylene	$C_{18}H_{10}$	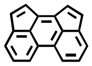	✓
Cyclopenta[*cd*]pyrene	$C_{18}H_{10}$	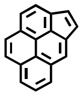	✓
Cyclopenta[*cd*]fluoranthene	$C_{18}H_{10}$	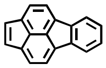	✓
Ethynyl-Substituted Species (purple structures in Figure A.3.)			
2-Ethynylnaphthalene	$C_{12}H_8$	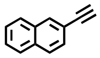	✓
1-Ethynylacenaphthylene	$C_{14}H_8$	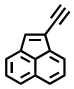	✓
3-Ethynylphenanthrene	$C_{16}H_{10}$	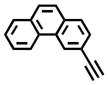	✓
2-Ethynylanthracene	$C_{16}H_{10}$	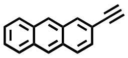	✓

Table A.6. *(continued)*

Product Name (by Class)	**Formula**	**Structure**	**First-Time Identification as Product of Propylene Pyrolysis?**
Bi-aryls (gray structures in Figure A.3.)			
Biphenyl	$C_{12}H_{10}$	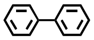	✓
1-Phenylnaphthalene	$C_{16}H_{12}$	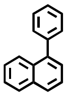	✓
2-Phenylnaphthalene	$C_{16}H_{12}$	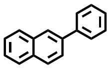	
Methyl-Substituted Aromatics and Acenaphthene (light blue structures in Figure A.3.)			
1-Methylnaphthalene	$C_{11}H_{10}$	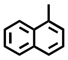	
2-Methylnaphthalene	$C_{11}H_{10}$	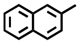	
3-Methylphenanthrene	$C_{15}H_{12}$	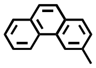	✓
1-Methylanthracene	$C_{15}H_{12}$	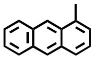	✓
2-Methylanthracene	$C_{15}H_{12}$	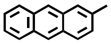	✓
1-Methylpyrene	$C_{17}H_{12}$	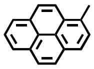	✓
2-Methylpyrene	$C_{17}H_{12}$	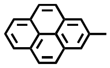	✓

Table A.6. *(continued)*

Product Name (by Class)	**Formula**	**Structure**	**First-Time Identification as Product of Propylene Pyrolysis?**
4-Methylpyrene	$C_{17}H_{12}$	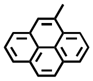	✓
Acenaphthene	$C_{12}H_{10}$	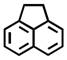	✓
Vinyl-Substituted Aromatics (pink structures in Figure A.3.)			
1-Vinylnaphthalene	$C_{12}H_{10}$	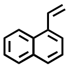	✓
2-Vinylnaphthalene	$C_{12}H_{10}$	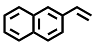	✓
Phenalene-Type Compounds (olive structures in Figure A.3.)			
Phenalene	$C_{13}H_{10}$		✓
7*H*-Benz[*de*]anthracene	$C_{17}H_{12}$	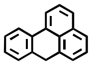	✓
6*H*-Benzo[*cd*]pyrene	$C_{19}H_{12}$	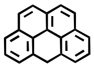	✓

Table A.7. PAH products of 1-pentene pyrolysis in Figure A.4.

Product Name (by Class)	**Formula**	**Structure**	**First-Time Identification as Product of 1-Pentene Pyrolysis?**
Benzenoid PAH (black structures in Figure A.4.)			
Naphthalene	$C_{10}H_8$	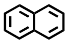	✓
Phenanthrene	$C_{14}H_{10}$	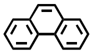	✓
Anthracene	$C_{14}H_{10}$	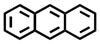	✓
Pyrene	$C_{16}H_{10}$	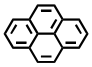	✓
Benzo[*c*]phenanthrene	$C_{18}H_{12}$	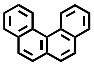	✓
Triphenylene	$C_{18}H_{12}$	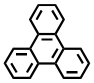	✓
Benz[*a*]anthracene	$C_{18}H_{12}$	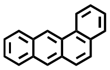	✓
Chrysene	$C_{18}H_{12}$	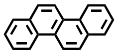	✓
Benzo[*e*]pyrene	$C_{20}H_{12}$	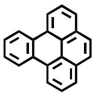	✓
Perylene	$C_{20}H_{12}$	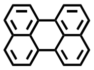	✓
Benzo[*a*]pyrene	$C_{20}H_{12}$	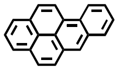	✓

Table A.7. *(continued)*

Product Name (by Class)	**Formula**	**Structure**	**First-Time Identification as Product of 1-Pentene Pyrolysis?**
Benzo[*ghi*]perylene	$C_{22}H_{12}$	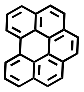	✓
Anthanthrene	$C_{22}H_{12}$	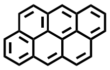	✓
Dibenz[*a,j*]anthracene	$C_{22}H_{14}$	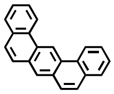	✓
Dibenz[*a,h*]anthracene	$C_{22}H_{14}$	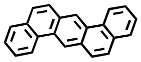	✓
Benzo[*b*]chrysene	$C_{22}H_{14}$	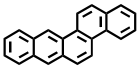	✓
Coronene	$C_{24}H_{12}$	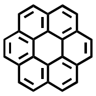	✓
Naphtho[2,1-*a*]pyrene	$C_{24}H_{14}$	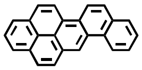	✓
Dibenzo[*cd,lm*]perylene	$C_{26}H_{14}$	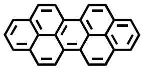	✓
Fluoranthene Benzologues (dark blue structures in Figure A.4.)			
Fluoranthene	$C_{16}H_{10}$	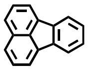	✓
Benzo[*a*]fluoranthene	$C_{20}H_{12}$	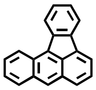	✓

Table A.7. *(continued)*

Product Name (by Class)	**Formula**	**Structure**	**First-Time Identification as Product of 1-Pentene Pyrolysis?**
Benzo[*j*]fluoranthene	$C_{20}H_{12}$	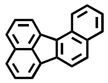	✓
Benzo[*b*]fluoranthene	$C_{20}H_{12}$	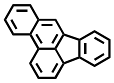	✓
Benzo[*k*]fluoranthene	$C_{20}H_{12}$	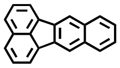	✓
Indeno[1,2,3-*cd*]pyrene	$C_{22}H_{12}$	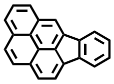	✓
Indene Benzologues (green structures in Figure A.4.)			
Indene	C_9H_8	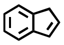	✓
Fluorene	$C_{13}H_{10}$	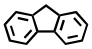	✓
Benz[*e*]indene	$C_{13}H_{10}$	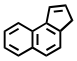	✓
Benz[*f*]indene	$C_{13}H_{10}$	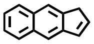	✓
4*H*-Cyclopenta[*def*]phenanthrene	$C_{15}H_{10}$	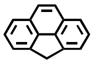	✓
Inden[2,1-*a*]indene	$C_{16}H_{10}$	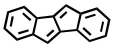	✓
Benzo[*a*]fluorene	$C_{17}H_{12}$	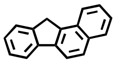	✓

Table A.7. *(continued)*

Product Name (by Class)	**Formula**	**Structure**	**First-Time Identification as Product of 1-Pentene Pyrolysis?**
Benzo[*b*]fluorene	$C_{17}H_{12}$	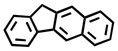	✓
4*H*-Cyclopenta[*def*]chrysene	$C_{19}H_{12}$	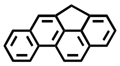	✓
4*H*-Benzo[*def*]-cyclopenta[*mno*]chrysene	$C_{21}H_{12}$	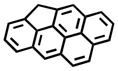	✓
Cyclopenta-Fused PAH (red structures in Figure A.4.)			
Acenaphthylene	$C_{12}H_8$		✓
Pyracylene	$C_{14}H_8$	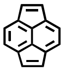	✓
Acephenanthrylene	$C_{16}H_{10}$	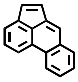	✓
Aceanthrylene	$C_{16}H_{10}$	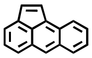	✓
Cyclopent[*hi*]acephenanthrylene	$C_{18}H_{10}$	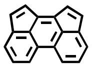	✓
Cyclopenta[*cd*]pyrene	$C_{18}H_{10}$	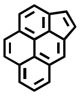	✓
Cyclopenta[*cd*]fluoranthene	$C_{18}H_{10}$	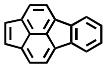	✓

Table A.7. *(continued)*

Product Name (by Class)	**Formula**	**Structure**	**First-Time Identification as Product of 1-Pentene Pyrolysis?**
Ethynyl-Substituted Species (purple structures in Figure A.4.)			
2-Ethynylnaphthalene	$C_{12}H_8$	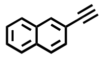	✓
1-Ethynylacenaphthylene	$C_{14}H_8$	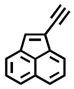	✓
3-Ethynylphenanthrene	$C_{16}H_{10}$	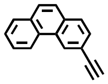	✓
2-Ethynylanthracene	$C_{16}H_{10}$	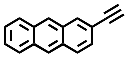	✓
2-Ethynylpyrene	$C_{18}H_{10}$	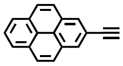	✓
Bi-aryls (gray structures in Figure A.4.)			
Biphenyl	$C_{12}H_{10}$	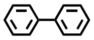	✓
1-Phenylnaphthalene	$C_{16}H_{12}$	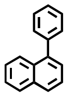	✓
2-Phenylnaphthalene	$C_{16}H_{12}$	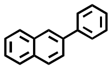	✓
Methyl-Substituted Aromatics and Acenaphthene (light blue structures in Figure A.4.)			
1-Methylnaphthalene	$C_{11}H_{10}$	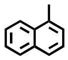	✓

Table A.7. *(continued)*

Product Name (by Class)	**Formula**	**Structure**	**First-Time Identification as Product of 1-Pentene Pyrolysis?**
2-Methylnaphthalene	$C_{11}H_{10}$	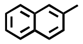	✓
3-Methylphenanthrene	$C_{15}H_{12}$	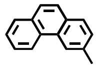	✓
1-Methylanthracene	$C_{15}H_{12}$	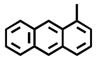	✓
2-Methylanthracene	$C_{15}H_{12}$	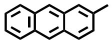	✓
1-Methylpyrene	$C_{17}H_{12}$	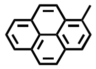	✓
2-Methylpyrene	$C_{17}H_{12}$	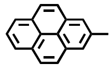	✓
4-Methylpyrene	$C_{17}H_{12}$	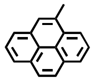	✓
Acenaphthene	$C_{12}H_{10}$	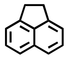	✓
Vinyl-Substituted Aromatics (pink structures in Figure A.4.)			
1-Vinylnaphthalene	$C_{12}H_{10}$	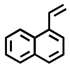	✓
2-Vinylnaphthalene	$C_{12}H_{10}$	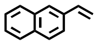	✓

Table A.7. *(continued)*

Product Name (by Class)	**Formula**	**Structure**	**First-Time Identification as Product of 1-Pentene Pyrolysis?**
Phenalene-Type Compounds (olive structures in Figure A.4.)			
Phenalene	$C_{13}H_{10}$		✓
7*H*-Benz[*de*]anthracene	$C_{17}H_{12}$	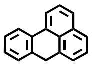	✓
6*H*-Benzo[*cd*]pyrene	$C_{19}H_{12}$	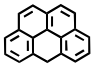	✓

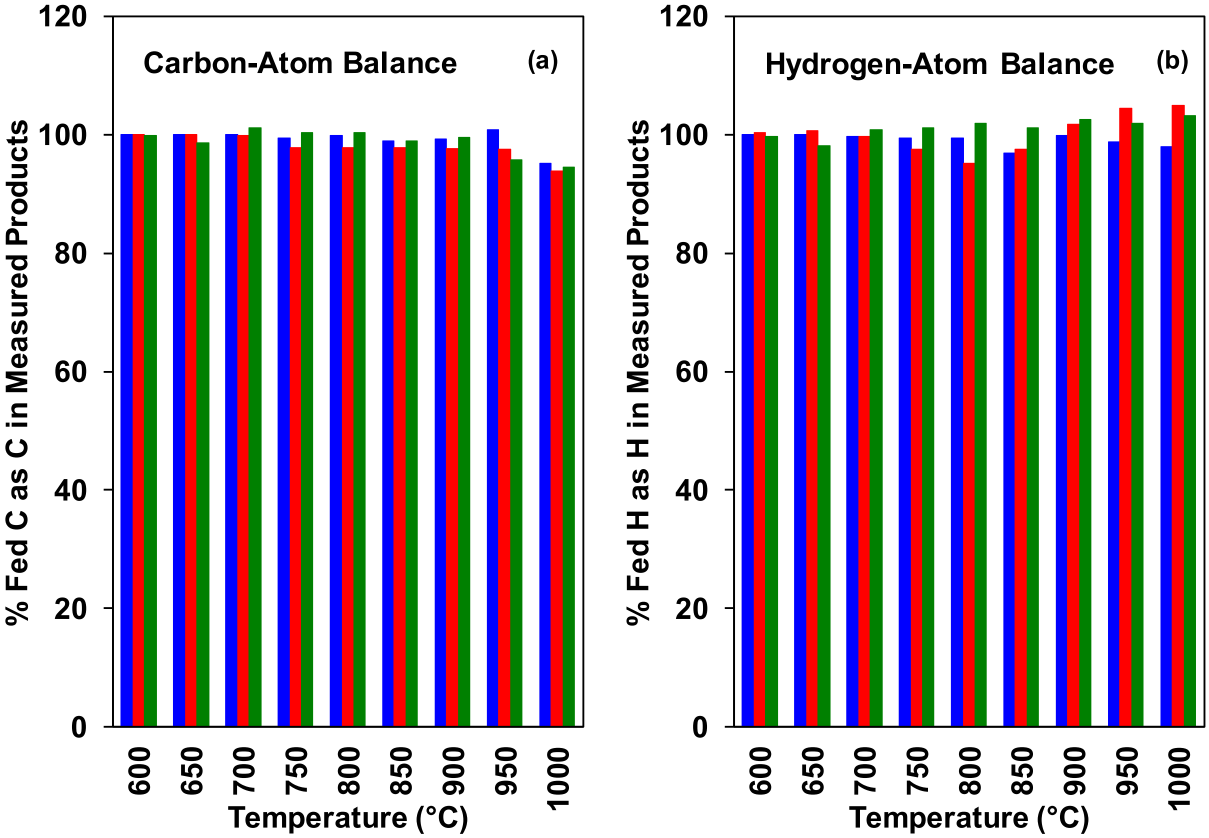

Figure A.1. (a) carbon-atom balance and (b) hydrogen-atom balance of propylene pyrolysis (blue bars), 1-butene pyrolysis (red bars), and 1-pentene pyrolysis (green bars) at 0.31 s.

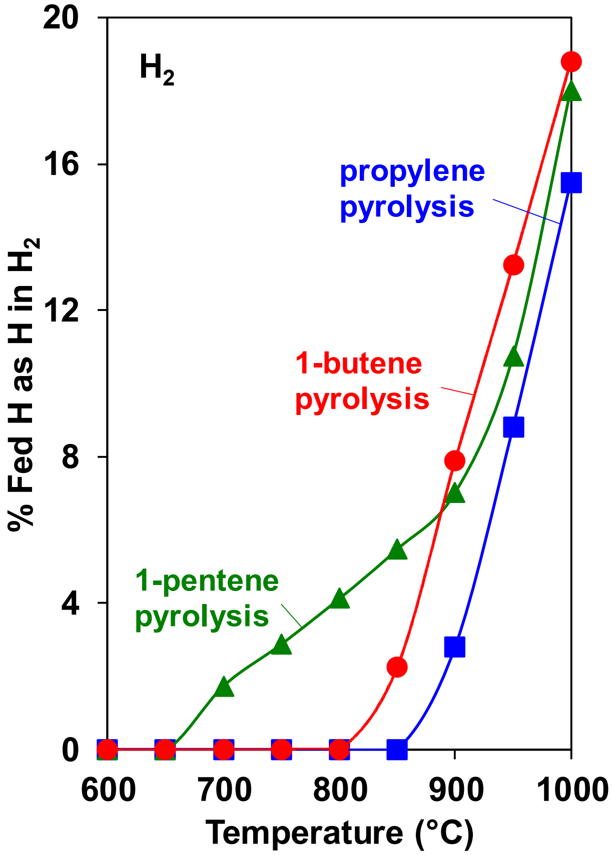

Figure A.2. Yield, as function of temperature, of product H_2 from propylene pyrolysis (blue squares and curve), 1-butene pyrolysis (red circles and curve), and 1-pentene pyrolysis (green triangles and curve) at 0.31 s.

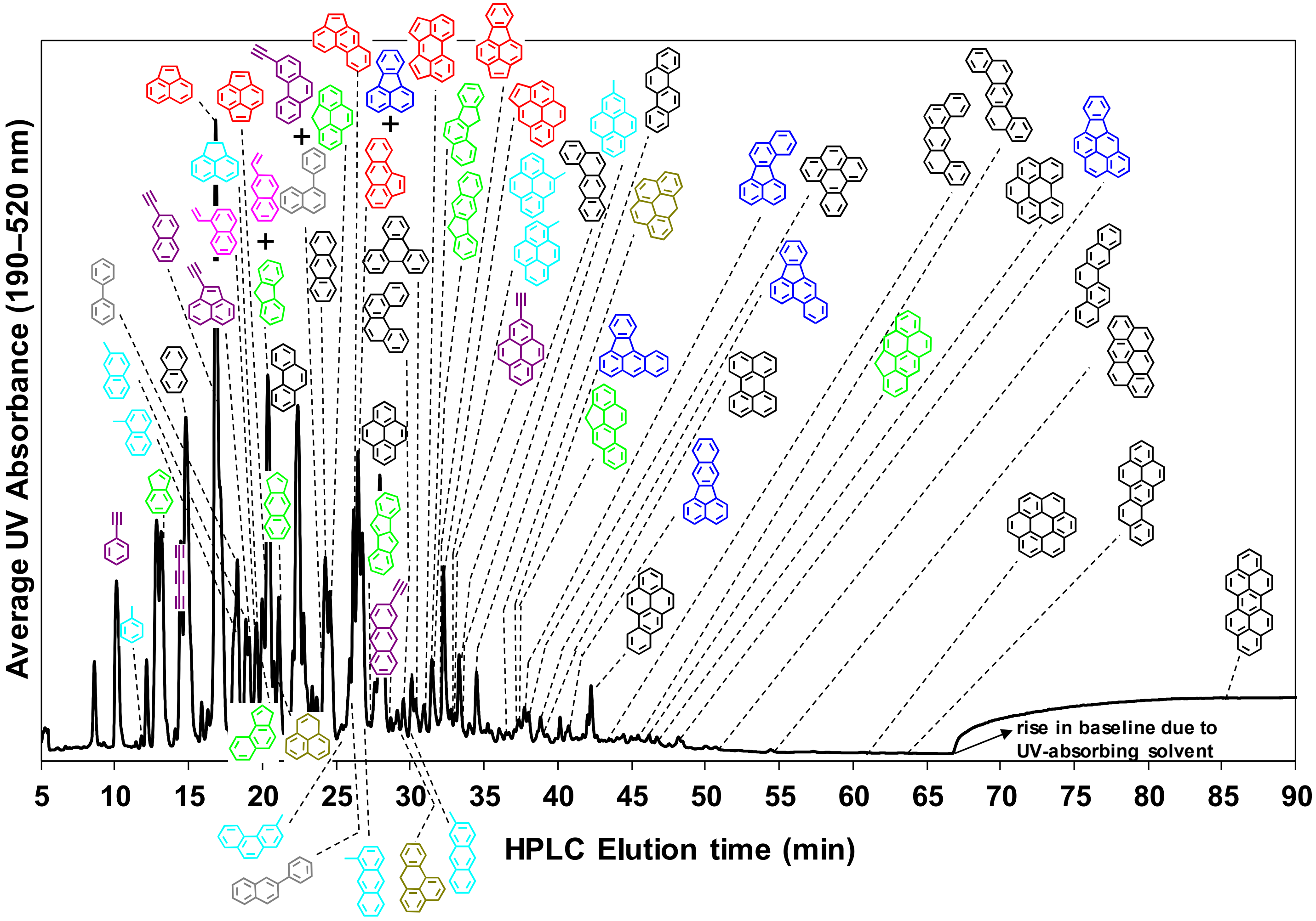

Figure A.3. HPLC chromatogram of the products of 1-pentene pyrolysis at 1000 °C and 0.31 s. The product compounds are color-coded by structural class: benzenoid PAH (black), ethynyl-substituted species (purple), vinyl-substituted PAH (pink), cyclopenta-fused PAH (red), fluoranthene benzologues (dark blue), indene benzologues (green), methyl substituted aromatics and acenaphthene (light blue), bi-aryls (grey), and phenalene-type compounds (olive). The names, molecular formulae, and structures of all the PAH products from propylene pyrolysis appear in Table A.6 in the Appendix.

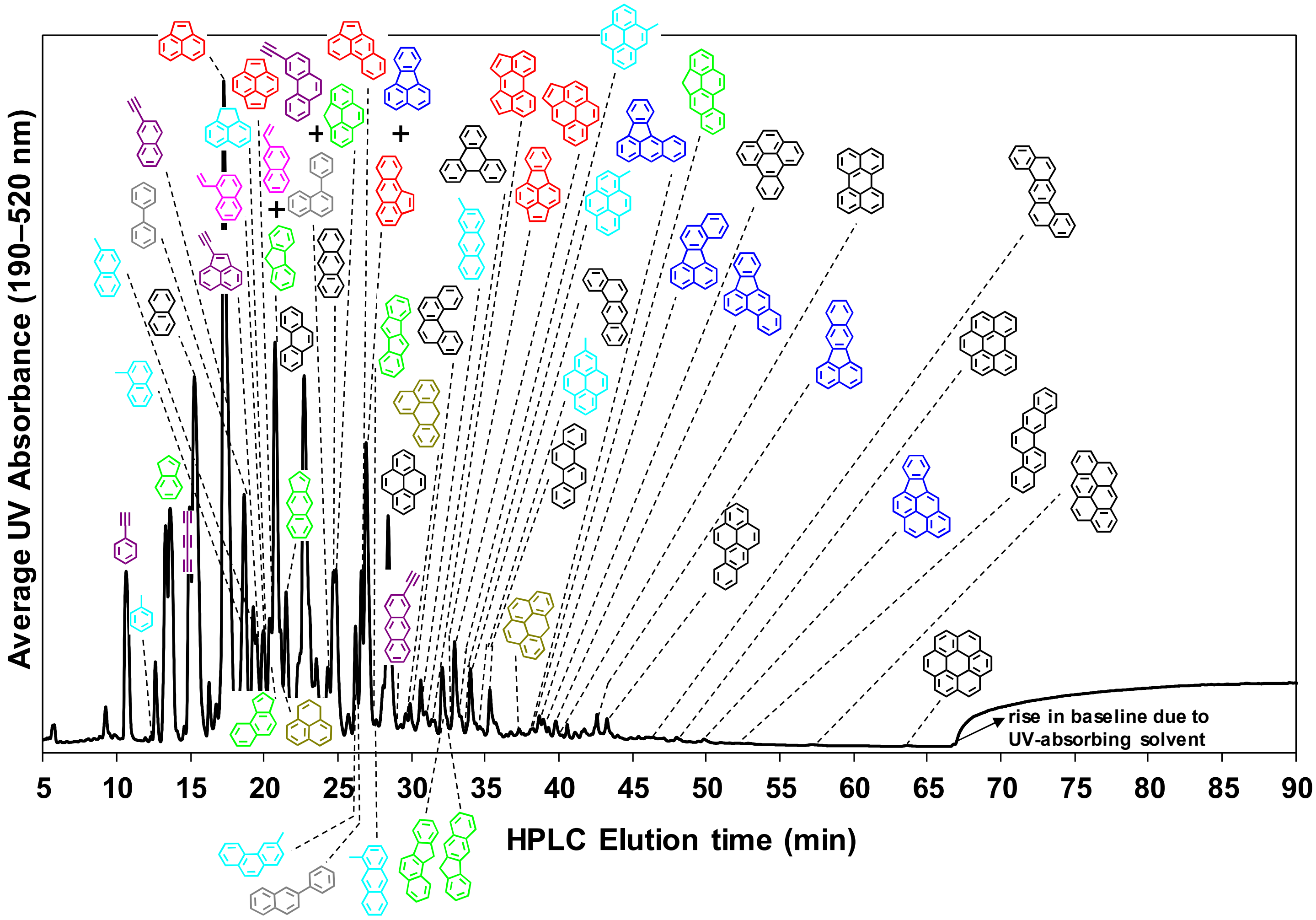

Figure A.4. HPLC chromatogram of the products of propylene pyrolysis at 1000 °C and 0.31 s. The product compounds are color-coded by structural class: benzenoid PAH (black), ethynyl-substituted species (purple), vinyl-substituted PAH (pink), cyclopenta-fused PAH (red), fluoranthene benzologues (dark blue), indene benzologues (green), methyl substituted aromatics and acenaphthene (light blue), bi-aryls (grey), and phenalene-type compounds (olive). The names, molecular formulae, and structures of all the PAH products from 1-pentene pyrolysis appear in Table A.7 in the Appendix.

Vita

Eva Christine Caspary was born in Mainz, Germany, in 1987. She obtained her Bachelor's in Process Engineering from the University of Applied Sciences in Mannheim, Germany in the year 2010. During the time of her doctoral studies, Eva Caspary has co-authored one peer-reviewed journal article and has had seven conference and poster presentations at various meetings in America, Europe, and Asia. She anticipates receiving her doctoral degree in Spring 2017.